HIV-1 SUBTYPE B AND C GP120-MEDIATED APOPTOSIS OF BYSTANDER CD4+ T LYMPHOCYTES

NATASHA CAMILLA PILLAY

A dissertation submitted to the Faculty of Health Sciences, University of the Witwatersrand, in fulfillment of the requirements for the degree of Master of Science in Medicine

Johannesburg, September 2011

DECLARATION

I, Natasha Camilla Pillay declare that this dissertation is my own work. It is being submitted for the degree of Master of Science in Medicine, in the University of the Witwatersrand, Johannesburg. It has not been submitted before for any degree or examination at this or any other University.

_____

Natasha Camilla Pillay

_____ day of _____, 2011

DEDICATION

This work is dedicated to my parents. Thank you for giving me this opportunity and for always supporting me and believing in me.

To the rest of my family and friends, thank you for your encouragement, love and continuous support.

To Levan, thank you for being by my side, for, loving me, motivating me and believing in me.

I love you all dearly!

ABSTRACT

Human Immunodeficiency Virus type 1 (HIV-1) is the causal agent of AIDS, and currently infects 33.3 million individuals worldwide. The gradual depletion of CD4+ T lymphocytes is a characteristic feature of a progressive HIV-1 infection. During HIV-1 infection the number of infected CD4+ T lymphocytes is fewer than the number of CD4+ T lymphocytes that are depleted, therefore suggesting a role for HIV-mediated apoptosis of uninfected bystander CD4+ T lymphocytes. Apoptosis, also known as programmed cell death, is a highly regulated, normal physiological process that results in the disposal of unwanted or corrupted cells such as virally infected cells. Several HIV-1 proteins are involved in HIV-1-mediated apoptosis, of which the envelope (Env) glycoprotein gp120 subunit is the most effective. However, the true mechanism of gp120-mediated apoptosis of uninfected CD4+ T lymphocytes is not fully understood and remains controversial. Furthermore, research focusing on HIV-1 subtype C Env-mediated apoptosis is limited. This study compared the ability of CCR5-utilizing soluble monomeric HIV-1 subtype C gp120 ($gp120^{ZM651}$), monomeric HIV-1 subtype B gp120 ($gp120^{BaL}$) and trimeric/oligomeric HIV-1 subtype C gp140 ($gp140^{AncC}$) to induce apoptosis of uninfected Jurkat T lymphocytes and activated CD4+ T lymphocytes via CD4 and CD4/CCR5 signalling, respectively. All three Env glycoproteins were expressed in HEK 293T cells, purified by lectin affinity chromatography and characterized by assessing their binding capabilities to monoclonal antibodies IgGb12, 17b (in the presence and absence of soluble CD4) and 2G12. Purified recombinant $gp120^{BaL}$, $gp120^{ZM651}$ and $gp140^{AncC}$ were found to

be functional and conformationally intact and subsequently added in different concentrations to uninfected Jurkat T lymphocytes and activated CD4+ T lymphocytes. Apoptosis was detected by flow cytometry using Annexin V/7-AAD staining for up to 48 hours post treatment, and further confirmed by TUNEL analysis at 65 hours post treatment. Recombinant $gp120^{BaL}$, $gp120^{ZM651}$ and $gp140^{AncC}$ induced low levels of apoptosis in the Jurkat T lymphocytes (6.1%, 5.0% and 6.8%, respectively) and higher levels of apoptosis in the activated CD4+ T lymphocytes (13.3%, 15.6% and 11.5%, respectively) via TUNEL analysis of chromosomal DNA fragmentation. Moreover, comparable levels of apoptosis were observed between the monomeric gp120 and trimeric/oligomeric gp140 forms in both cell types. Interestingly, the subtype C $gp140^{AncC}$ induced higher levels of apoptosis than subtype C $gp120^{ZM651}$ and subtype B $gp120^{BaL}$ in activated CD4+ T lymphocytes during the Annexin V/7-AAD analysis while the subtype C $gp120^{ZM651}$ induced higher levels of apoptosis than subtype C $gp140^{AncC}$ and subtype B $gp120^{BaL}$ in activated CD4+ T lymphocytes during the TUNEL analysis. Overall, these results suggest that soluble gp120 is able to mediate low levels of apoptosis via CD4 signalling only in Jurkat T lymphocytes, and these levels are enhanced in activated CD4+ T lymphocytes, possibly due to engagement of gp120 with CD4 and the CCR5 co-receptor on the surface of the target cell.

AKNOWLEDGEMENTS

To my supervisor, Dr Maria Papathanasopoulos, thank you for all your support, patience and invaluable insight on this project. Your time and guidance has been much appreciated.

To my co-supervisor, Dr Natalie Whalley, thank you for your time and assistance. Also, for always being so willing to discuss work and for the kind advise and opinions.

To Dr Chrisna Durandt, for your assurance and assistance with all of the flow cytometry work. Thank you for all those hours that you spent with me analysing and discussing the data. Your patience and kindness was remarkable.

To Thenusha Naidoo, thank you for your amazing friendship and support. For all the tears, giggles and memorable times together in the lab. I am so grateful to have shared this experience with you.

To Naazneen Moola, Mark Killick and Nichole Cerutti, thank you for all the kind advice and always willing to listen and lend a helping hand wherever you can. Thank you Naaz for your assistance with the protein purification studies and all of the helpful tips during the cell culture experiments. Mark, thank you for your continuous support throughout this study, for all your help on every aspect of this project. Nichole, thank

you for your assistance whenever needed, giggles, moral support and experienced advice.

To Maria Antropova, thank you for your love, support and for making this journey easier.

To Dr Abdullah Ely, thank you for being so helpful and for always being there when I needed you. You are an awesome friend and collegue.

To the Red Cell Membrane Unit, thank you for always being so welcoming and helpful.

To the PRF, NRF and the University of the Witwatersrand for the financial support.

TABLE OF CONTENTS

LIST OF FIGURES

LIST OF TABLES

LIST OF ABBREVIATIONS

7-AAD	7-amino-actinomysin
AIDS	Acquired Immune Deficiency Syndrome
bp	Base pairs
BSA	Bovine Serum Albumin
CA	Capsid Protein
$CaCl_2$	Calcium Chloride
CCR5	Chemokine (C-C Motif) Receptor 5
CD4+	CD4 Positive
CD4	Cluster of Differentiation 4
CD3	Cluster of Differentiation 3
CD8	Cluster of Differentiation 8
CRFs	Circulating Recombinant Forms
CXCR4	CXC Chemokine Receptor 4
DMEM	Dulbecco's Modified Eagle Medium
DMSO	Dimethyl Sulfoxide
DNA	Deoxyribonucleic Acid
E. coli	*Escherichia coli*
ECD	Phycoerythrin-Texas Red-X
EDTA	Ethylenediamine tetraacetic acid
ELISA	Enzyme-Linked Immunosorption Assay
Env	Envelope
FCS	Fetal Calf Serum
FITC-dUTP's	Fluorescein Isothiocyanate -labelled-2'-deoxyuridine 5'- triphosphates
gp120	Envelope Glycoprotein 120
gp160	Envelope Glycoprotein 160
gp140	Envelope Glycoprotein 140

gp41	Transmembrane Glycoprotein 41
$gp120^{BaL}$	Subtype B envelope glycoprotein 120
$gp120^{ZM651}$	Subtype C envelope glycoprotein 120
$gp140^{AncC}$	Ancestral subtype C envelope glycoprotein 140
HAART	Highly Active Antiretroviral Therapy
HEK 293T cells	Human Embryonic Kidney 293T cells
HIV-1	Human Immunodeficiency Virus Type 1
HIV-2	Human Immunodeficiency Virus Type 2
hIL-2	Human Interleukin 2
HRP	Horseradish Peroxidase
IN	Integrase
kDa	KiloDaltons
LAV	Lymphadenopathy-Associated Virus
LB Broth	Luria-Bertani Broth
MA	Matrix Protein
MMP	methyl α-D-mannopyranoside
Mw	Molecular Weight Marker
NaCl	Sodium Chloride
NaOH	Sodium Hydroxide
NC	Nucleocapsid Protein
NIH	National Institute of Health
PBMC’s	Peripheral Blood Mononuclear Cells
PBS	Phosphate Buffered Saline
PBS-T	Phosphate Buffered Saline containing Tween-20
PC7	Phycoerythrin-Cy7
PE	Phycoerythrin
PFA	Paraformaldehyde
PHA	Phytohaemaglutinin
PIC	Preintegration Complex
PR	Protease
R5	CCR5-utilizing

RNA	Ribonucleic Acid
RPMI	Roswell Park Memorial Institute Medium
RT	Reverse Transcriptase
SANBS	South African National Blood Bank Services
sCD4	Soluble Cluster of Differentiation 4
sH_2O	Sterile Sabax water
SDS-PAGE	Sodium Dodecyl Sulphate Polyacrylamide Gel Electrophoresis
SIV	Simian Immune Deficiency Virus
TAE Buffer	Tris-Acetate-EDTA Buffer
Tdt	Terminal deoxynucleotidyl transferase
TBS	Tris-Buffered Saline
T-TBS	Tris-Buffered Saline containing Tween-20
TUNEL	Tdt-mediated dUTP Nick End Labeling
UV light	Ultra Violet light
V1/2/3/4/5	Variable Loop 1/2/3/4/5
X4	CXCR4-utilizing

CHAPTER 1: INTRODUCTION

1.1 Human Immunodeficiency Virus and AIDS

Acquired Immune Deficiency Syndrome (AIDS) was given its name in 1982 by the United States Centre for Disease Control and Prevention (CDC) [1]. It is commonly defined by the disruption and loss of cellular immune responses due to a decline in CD4+ T helper lymphocytes and the occurrence of opportunistic infections such as candidiasis and pneumonia [2-4]. The initial clinical encounter of AIDS was reported in the United States of America in 1981 after previously healthy young homosexual men began to develop unusual diseases such as Kaposi's sarcoma and pneumonia [2, 3]. Eventually, AIDS became apparent in the heterosexual population resulting in a global epidemic.

In 1983, Luc Montagnier and his research team reported the discovery of a new retrovirus as the cause of AIDS and named it lymphadenopathy-associated virus (LAV) [5]. This discovery was confirmed by Robert Gallo and his research team who had renamed the virus as the human T-cell lymphotropic virus type 3 (HTLV-III) [5, 6]. In 1986, after reaching a consensus, the retrovirus was finally renamed Human Immunodeficiency Virus (HIV) [7].

HIV destroys and disables the immune system by establishing prolonged infections within major immune defence cells such as the $CD4^+$ T helper lymphocytes, macrophages and dendritic cells, resulting in the production of weak neutralizing

antibodies and antigen specific cellular immune responses involving cytotoxic CD8+ T lymphocytes and CD4+ helper T lymphocytes [4]. Transmission of infection occurs by bodily fluids (semen, blood and breast milk) that contain virus particles and this is commonly facilitated by unprotected sexual intercourse, use of contaminated needles and from mother-to-child by breast feeding or intra-, peri- or post partum [8] [1].

1.2 HIV subtypes and groups

HIV shows incredible genetic diversity due to its high mutation rate and this has contributed to the development of multiple variants or strains. HIV type 1 (HIV-1) and HIV type 2 (HIV-2) are the two main types of HIV that originated in central West Africa by zoonotic transmission of Simian Immunodeficiency Virus (SIV) from the chimpanzee (*Pan troglodytes)* [9] and sooty mangabey monkeys (*Cercoebus atys*) [10], respectively. HIV-1 is the most virulent and predominant type globally while HIV-2, with partial homology to HIV-1, is less virulent and commonly found in central West Africa [10].

Owing to the emergence of multiple and genetically different strains, HIV-1 was classified into 3 groups: M (major), N (non-M/non-O) and O (outlier) based on the envelope sequences [11]. Groups N and O isolates are quite rare, while Group M isolates constitute the cause of the global epidemic. More recently, Group P has been introduced into the classification of HIV-1, containing an HIV-1 isolate derived from

gorilla SIV [12]. Group M is sub-divided into 9 genetically different subtypes: A-D, F, G, J and K based on the entire genome [11]. The subtypes show up to 30% and 15% diversity in their envelope (Env) glycoprotein and gag amino acid sequences, respectively [11]. The most prevalent subtypes include subtypes A, B, C and D. Subtype B is found mainly in North America, North Africa, Asia and west and central Europe, while subtypes A, C and D are found mainly in Africa [11]. Different subtypes are able to infect a single individual and recombination of their genetic material occurs to produce new viruses [13, 14]. If the new viruses are viable, able to survive or be transmitted, and are identified in epidemiologically non-related individuals, they are known as a circulating recombinant forms (CRFs) [13, 14]. There has been an increased incidence of CRFs which now contribute significantly to global HIV pandemic [15, 16]. There are currently 49 identified CRFs circulating globally, and this number is expected to increase (Los Alamos National Laboratory http://www.hiv.lanl.gov/content/sequence/HIV/CRFs/CRFs.html).

1.3 What is the significance of the HIV/AIDS epidemic globally and in Sub-Saharan Africa?

There are currently 33.3 million individuals worldwide who are living with HIV infection [17]. In 2009, up to 1.8 million people died of AIDS and an estimated total of 2.6 million new infections occurred globally [17]. However, there has been a significant reduction in the number of AIDS-related deaths and progress in the prevention of HIV

infection, since antiretroviral treatments have become more readily available in less developed countries. In 1997, an estimated 3.2 million new infections occurred, while in 2009, the number of new infections dropped by 21% [17]. In the same regard, there were 2.1 million AIDS–related deaths in 2004 which dropped to 1.8 million in 2009 [17]. In addition, there has been an estimated 19% decrease in AIDS-related deaths among children all over the globe between 2004 and 2009 [17]. Sub-Saharan Africa still accounts for 72% (1.3 million adults and children) of the worlds AIDS-related deaths and 68% of the total number of people living with HIV globally[17]. HIV contributes to the poverty and economic distress that is experienced by Sub-Saharan Africa but treatment availability has improved and as a result AIDS-related death rates have decreased [17]. Even though the epidemic seems to be stabilizing in various countries, it prevails in other countries such as Eastern Europe and Central Asia due to increased numbers of new infections [17].

AIDS-induced deaths, the occurrence of opportunistic infections and viral replication can be controlled by Highly Active Antiretroviral Therapy (HAART) [18, 19], which is a combination of three different drugs that target different stages of the HIV life cycle [20]. Most clinically approved drug regimens include drugs that are directed towards the 3 viral enzymes, reverse transcriptase (RT), integrase (INT) and protease (PR) as well as those targeting viral entry [21, 22]. Owing to the high mutation rate and lack of proofreading ability of RT [23], the virus easily develops resistance to many antiretroviral drug regimens. For this reason, the discovery or development of a

vaccine against HIV and AIDS remains an ongoing struggle. Despite the struggle, since 2004, more than 5 million people are now receiving HAART globally [17].

1.4 The biology of HIV-1 and the structural organization of its genome

As shown in Figure 1.1, mature HIV-1 virions are roughly spherical and encapsulated by a double layered cholesterol and sphingomyelin-rich phospholipid envelope which is obtained from the host cell phospholipid membrane [24-26]. Trimeric Env glycoprotein spikes are embedded within the phospholipid envelope, each consisting of a surface glycoprotein (gp120) and a transmembrane glycoprotein (gp41) [27]. Two identical single plus strands of viral RNA (ssRNA) associated with nucleocapsid proteins [28-30], accessory proteins Vpr, Vif and Nef and essential viral enzymes such as RT, INT and PR are located within the bullet-shaped capsid core [31-33]. The RT has DNA polymerase and RNase H (RH) functions to assist in the conversion of ssRNA to double stranded complementary DNA (dsDNA) [34]. The capsid is separated from the phospholipid envelope by a protein matrix layer that ensures the integrity of the virion [35] (Figure 1.1).

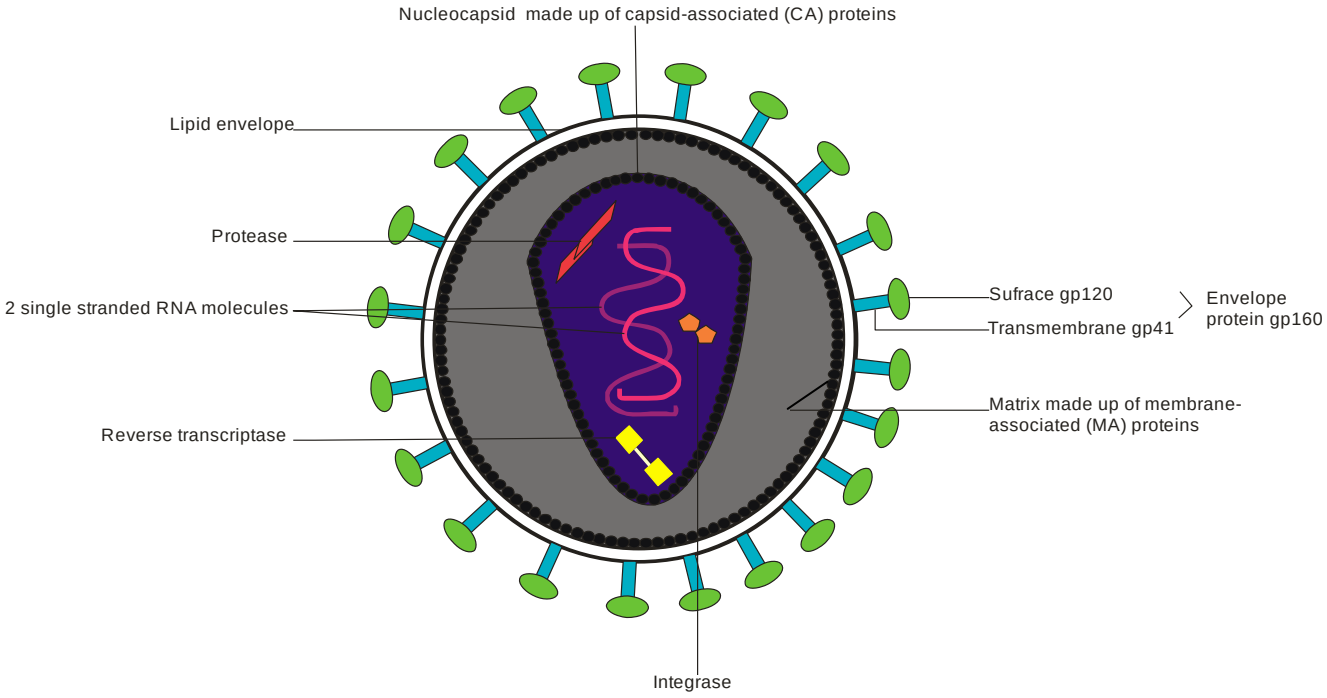

Figure1.1: The structure and biology of an HIV particle

The HIV-1 genome contains 9 genes, encoding for structural, accessory and regulatory proteins, each holding a unique function [36-41]. Structural proteins are encoded by the *gag, env* and *pol* genes [38-42]. The *gag* gene encodes viral capsid (p24) and matrix (p17) proteins, all of which are essential for viral assembly [32, 41, 43-45]. Important viral enzymes: RT, PR and INT are expressed by the *gag-pol* open reading frame, by ribosomal frame shifting [46]. *Env* encodes the large Env glycoprotein precursor gp160, which is cleaved by host cellular proteases to produce gp120 and gp41 [41]. Regulatory genes *tat* and *rev* encode for proteins that are essential for the regulation of viral protein transcription and translation [37, 41, 42].

Accessory genes *vif, vpr, vpu* and *nef* encode proteins that assist in viral infection and protect the virus during its life cycle [37, 41, 42, 47, 48].

1.5 HIV-1 lifecycle

Viral entry, reverse transcription of viral RNA, integration of the complementary viral DNA into the host genome, transcription, translation, viral assembly, release and maturation are essential for the completion of the life cycle and each process poses as a possible drug target. These processes are described briefly.

1.5.1 Viral Entry

Env glycoproteins, gp120 and gp41 mediate fusion of the viral and host cell membranes and ultimaltely viral entry into the target cell [27]. The interaction between the viral gp120 and the host CD4 induces several conformational changes that include the exposure of co-receptor binding sites on gp120 [49-51]. The co-receptor binding sites are recognized by chemokine co-receptors, CXCR4 and/or CCR5 [51-53]. Following the gp120-co-receptor interaction, the gp120 component is shed and the gp41 hydrophobic fusion peptide or ectodomain becomes exposed [27] [50, 54]. The gp41 fusion peptide then folds over to acquire a coiled conformation which is known as a six helix bundle which results in the fusion of both membranes and entry of the viral core particle into the host cell [55].

1.5.2 Host cell proteins involved in HIV-1 entry

1.5.2.1 CD4 receptor

CD4 is a glycoprotein that is expressed on the surface of some T lymphocytes. CD4 is made up of an intracellular cytoplasmic domain, transmembrane domain and an extracellular unit of four domains comprising of two constant and two variable immunoglobulin-like domains [56] [57]. CD4 assists in T lymphocyte activation and is able to elicit an efficient immune response by directly interacting with Major Histocompatibility complex (MHC) class II on Antigen Presenting Cells (APCs) via its first variable domain (D1) [58-60]. The intracellular domain is involved in the initiation of signalling cascades within an activated T lymphocyte [61]. HIV-1 uses CD4 as its primary receptor to gain entry into the host cells [49, 62, 63] by binding to the amino terminal of D1 on the CD4 receptor via specific residues on its outer Env glycoprotein gp120 [64-66].

1.5.2.2 CXCR4 and CCR5 co-receptors

CXCR4, a α-chemokine receptor expressed on T lymphocytes and CCR5, a β-chemokine receptor expressed on T lymphocytes and macrophages, are part of the seven transmembrane G-protein coupled receptor family [67-69]. CXCR4 was discovered as a co-receptor used by HIV-1 during entry and the discovery of CCR5 as another co-receptor used by macrophage-tropic HIV-1 isolates followed [52, 53, 68, 70]. HIV-1 entry into host cells and subsequent replication is efficient only in the

presence of a chemokine co-receptor [53, 70, 71]. The first and second extracellular loops of CXCR4 and the second and third extracellular loops of CCR5 have been shown to play an important role during gp120 binding and HIV-1 entry [72] [73].

The type of co-receptor used depends on the cell type and phase of HIV-1 infection and contributes to the pathogenesis of virus [55]. HIV-1 transmissible Macrophage (M)-tropic strains or non-syncytia inducing strains (NSI) utilize the CCR5 co-receptor while HIV-1 T lymphocyte (T)-tropic strains or syncytia-inducing strains (SI) utilize the CXCR4 co-receptor [52, 53, 68]. During subtype A, B and D infection, M-tropic strains occur predominantly during early infection and T-tropic strains predominate during the later stages of infection resulting in accelerated disease progression to AIDS [74, 75] [76]. During the transition of M-tropic strains to T-tropic strains, the emergence of dual tropic viruses (R5X4) may also occur [76] [77]. In contrast to the switch in tropism observed, previous studies have demonstrated that M-tropic viruses predominate at various stages of HIV-1 subtype C infection and that T-tropic viruses are quite rare even during the later stages of infection [78, 79], although an increase in T-tropic viruses has been described recently [80]. Interestingly, a recent study showed that ARV exposed subtype C isolates from Zimbabwe exhibited a T-tropic phenotype, suggesting that the ARV therapy may have possibly created an environment that stimulates the emergence of T-tropic viruses [81].

1.5.3 Viral proteins involved in HIV-1 entry

1.5.3.1 Envelope glycoproteins

Env glycoprotein gp160 precursors are processed within the rough endoplasmic reticulum (ER) [27, 82] followed by a series of modifications such as disulphide bond formation and the addition of N-linked high mannose oligosaccharides [82, 83]. Trimers of gp120 and gp41 are generated after gp160 is cleaved by host proteases in the Golgi apparatus [82, 84-86]. Non-covalent interactions exist between the gp41 hydrophobic ectodomain and the amino and carboxyl terminals of gp120, which further facilitate the shedding of gp120 from the virion post CD4 binding [27, 87]. Mature Env glycoproteins are formed in the Golgi apparatus once the gp120 subunit is glycosylated (addition of complex sugars) [83]. Mature Env glycoproteins are then transported to the host cell membrane where they are acquired along with host phospholipids by the viral particles upon budding [27]. The gp120 component is exposed on the viral membrane surface while gp41 component spans the membrane [27].

1.5.3.2 The structure of HIV-1 gp120

The conformationally flexible gp120 glycoprotein consists of five disulphide-linked hypervariable domains or loops (V1, V2, V3, V4 and V5) which are exposed on the viral surface, with five highly conserved regions (C1, C2, C3, C4 and C5) that are buried within the gp120 core [27, 83, 88-90]. The gp120 core is composed of an inner

domain containing the V1 and V2 loops that interact with the gp41 subunit, a four-stranded beta-bridging sheet containing the co-receptor binding site and a highly glycosylated outer domain containing the V3 and V4 loops exposed on the viral surface [27]. Both the inner and outer gp120 domains contribute to CD4 interactions [27].

Exposure of the highly conserved co-receptor binding sites induced by the binding of gp120 to the CD4 receptor on T lymphocytes requires the movement of the V1, V2 and V3 loops [91]. The V1 and V2 regions are within close proximity of one another and are believed to shield the V3 region [91]. The absence of the V1/V2 regions has been shown to increase viral susceptibility to neutralizing antibodies [91]. The V3 region has been the major focus of many studies since it contains an important neutralization domain and is able to co-ordinate co-receptor usage [71, 92-95]. This region is highly immunogenic and therefore exposed to strong immune pressures that increase its antigenic diversity [96].

1.5.3.3 Interactions between gp120-CD4 and gp120-co-receptors

It has been shown that CD4 receptors form hydrogen bonds with amino acid residues that surround a deep pocket in gp120 via Phenylalanine-43 which has been shown to be extremely important for gp120 binding [27, 65, 97, 98]. In addition, the interaction between Asparagine-368 on gp120 and Arginine-59 on CD4 is believed to be important for gp120-CD4 interactions [27, 65, 97, 98]. Even though the V3 loop has

been implicated as the major determinant of co-receptor usage, there is evidence implicating the involvement of other gp120 conserved regions in co-receptor usage [51, 71, 99].

1.5.3.4 The structure of HIV-1 gp41 and the fusion process

In addition to its role in mediating fusion of the host and viral cell membranes, gp41 is also involved in the trimerization of Env glycoproteins [100]. It consists of an ectodomain (N-terminal) which contains a hydrophobic fusion peptide, a tryptophan-rich membrane-spanning anchor and a cytoplasmic tail [85]. The ectodomain is a coiled coil structure which is believed to undergo conformational changes that ultimately allow fusion and viral entry [85, 101].

Subsequent to the gp120-co-receptor interaction, the gp41 fusion peptide is exposed and inserted into the host cell membrane [85, 102, 103], leading to the formation of a pre-hairpin intermediate which consists of a two-heptad repeat (HR) region, an N-terminal HR region within the host cell membrane and a C-terminal HR region within the viral membrane [103, 104]. Three parallel N-terminal HRs form a coiled-coil structure that lies anti-parallel to three C-terminal HRs. Interhelical interactions between the N-terminal HRs and C-terminal HRs result in the formation of the six-helix bundle which pulls the viral and host cell membranes towards each other, thereby mediating fusion [85, 103]. A fusion pore that facilitates the passage of the

viral core into the host cell develops during the assembly of the six-helix bundle [105, 106].

1.5.4 Viral replication, assembly and budding

Post viral fusion, the viral core is uncoated and the genetic material along with essential viral proteins and enzymes are released into the cytoplasm [107]. RT converts each of the ssRNA molecules into dsDNA with the help of host deoxy-nucleotriphosphates (dNTPs) [108]. Subsequently, a Pre-Integration Complex (PIC) including the complementary dsDNA, integrase, matrix protein and Vpr is formed [109, 110]. Vpr proteins contain nuclear localization signal sequences within the PIC and subsequently assist in importing the complex into the nucleus where it can be integrated into the host genome [111]. Integrase facilitates the translocation of the PIC through the nuclear pores and the integration of the dsDNA into the host genome where it is transcribed and expressed along with the host's genes [109, 112, 113]. Rev proteins recognize viral mRNA transcripts and export them from the nucleus into the cytoplasm where they are protected from degradation, spliced and translated into viral proteins [40, 114]. All newly synthesized viral structural Gag proteins and enzymes migrate to lipid rafts within the plasma membrane where the assembly of immature virions takes place [115]. A lipid membrane is acquired from the infected host cell [27] and maturation of immature virions during budding out of the host cell relies on the complete proteolytic cleavage of the Gag and Gag-Pol proteins by the viral protease [116, 117].

1.6 HIV-1/AIDS disease progression

HIV-1 infection and disease progression in the absence of HAART usually occurs via distinct stages or phases and since the rate of HIV-1 disease progression to AIDS is dependent on numerous factors such as host immune responses, host and viral genetics and co-infections, the state of disease therefore varies with each individual [118-121]. The first phase, known as the acute or primary phase is characterized by a decrease in CD4+ T lymphocytes caused by rapid viral replication which in turn correlates with an increase in cytotoxic CD8+ T lymphocytes [122]. It is during this phase that seroconversion takes place [122]. The chronic or asymptomatic phase which can last up to 10 years is accompanied by the stabilization of viral replication. This causes plasma viral loads to reach a viral set point that ultimately defines the rate of disease progression to AIDS [123, 124]. During the asymptomatic phase, the levels of circulating CD4+ T lymphocytes normalize, however, intense immune activation as well as a gradual decrease in CD4+ T lymphocytes leads to the deterioration of the immune system which increases the host's susceptibility to opportunistic infections resulting in the progression to AIDS [123-126]. The final AIDS phase is associated with an increase in viral load which correlates with a decrease in CD8+ T lymphocytes and in the production of neutralizing antibodies [123, 127]. During the course of HIV-1 infection, there is a loss of both infected and uninfected CD4+ T lymphocytes and several processes are known to contribute. However, one of the main strategies that HIV-1 utilizes to attack the immune system is its ability to

manipulate and disrupt the balance of apoptosis, which is a host cell defence mechanism [123]. Apoptosis, during the chronic phase of HIV-1 infection has been proposed as one of the processes that contribute to the depletion of uninfected CD4+ T lymphocytes and an increase in CD4+ T lymphocyte depletion correlates with an increase in disease progression [128-131]. Furthermore, HAART has been shown to reduce the levels of CD4+ T lymphocyte apoptosis within infected individuals [132, 133].

1.7 HIV-1 - mediated bystander CD4+T lymphocyte apoptosis

Several HIV-1 encoded proteins are able to induce apoptosis (extrinsically or intrinsically) of both infected and uninfected T lymphocytes during HIV-1 infection via several mechanisms [134]. HIV-1 mediated apoptosis of uninfected bystander T lymphocytes is believed to be the cause of CD4+ T lymphocyte depletion since the number of infected lymphocytes is less than the number of lymphocytes undergoing apoptosis [135]. In addition, apoptosis of uninfected bystander T lymphocytes has been observed in the peripheral blood and lymph nodes of HIV-1 infected individuals and similar results were obtained in animal models [136-138]. Uninfected bystander T lymphocyte death can occur via the direct/indirect influence of HIV proteins, which are released by infected lymphocytes, or by activation-induced cell death (AICD), which is

caused by continuous antigenic stimulation and is mediated by the Fas-FasL pathway [132, 139].

This phenomenon has been intensely researched for more than a decade, however the true mechanisms are not fully understood and therefore HIV-1-mediated apoptosis of CD4+ T lymphocytes remains a controversial issue.

1.7.1 Apoptosis

Apoptosis, also known as programmed cell death, is a complex and highly regulated process that results in the self-destruction of cells in response to receptor mediated (extrinsic) or non-receptor mediated (intrinsic) signals, [134, 140]. Apoptosis is not only required for the regulation of normal physiological and developmental processes of multicellular organisms but also for the elimination of harmful cells [141, 142]. Cells that are undergoing apoptosis are characterized by chromosome condensation and fragmentation, phosphotidylserine (PS) externalization, mitochondrial membrane disruption, cell shrinkage and cell fragmentation ultimately leading to the formation of ‘apoptotic bodies’ [134, 140, 143]. During apoptosis, serine proteases known as cysteine-dependant aspartate-specific proteases (caspases) are activated by proteolytic cleavage of their procaspase forms [134, 144, 145]. Activated caspases act as catalysts and mediate apoptosis by cleaving and inactivating protein substrates which are normally essential for the prevention of apoptosis [134, 144, 145]. In

addition, cleavage of the linker DNA between nucleosomal units occurs during the later stages of apoptosis, resulting in the fragmentation of DNA into multiples of the 180 base pair (bp) nucleosomal unit [146].

1.7.1.1 Extrinsic Apoptosis and HIV-1 infection

Extrinsic apoptosis requires an external death signal that interacts specifically with death receptors on cell surfaces [147]. Death receptors (DR), belonging to the Tumor Necrosis Factor Receptor (TNFR) superfamily include Fas (CD95), TNF receptor 1 (TNFR1) and 2 (TNFR2) [147] and TNF-related apoptosis inducing ligand (TRAIL) receptors DR4 and DR5 [147-150]. These death receptors consist of a cysteine-rich extracellular domain and an intracellular cytoplasmic death domain (DD) (conserved sequence) which is involved in the recruitment of adaptor molecules, such as Fas-associated DD (FADD) and the formation of a death-inducing signaling complex (DISC) [148]. Each death receptor interacts with its cognate death ligand, for example: FasL interacts with Fas DR [151], undergoes trimerization and subsequently activates a caspase-dependent signalling cascade that terminates in apoptosis [148].

Briefly, the Fas cell death pathway requires the binding of the Fas ligand (FasL) to the Fas death receptor resulting in the formation of Fas trimers which activate the death receptor [148, 151]. The activated death receptor then recruits the adaptor molecule

Fas-associated DD (FADD) via DD signalling. Further interactions of FADD with cytosolic proteins as well as procaspase 8 leads to the formation of a death-inducing signalling complex (DISC) [148]. The formation of this complex leads to the activation of caspase 8 which in turn activates effector caspases; 6, 7 and 3 [144, 145]. Activated caspase 3 cleaves specific cellular substrates that include DNA repair enzymes and cytoskeletal proteins which ultimately results in cell death [144]. The DR5/DR4 and TNFR1 cell death pathways occur in the same manner as the Fas cell death pathway in the presence of TRAIL and TNF ligands, respectively.

During HIV-1 infection, TRAIL has been found to be expressed by macrophages, monocytes and neurons [152-154] while Fas, FasL and TNF have shown to be expressed by macrophages, CD4+ and CD8+ T lymphocytes and in the patient plasma [155-157]. Studies have shown an increased expression of FasL, TNF, TNFR1 and TNFR2 within HIV-1 infected individuals and the resulting increase in Fas, TNFR1 and TNFR2-mediated apoptosis of CD4+ and CD8+ T lymphocytes has been correlated with disease progression [155, 156]. Furthermore, natural killer cells are able to utilize the Fas-pathway to mediate the destruction of HIV-1 infected lymphocytes [158]. It is evident that TRAIL plays a major role during HIV-1 infection and has therefore been suggested as being responsible for the apoptosis of uninfected bystander CD4+ T lymphocytes within HIV-1 infected tissues [147].

1.7.1.2 Intrinsic Apoptosis and HIV infection

Alternatively, the intrinsic Fas-independent pathway, which is also known as the mitochondrial-dependant apoptotic pathway, can be activated by intracellular and extracellular stress signals and is regulated by specific pro-apoptotic factors that belong to the Bcl-2 protein family (Table 1.1) [159-162]. These proteins regulate the permeability and membrane potential of the mitochondrial membrane by forming pores in the mitochondrial membrane, resulting in the influx of water which eventually leads to the rupturing of the outer mitochondrial membrane [163-165]. Subsequently, pro-apoptotic proteins and cytochrome c are released from the inter-membrane space into the cytosol [166-168]. Pro-apoptotic factors assist cytochrome c to form an apoptosome consisting of Apoptotic Protease Activating Factor 1 (APAF-1) and procaspase 9. This process initiates a caspase cascade similar to the extrinsic pathway that ultimately results in the activation of effector caspases (6, 7 and 3) and cell death [145]. DNA fragmentation and nuclear condensation is induced in a caspase-independent manner by the translocation of cytochrome c activated proteins, Apoptosis-inducing factor (AIF) and Endonuclease G (EndoG) from the mitochondria to the nucleus [161, 166, 169, 170]. If however, the signals transmitted from activated death receptors are too weak and are unable to result in the apoptosis of a cell, the signals are amplified via the mitochondrial apoptotic pathway. In this case, active caspase 8 cleaves and activates proapoptotic protein Bid producing a truncated Bid which moves into the mitochondria and interacts with proapoptotic proteins Bax and

Bak [171-173]. These proteins contain conserved domains which allow the formation of oligomers, resulting in the release of cytochrome c [174-177]. The downstream effects thereafter are identical to those described in the intrinsic pathway.

The Bcl-2 family consists of anti-apoptotic proteins Bcl-2 and Bcl-XL and pro-apoptotic proteins Bid, Bik, Noxa, Bim, Bax and Bak which regulate apoptosis by influencing cytochrome c release [159]. All anti- and pro-apoptotic proteins share homology in their Bcl2-homology domains [159]. The general functions of the Bcl-2 proteins are described in Table 1.1 [159, 163, 178].

Table 1.1: General functions of pro-apoptotic and anti-apoptotic proteins that belong to the Bcl-2 family

Bcl-2 family members	Function in mitochondrial apoptosis	**References**
Anti-apoptotic Bcl-2 and Bcl-XL	Prevent the release of cytochrome c	**[159, 163, 178]**
Pro-apoptotic Bid, Bax and Bak	Promote the release of cytochrome c	**[159, 163, 178]**
Pro-apoptotic Bik, Noxa and Bim	**Inhibit Bcl-2 and Bcl-XL**	**[159, 163, 178]**

In addition to activating the extrinsic pathway, HIV-1 proteins have the ability to change the mitochondrial membrane potential by disrupting the balance between anti-apoptotic and pro-apoptotic proteins. Increased TNF-α levels and consequent loss of mitochondrial membrane potential have been observed in acutely HIV infected individuals [166, 179-181]. In addition, Env-induced syncytia have been shown to undergo intrinsic apoptosis via Bax mediate loss of mitochondrial membrane potential [166, 179-181]. Within HIV-1 infected individuals, the levels of Bcl-2 expression are low, however this varies according to the stage of disease and may be related to immune activation or other factors, for example, TNF-α induced NF-κβ upregulation has been implicated in increased Bcl-2 expression and apoptosis prevention and establishment of viral reservoirs [182] [183]. In contrast, the levels of Bax [184, 185] and Bim [186] and Reactive Oxygen Species (ROS) [180, 187] are much higher in infected individuals. HIV-1 is able to induce the release of cytochrome c and AIF via the activation of the p53 pathway [184]. Furthermore, there have been reports of p53 regulation of Bax [188-190] and Bak [189]. The impact of HIV-1 proteins on apoptosis is cell-type specific and these proteins can function as pro/anti- apoptotic molecules, depending on the scenario [134].

1.7.2 The involvement of HIV-1 encoded proteins in bystander T cell apoptosis

Both uninfected and infected CD4+ T cell death is believed to be caused by viral encoded proteins such as Tat, Nef, Vpr, protease, Vpu and gp120 [191, 192]. The

apoptotic properties of proteins that promote bystander T cell death are described briefly below:

1.7.2.1 Tat, Nef, Vpr, protease and Vpu - induced apoptosis

Tat, secreted by HIV-1 infected T lymphocytes, is involved in the induction of apoptosis in uninfected bystander T lymphocytes [193] by enhancing their susceptibility to Fas-mediated apoptosis by upregulating Fas/FasL [194-196] and by increasing TRAIL expression on monocytes and macrophages which then interact with uninfected bystander lymphocytes [152, 153]. Tat is also able to induce apoptosis intrinsically by upregulating caspases 8 expression, Bax expression and modulating caspase 10 expression [185, 197, 198] and downregulating or upregulating Bcl-2 [185, 199].

Nef is able to function as an anti or pro-apoptotic protein and with such control over the apoptosis process, is able to protect HIV-1 infected lymphocytes from CD8+ cytotoxic T lymphocytes (CTL) attack, and gp120-CD4 mediated apoptosis by downregulating the surface expression of Major Histocompatibility Complexes I (MHC I) [200] and CD4 [201], respectively, while promoting uninfected bystander lymphocyte death by inducing Fas ligand (FasL) expression [202].

Vpr is able to induce apoptosis by causing G2/M transition phase cell cycle arrest in proliferating infected lymphocytes through the inactivation of a G2/M transition regulator [203-205] and is also able to interact directly with the mitochondrion permeability transition pore ultimately resulting in the release of cytochrome c [206, 207]. Vpu disrupts the integrity of the cell membrane and ultimately, cell viability by forming ion channels in the cell membrane, promoting viral release/budding [208]. Vpu has also been implicated in bystander killing [209-211].

HIV-1 protease is predominantly a pro-apoptotic protein and has been shown to modulate the expression of caspase 8 by associating with the extrinsic Fas-independent apoptotic pathway [212] and Bcl-2 [213] therefore promoting mitochondrial dysfunction within HIV-1 infected T lymphocytes. Similarly, Vpu downregulates CD4 and Bcl-XL [214] expression, compromises the integrity of the cell membrane by increasing its permeability [215] and promotes Fas-mediated apoptosis [216] within HIV-1 infected T lymphocytes.

1.7.2.2 gp120-induced apoptosis

Finally and most importantly, gp120 has been demonstrated as the major pro-apoptotic HIV-1 protein that can be presented in a variety of forms [123, 192, 217-219]. Each form is capable of engaging the CD4, CCR5 and/or CXCR4 receptors,

and signalling through these receptors can activate apoptotic pathways within both infected and uninfected CD4+ T lymphocytes [192, 220-224]. During the entry process, gp120 monomer is shed, allowing gp41 to mediate fusion [225]. Thus, in an infected individual gp120 exists as shed soluble gp120 (sgp120), intact gp120 on the virion and as newly formed gp120 assembled on the membrane of an infected CD4+ T lymphocyte [123, 192].

Free sgp120, is able to induce apoptosis via CD4–mediated signalling and signalling via both the co-receptors on uninfected and infected T lymphocytes. In addition, gp120 (monomeric or trimeric/oligomeric) expressed on infected lymphocytes is able to interact with CD4 and both the co-receptors on uninfected T lymphocytes resulting in either apoptotic signalling or cell-cell fusion events i.e. the development of syncytia or the occurrence of an hemifusion event. Both sgp120 and membrane bound gp120 are able to induce both extrinsic and intrinsic apoptotic pathways [192, 218, 219, 224, 226-229]. Syncytia are huge multinucleated cells that eventually become unstable and undergo apoptosis [123, 192]. Internalized gp120 acts as an anti-apoptotic protein by assisting in the dowregulation of CD4 on host cell surface, preventing gp120-CD4 signalling that could result in apoptosis of the infected T lymphocyte [230].

The ability of sgp120 to induce apoptosis through CD4 and/or the CCR5 or CXCR4 co-receptors interactions has been investigated in uninfected CD4+ T lymphocytes,

monocyte derived macrophages (MDMs) and various other cell lines [220, 224, 231-234] and the membrane tyrosine phosphatase CD45 has shown to be an important regulator [235]. Results show that sgp120 (R5 and/or X4-utilizing) can induce apoptosis in uninfected cell lines via the extrinsic pathway [224, 236] intrinsic pathway [237], caspase independent pathways [238], caspase dependent pathways [239], and by inducing an anergic state [240].

Activation of the intrinsic pathway within uninfected CD4+ T cells induced by X4 sgp120 interactions correlates with a significant alteration in the expression of proteins that are involved in mitochondrial functioning, cell metabolism, cytoskeleton and cell cycle [241]. Differences between R5 and X4 sgp120-induced apoptosis have been described. For example, apoptosis mediated by the R5 sgp120 does not involve the activation of MAPK p38, as does X4 sgp120 [231]. Furthermore, Perfettini *et al.*(2005) found that X4 sgp120-mediated apoptosis was caspase-dependent and CD4 independent [219]. In contrast, Vlahakis *et al*.(2001) and Algeciras-Schimnich *et al.*(2002) showed that X4 sgp120 interactions induced caspase-independent apoptosis and R5 sgp120 interactions resulted in caspase 8-dependent Fas-mediated apoptosis which was dependant on CD4 binding [238] [224].

In addition to CD4+ T lymphocyte apoptosis, gp120 has been implicated as a major contributor to the apoptosis of neuronal cells [242-244]. This results in the development of neuronal damage and dementia within AIDS patients [245, 246].

Chemokine co-receptors have also been shown to be involved in gp120-mediated apoptosis of neuronal cells and interestingly, thought to be CD4 independent [247, 248]. RNA-activated protein kinase signalling has been suggested as a mechanism for gp120-mediated apoptosis of neurons [249]. However, in a recent study, the treatment of neuronal cells with a cytokine known as Platelet-derived growth factor (PDGF) was able to reduce the amount of gp120-mediated apoptosis within neurons [243]. In addition, gp120-mediated apoptosis of cardiomyocytes and hepatocytes have also been implicated as part of the complications induced by HIV-1 infection [250, 251].

Studies that evaluate the ability of cell surface expressed gp120 to induce apoptosis in co-cultured uninfected cells show a similar trend to that seen with sgp120 [220, 224, 252]. Interestingly, it has been reported that a productive infection is not required for the induction of apoptosis in uninfected T lymphocytes, but the presence of infected dying T lymphocytes is required instead [253].

Evidently, the gp120 - CD4 interaction activates various apoptotic proteins that participate in both extrinsic and intrinsic apoptotic pathways. Even though there is supporting evidence of sgp120-mediated apoptosis in uninfected T lymphocytes, the true mechanism of this process remains unclear. Understanding the apoptosis of uninfected bystander T lymphocytes could lead to the development of therapies that could decrease the levels of apoptosis and most importantly, maintain CD4+ T lymphocyte populations.

1.8 Study Perspective

Most studies have been conducted using subtype B gp120 and since subtype C is the predominant HIV-1 subtype worldwide, as well as in the heterosexual population in South Africa [15, 254], additional research on this subtype is required. The overall aim of this project is to evaluate and compare the ability of recombinant subtype B and C R5 Env glycoproteins to mediate apoptosis of Jurkat T lymphocytes via gp120-CD4 signalling and of CD4+ T lymphocytes via gp120-CD4 and co-receptor CCR5 signalling.

This was achieved through the following objectives:

1. To express, purify and characterize the R5 HIV-1 subtype B and C recombinant monomeric gp120 from isolates BaL ($gp120^{BaL}$) and 96ZM651 ($gp120^{ZM651}$) as well as the trimeric/oligomeric Ancestral subtype C gp140 ($gp140^{AncC}$).
2. To evaluate the ability of the purified recombinant $gp120^{BaL}$, $gp120^{ZM651}$ and $gp140^{AncC}$ to induce apoptosis of HIV-1 uninfected Jurkat T lymphocytes via engagement with the CD4 receptor, using flow cytometry.
3. To examine the contribution of CD4 and/or CCR5 receptor engagement with the purified recombinant $gp120^{BaL}$, $gp120^{ZM651}$ and $gp140^{AncC}$ on triggering apoptosis of HIV-1 uninfected enriched CD4+ T lymphocytes [isolated from peripheral blood mononuclear cells (PBMC's)], using flow cytometry.

CHAPTER 2: MATERIALS AND METHODS

2.1 Mammalian cell lines, bacterial cell lines, expression plasmids, recombinant proteins and antibodies used in this study

Human Embryonic Kidney (HEK) 293T adherent cells were available in our laboratory, and used for the expression of the recombinant HIV-1 Env glycoproteins. The human T cell leukemic, Jurkat Clone E6-1 (Jurkat T lymphocytes) suspension cell line was purchased from Highveld Biologicals, Catalogue number: 177 (South Africa), and used to determine Env-mediated apoptosis via CD4 binding. CD8 depleted CD4+T lymphocytes were isolated from fresh buffy coats purchased from the South African National Blood Bank Services (SANBS), and each donor was used seperately to determine Env-mediated apoptosis via CD4 and co-receptor binding (buffy preparations were not pooled) . (No ethics was required for the use of the buffy coats from the SANBS (see ethics waiver in Appendix B). All mammalian cell lines were incubated in a water jacketed 37°C, 5% CO_2 incubator.

Escherichia coli (E .coli) DH5α cells were available for use in our laboratory, and used in the transformation experiments and preparation of Env expression plasmids.

Env expression plasmids used in this study are described in Table 2.1 and the commercially available HIV-1 recombinant Env glycoproteins that were used in the Enzyme-Linked Immunosorbent Assays (ELISAs) are described in Table 2. 2.

Affinity purified sheep anti-HIV-1 gp120 (D7324; Aalto Bio Reagents Ltd, Ireland) was used to coat 96-well ELISA plates (Nunc, Roskilde, Denmark) for the capture of $gp120^{BaL}$, $gp120^{ZM651}$ and $gp140^{AncC}$ in the capture ELISAs. The primary and secondary antibody probes used in the ELISAs for the conformational and functional analyses of the purified recombinant glycoproteins are described in Table 2.3. In addition, the antibodies used in the Western Blot analyses are described in Table 2.4.

Table 2.1: Expression plasmids used for the transient expression and purification of monomeric and trimeric/oligomeric recombinant HIV-1 Env glycoproteins.

EXPRESSION PLASMID	CATALOGUE NUMBER	AKNOWLEDGEMENT	PURPOSE IN THE STUDY
HIV-1 p96ZM651gp120-CD5-opt (subtype C) expression plasmid	8661	Obtained from the NIH AIDS Research and Reference Reagent Program, Division of AIDS, NIAID, NIH: p96ZM651gp120-CD5-opt from Drs Yingying Li, Feng Gao and Beatrice H. Hahn	Transient expression and purification of monomeric recombinant 96ZM651gp120 ($gp120^{ZM651}$)
HIV-1 pciNEO-BaLgp120 (subtype B) expression plasmid	N/A	Available in our laboratory	Transient expression and purification of monomeric recombinant BaLgp120 ($gp120^{BaL}$)
Ancestral subtype C gp140 expression plasmid	N/A	Obtained from Dr Richard Wyatt, Vaccine Research Centre, NIH	Transient expression and purification of trimeric/oligomeric recombinant gp140 ($gp140^{AncC}$)
Empty pcDNA 3.1 expression plasmid (mock control)	N/A	Available in our laboratory	Transient expression and purification of a mock control which was used in apoptosis assays.

Table 2.2: Recombinant proteins used in the ELISAs and Western Blot analyses.

RECOMBINANT PROTEINS	CATALOGUE NUMBER	AKNOWLEDGEMENT	PURPOSE IN THE STUDY
HIV-$1_{96ZM651}$gp120	10080	Obtained from the NIH AIDS Research and Reference Reagent Program, Division of AIDS, NIAID, NIH: HIV-$1_{96ZM651}$gp120 from DAIDS, NIAID	Positive control in Western blots and ELISAs
HIV-1_{BaL}gp120	4961	Obtained from the NIH AIDS Research and Reference Reagent Program, Division of AIDS, NIAID, NIH: HIV-1_{BaL}gp120 from DAIDS, NIAID	Positive control in Western blots and ELISAs
Full length soluble CD4 (sCD4)	N/A	Obtained from Progenics Pharmaceuticals Inc. Lot# 63	Confirm CD4 binding of recombinant $gp120^{ZM651}$ in CD4 binding ELISAs
Wild type two domain soluble CD4 (wt2dsCD4)	N/A	Available in our laboratory	Conformational analysis of the recombinant HIV-1 Env glycoproteins using capture ELISAs

Table 2.3: Primary and secondary antibodies used in the ELISAs

ANTIBODIES	CATALOGUE NUMBER	ACKNOWLEDGEMENT	PURPOSE IN THE STUDY
Human HIV-1 gp120 Monoclonal antibody (MAb) (IgG1 b12)	2640	Obtained from the NIH AIDS Research and Reference Reagent Program, Division of AIDS, NIAID, NIH: HIV-1 gp120 MAb (IgG1 b12) from Dr. Dennis Burton and Carlos Barbas	Primary antibody used in capture ELISAs
Human HIV-1 gp120 MAb (17b)	4091	Obtained from the NIH AIDS Research and Reference Reagent Program, Division of AIDS, NIAID, NIH: HIV-1 gp120 MAb (17b) from Dr. James E. Robinson	Primary antibody used in capture ELISAs
Human HIV-1 gp120 MAb (2G12)	1476	Obtained from the NIH AIDS Research and Reference Reagent Program, Division of AIDS, NIAID, NIH: HIV-1 gp120 MAb (2G12) from Dr. Hermann Katinger	Primary antibody used in capture ELISAs
Human HIV-1 gp120 MAb (48D)	1756	Obtained through the NIH AIDS Research and Reference Reagent Program, Division of AIDS, NIAID, NIH: HIV-1 gp120 MAb (48d) from Dr. James E. Robinson	Primary antibody used in CD4 binding ELISAs
ECL™ Anti-human IgG Horseradish peroxidase (HRP)-linked whole antibody (from sheep)	NA933V	Obtained from GE Healthcare UK Limited, Little Chamfont Buckinghamshire, England	Secondary antibody used in all ELISAs

Table 2.4: Antibodies used during Western Blot Analyses for the detection of recombinant HIV-1 Env glycoproteins.

ANTIBODIES	CATALOGUE NUMBER	AKNOWLEDGEMENT
HIV positive plasma 16 and 20 (primary antibody used)	N/A	Obtained from SANBS
Anti-human IgG (Fc specific) Alkaline phosphatase conjugate (from goat) (secondary antibody used)	A-9544	Obtained from Sigma-Aldrich, Steinheim, Germany

All antibodies used in the flow cytometric analyses (shown below in Table 2.5) were obtained from Beckman Coulter Inc, Fullerton, CA, USA.

Table 2.5: Flow cytometry antibodies used during the detection of early/late apoptosis and DNA fragmentation.

ANTIBODIES	PART NUMBER	PURPOSE IN THE STUDY
R-Phycoerythrin (PE)-labelled anti-CD4 antibody probe (IOTest® CD4-PE) (CD4-PE)	IM0449U	Confirm the presence of CD4+ lymphocytes (from blood and Jurkat T lymphocytes)
Phycoerythrin-Texas Red-X (ECD)-labelled CD8 antibody(Cyto-Stat®/Coulter Clone®T8-ECD) (CD8-ECD)	6604728	Confirm the depletion of CD8+ T lymphocytes
Phycoerythrin-Cy7 (PC7)-labelled CD3 antibody (IOTest® CD3-PC7) (CD3-PC7)	6607100	Used for the selection of CD3+ CD4+ CD8- T lymphocytes

2.2 Isolation of $gp120^{BaL}$, $gp120^{ZM651}$ and $gp140^{AncC}$ plasmid DNA

2.2.1 Production of competent *E. coli* DH5α cells

Under sterile conditions, 10µl of *E. coli* DH5α cells were added to 10ml of Luria Bertani (LB) broth (Appendix A.1) incubated in a shaking incubator overnight at 37°C and subsequently diluted 40 times with fresh LB broth before being incubated at 37°C

for another hour in a shaking incubator. This was to allow optimal growth and to obtain an optical density of 0.4 at 600nm. Cell cultures were centrifuged at 300xg for 10 minutes at 4°C, the cell pellet was resuspended in 10ml of ice-cold transformation buffer (Appendix A.1), incubated on ice for 30 minutes and centrifuged again at 300xg for 10 minutes at 4°C. Finally, the supernatant was discarded and the bacterial cell pellet was resuspended in 1ml of ice-cold transformation buffer. Competent *E. coli* DH5α cells were stored at -80°C in 100µl aliquots until required for use.

2.2.2 Bacterial transformation with Env expression plasmids

Under sterile conditions, 2µl of each Env expression plasmid ($gp120^{BaL}$, $gp120^{ZM651}$ or $gp140^{AncC}$) was incubated with 25µl of competent *E. coli* DH5α cells for 30 minutes on ice. The mixture was then heat shocked in a 42°C water bath for 90 seconds and 200µl of LB broth was added to the cells. The cells were incubated at 37°C in a shaking incubator for an hour before being spread onto LB agar plates containing 100µg/ml ampicillin (Appendix A.1.) using a sterile glass rod. The plates were then incubated overnight at 37°C. Ampicillin resistant, transformed *E. coli* DH5α cells (those containing the plasmids) grew as single colonies on the agar plate and a single bacterial colony was picked off the plate, inoculated into 250ml of fresh LB broth containing 100µg/ml ampicillin and incubated on a shaker at 37°C overnight. Glycerol stocks of $gp120^{BaL}$, $gp120^{ZM651}$ and $gp140^{AncC}$ transformed *E. coli* DH5α cells were produced under sterile conditions and stored in cryovials (Nunc, Roskilde, Denmark)

at -80°C until required for use. Briefly, 200µl of 100% glycerol (Merck, Hohenbrunn, Germany) was added to 800µl of each culture, and mixed well. The glycerol protects the bacterial cells from being punctured and killed by ice crystals that form in the LB broth during freezing.

2.2.3 Large scale expression plasmid preparations

Recombinant $gp120^{BaL}$, $gp120^{ZM651}$ and $gp140^{AncC}$ expression plasmids were extracted from the overnight cultures produced (mentioned in section 2.2.2), using a Qiagen QIAfilter™ Plasmid Maxi Kit (Qiagen, Maryland, USA) according to the manufacturer's instructions. Briefly, the overnight cultures were centrifuged at 6000xg for 15 minutes and the pellet was resuspended in Buffer P1 (Appendix A.1.2) to produce a homogenous mixture. Buffer P2 (Appendix A.1.2) was then added to the homogenous mixture to lyse and denature the bacterial cells for the release of the plasmids, subsequently mixed vigorously and incubated at room temperature for 5 minutes before chilled buffer P3 (Appendix A.1.2) was added. Buffer P3 neutralizes and renatures the plasmid DNA.

After vigorously inverting a few times, the lysate was poured into QIAfilter™ maxi cartridges and incubated at room temperature for 10 minutes. During this time, a QIAGEN-tip 500 was equilibrated with QBT buffer (Appendix A.1.2) by gravity flow to prepare the column for plasmid DNA binding. The cap at the outlet nozzle of the

QIAfilter^{TM} cartridge was removed and the plunger was gently inserted into the filter allowing the cell lysate to be filtered through the previously equilibrated QIAGEN-tip 500. The cell lysate filtered through the resin by gravity flow and the QIAGEN-tip 500 was then washed twice with buffer QC (Appendix A.1.2). The plasmid DNA was then eluted with buffer QF (Appendix A.1.2) and precipitated by the addition of isopropanol (Merck, Hohenbrunn, Germany). After mixing the eluted DNA in the isopropanol, the plasmid DNA was centrifuged at 15000xg for an hour at 4°C. The supernatant was carefully discarded and the pellet was washed with room temperature 70% ethanol (Merck, Hohenbrunn, Germany) (Appendix A.1) and centrifuged again at 15000xg for 30 minutes at 4°C.

The supernatant was carefully discarded and the pellet was air dried completely before being dissolved in sterile Sabax water (sH_2O) (Dismed Criticare, Midrand, South Africa). The concentration of the isolated recombinant gp120^{BaL}, gp120^{ZM651} and gp140^{AncC} plasmid DNA was measured spectrophotometrically (Nanodrop Technologies Inc; Wilmington, DE) and stored at -20ºC until used for the transfections of mammalian HEK 293T cells.

The isolated recombinant gp120^{BaL}, gp120^{ZM651} and gp140^{AncC} plasmids DNA were resolved on 0.8% agarose (Sigma-Aldrich, Steinheim, Germany) gels (Appendix A.1.3) submerged in 1XTris-Acetate-EDTA (TAE) buffer (Appendix A.1.3) using the Bio-Rad Gel Tank System (Bio-Rad; Hercules, CA). Each DNA sample, including the

O' GeneRuler^{TM} DNA ladder mix (range 50bp-10kb) (Fermenta, Ontario, Canada), was mixed with 6X DNA loading buffer (Appendix A.1.3) before being loaded into the wells in the gel. The gels were resolved at a current of 100V for approximately 1.5 hours and subsequently visualized under UV light using the Versadoc^{TM} Imaging System (Bio-Rad; Hercules, CA) to ensure that the expression plasmids were present and not degraded.

2.3 Expression of recombinant gp120^{BaL}, gp120^{ZM651} and gp140^{AncC} using mammalian HEK 293T cells

2.3.1 Maintenance of HEK 293T cell lines

The HEK 293T adherent cell line was propagated in 75cm^3 flasks (Nunc, Roskilde, Denmark) and maintained in complete Dulbecco's Modified Eagle Medium (DMEM) (Sigma-Aldrich, Steinheim, Germany) [DMEM supplemented with 10% heat-inactivated fetal calf serum (FCS) (Gibco; Grand Island, USA), L-Glutamine (200nM) (Gibco; Grand Island, USA), Penicillin (1000µg/ml) and Streptomycin (1000µg/ml) (Gibco; Grand Island, USA)].

HEK 293T cells were split when confluent, and diluted as required. The complete DMEM was discarded and the cells were washed with 5ml of 1X Dulbecco's Phosphate Buffered Saline (PBS) (no calcium chloride and magnesium chloride) (Sigma-Aldrich, Steinheim, Germany) and trypsinized with 1ml of 0.25%

Trypsin/EDTA (Sigma-Aldrich, Steinheim, Germany) for one minute at room temperature and then for 2-5 minutes in a 37°C incubator. Thereafter, 10ml of complete DMEM was added to inactivate the trypsin (FCS inactivates trypsin) and to gently resuspend the cells and disperse any clumps. Finally, the cells were diluted ten times (or as required) in fresh complete DMEM: 9ml of cells were discarded or transferred as 1ml aliquots into new 75cm^3 flasks, and 9ml of fresh complete DMEM were added to each ml of split cells.

2.3.1.1 HEK 293T cell stocks

HEK 293T cell stocks were prepared in a filter sterilized (0.22 µM Acrodisc® 25 mm syringe filters; Pall Corporation, Ann Arbor, USA) freezing mix (Appendix A.2). Briefly, trypsinized cells were resuspended in complete DMEM, centrifuged at 200xg for 10 minutes and subsequently resuspended in freezing mix, ensuring that there were 1X10^6 cells/ml. Cell stocks were transferred into the Nalgene^{TM} Cryo 1ºC freezing container (USA) and stored at -80ºC overnight to ensure a -1ºC/min rate of cooling. The isopropanol within the freezing container was replaced each time before use. Finally, the cell stocks were transferred into a separate storage container at -80ºC for short storage periods or into liquid nitrogen for longer storage periods. HEK 293T cell lines were discarded after 20 passages, and new cell lines were propagated from frozen cell stocks.

2.3.1.2 HEK 293T cell counting

Trypsinised HEK 293T cells were counted using trypan blue solution (Sigma-Aldrich; Steinheim, Germany) on a haemocytometer to ensure cell viability and that the appropriate numbers of cells were used in the various assays. The cells were diluted five times with 0.4% trypan blue solution, counted under an inverted light microscope and the average number of cells was obtained. The average was then multiplied by the dilution factor (5) and divided by the volume of the haemocytometer ($1 \text{ X } 10^{-4} \text{ cm}^3$) to obtain the amount of cells/ml. The number of cells/ml was then multiplied by the total volume of cells collected to obtain the final amount of cells.

2.3.2 Optimisation of transfection conditions in HEK 293T mammalian cells

At approximately 70-80% confluency, HEK 293T cells were split (as outlined in section 2.3.1), counted (as outlined in section 2.3.1.2), seeded at $2.5 \text{ x } 10^6$ cells in 20ml of complete DMEM within a 75cm^3 flask and transfected 24 hours later with recombinant $gp120^{BaL}$ or $gp120^{ZM651}$ expression plasmids using either Calcium Chloride ($CaCl_2$) (Appendix A2.1) or Polyfect® transfection reagent (Qiagen, Maryland, USA). Optimal transfection condition for $gp140^{AncC}$ are already established in our laboratory (using the Polyfect® transfection reagent), thus experiments for this protein were not repeated.

2.3.2.1 Transfections using $CaCl_2$

When using $CaCl_2$, 62.5µl of 2.5M $CaCl_2$ (Appendix A.2.1) and 500µl of 2X HEPES solution (Appendix A.2.1) was added to 10µg of recombinant plasmid DNA (either $gp120^{BaL}$ or $gp120^{ZM651}$) and the mixture was subsequently made up to a total of 1ml with sH_2O. The transfection complexes were then incubated at room temperature for 15-20 minutes before being added to the medium in a drop-wise manner. The medium was then gently swirled over the surface of the adherent cells. A negative control was prepared in the exact same manner, but with the absence of plasmid DNA. The complete DMEM was replaced with 20ml of fresh medium 24 hours later and the cells were incubated for a further 48 hours before the DMEM containing the secreted proteins was harvested i.e. harvested at 72 hours. Since the proteins were secreted into the cell medium, supernatant samples (50µl) were taken at 24, 48 and 72 hours for the detection of protein expression by Sodium Dodecyl Sulphate–Polyacrylamide Gel Electrophoresis (SDS-PAGE) and Western blot analyses.

2.3.2.2 Transfections using the Polyfect reagent

When using the Polyfect® transfection reagent, 8µg of either $gp120^{BaL}$ or $gp120^{ZM651}$ was combined with 80µl of the Polyfect® transfection reagent and 300µl of incomplete DMEM (no additives). The combinations were incubated for 15 minutes at room temperature to allow the formation of transfection complexes and 1ml of

complete DMEM was subsequently added. The complexes were added to the culture medium of each flask, followed by gentle swirling of the medium over the surface of the adherent cells. A negative control was also prepared, as mentioned above in section 2.3.2.1. The procedure here after was performed in the exact same manner as in the $CaCl_2$ transfections (section 2.3.2.1). Culture supernatant were harvested at 72 hours and supernatant samples (50µl) were taken at 24, 48 and 72 hours for the detection of protein expression by SDS-PAGE and Western blot analyses.

2.3.3 SDS-PAGE and Coomassie staining

SDS-polyacrylamide gels (8%) comprising of an upper stacking and lower resolving gel component (Appendix A.3) were produced. Each sample (samples taken during the transfections or protein purification processes) (30µl) was combined with 2X loading buffer (30µl) (Appendix A.3), boiled for 5 minutes and cooled before being loaded onto duplicate SDS-polyacrylamide gels. The gels were submerged in running buffer (Appendix A.3) and exposed to a current of 10mA/gel until the dye front had passed through the stacking gel (for approximately 1 hour). The current was then increased to 20mA/gel and the gels were resolved over a period of 2 hours using the Amersham Biosciences Electrophoresis power supply EPS 301 power box. One of the resolved SDS-polyacrylamide gels was stained with Coomassie® Brilliant Blue R250 (Sigma-Aldrich; Steinheim, Germany) (Appendix A.5) overnight at room temperature with gentle shaking. Staining was followed by the addition of a destaining

buffer (40% Methanol and 7% Acetic Acid) (Appendix A.5) which was incubated with the gel while gently shaking until it turned clear. The clear SDS-polyacrylamide gel was visualized under white light and photographed with the Versadoc™ Imaging System (Bio-Rad; Hercules, CA) under white epiluminescence.

2.3.4 Western blot analysis

The second SDS-polyacrylamide gel was used for western blot analysis. All steps were carried out at room temperature. The gel, filter paper (Pierce, USA) and Hybond™-C-Extra nitrocellulose membrane (Amersham Biosciences UK Limited, Little Chatfont, England) were simultaneously equilibrated with transfer buffer (Appendix A.4) with gentle shaking at room temperature for 15 minutes. The proteins on the SDS- polyacrylamide gel were transferred onto the nitrocellulose membrane (Amersham Biosciences) using the Trans-Blot SD Semi-Dry Transfer Cell System (Bio-Rad, Hercules, CA) at a constant current of 250V, applied for 75 minutes. The membrane was subsequently blocked with 5% Blotting Grade Blocker (non-fat dry milk) (Biorad, Hercules, CA) in 50ml of 1X Tris-buffered saline (TBS) containing 0.1% Tween-20 (T-TBS) (Appendix A.4) overnight, and subsequently washed with 1X T-TBS 3 times for 5 minutes each by moderate shaking. The membrane was then incubated with 50ml of 1X T-TBS containing 0.5% Bovine Serum Albumin (BSA) (Appendix A.4) and a 1:2000 dilution of the primary antibody, pooled human sera 16 and 20 for 2 hours. The membrane was washed 3 times with 1X T-TBS for 5 minutes

each wash, was and then probed with the secondary Anti-human IgG (Fc specific) Alkaline phosphatase conjugate antibody (Sigma-Aldrich, Steinheim, Germany) at a 1:30000 dilution in 30ml of 1X T-TBS containing 0.5% BSA for one hour. Finally, the membrane was washed 3 times with 1X T-TBS for 5 minutes each, and incubated with 2.5ml of the NBT/BCIP (Roche, Mannheim, Germany) solution (Appendix A.4) in the dark until the protein bands were visible. The reaction was terminated upon the addition of sH_2O (Dismed Criticare). The western blot was photographed with the Versadoc^{TM} Imaging System (Bio-Rad; Hercules, CA) under white epiluminescence.

All further transfection experiments using gp120^{BaL}, gp120^{ZM651} and gp140^{AncC} were performed using the Polyfect® transfection reagent as described in section 2.3.2.2.

2.4 Purification and concentration of recombinant gp120^{BaL}, gp120^{ZM651} and gp140^{AncC} Env glycoproteins

The expression of all three recombinant Env glycoproteins including a mock control (empty expression plasmid) was upscaled using the Polyfect® transfection reagent. During large scale Polyfect transfections, 293 Serum-Free media (SFM II) (Gibco; Grand Island, USA) (containing only 200nM L-Glutamine) was used as the replacement medium instead of complete DMEM, at 24 hours post transfection. The absence of serum proteins or antibiotics eliminates any cause of interference with the subsequent purification of the recombinant proteins. The harvested media from

transfections of each recombinant protein was clarified by centrifugation at 4000xg for 10 minutes at 4°C, pooled and stored at -20ºC until purified (maximum of 3 days).

2.4.1 The preparation of the column and purification procedure

The Bio-Rad Biologic LP chromatography system (Bio-Rad, Hercules, CA) was used for the recombinant Env glycoprotein purification process. For each purification process, 200ml volumes of the clarified cell supernatants containing the expressed Env glycoprotein ($gp120^{BaL}$, $gp120^{ZM651}$ or $gp140^{AncC}$) and supernatants from mock transfected cells were each purified using *Galanthus nivalis* lectin (Sigma-Aldrich, Steinheim, Germany) [255]. This can be accomplished due to the highly glycosylated external front of gp120, which possesses a high affinity for the lectin sugar residues. For preparation of the column, the lectin was resuspended in 1X PBS before being packed into a 2ml column (Sigma-Aldrich, Steinheim, Germany). Before loading the supernatant samples ($gp120^{BaL}$, $gp120^{ZM651}$**,** $gp140^{AncC}$ or mock control) onto the lectin column, the column was washed and equilibrated with 10ml of 1X PBS. The supernatant samples were pumped through an adaptor and onto the column at a flow rate of 2ml/minute. Once the sample had been loaded onto the column, the column was subjected to two washing buffers (1X PBS and 1M NaCl) (Appendix A2.2) for 75 minutes at 2.5ml-3.5ml/min and finally the lectin-bound glycoprotein ($gp120^{BaL}$, $gp120^{ZM651}$ or $gp140^{AncC}$) was eluted from the column using a 50ml 0.75M methyl α-D-mannopyranoside (MMP) (Sigma-Aldrich, Steinheim, Germany) solution (Appendix

A2.2) at a flow rate of 2.5ml/minute. In addition, the mock control supernatant was purified in the same manner. Separate lectin columns were used for each $gp120^{BaL}$, $gp120^{ZM651}$**,** $gp140^{AncC}$ or mock Env preparation to prevent cross contamination of proteins.

2.4.2 Dialysis and concentration of the eluted recombinant Env glycoproteins

The eluted Env glycoproteins ($gp120^{BaL}$, $gp120^{ZM651}$ or $gp140^{AncC}$) and mock samples were transferred into Snakeskin® Pleated dialysis tubing (Thermo Scientific, Rockford, IL, USA) and dialyzed overnight in 2L of ice-cold 1X PBS at 4°C, with stirring. The following day, the 2L of 1X PBS was replaced with 2L of fresh, ice-cold 1X PBS and the Env glycoproteins and mock samples were dialyzed for a further 2-3 hours and subsequently concentrated in Amicon® Ultra-15 Centrifugal Filter devices (Molecular Weight cut off 50 kDA) (Millipore, Billerica, MA) by centrifugation at 4000x g for 3 min at 4°C. The Amicon® Ultra-15 Centrifugal Filter devices were equilibrated with 15ml of ice-cold 1X PBS before concentrating the eluted samples ($gp120^{BaL}$, $gp120^{ZM651}$**,** $gp140^{AncC}$ or mock control). Excess amounts of MMP bound to the purified, concentrated Env glycoproteins or mock control was removed by centrifugation in ice-cold 1X PBS at 4000x g for 3 min at 4°Cand subsequently aliquoted and stored at -80ºC until required.

After every purification process, the lectin column was rinsed with 0.01% Sodium Azide (Sigma-Aldrich, Steinheim, Germany) (Appendix A2.2) to prevent the risk of contamination. The entire protein purification process was monitored by obtaining 50µl aliquots of the clarified cell supernatants, flow through, washes, elutions and concentrated Env glycoprotein and mock control samples for SDS-PAGE and Western Blotting analyses (as described in Sections 2.3.3 and 2.3.4).

2.5 Quantification of the recombinant $gp120^{BaL}$, $gp120^{ZM651}$ and $gp140^{AncC}$

The recombinant $gp120^{BaL}$, $gp120^{ZM651}$ and $gp140^{AncC}$ Env glycoproteins were quantified using the Pierce BCA™ protein assay kit (Thermo Scientific, Rockford, IL, USA) and the procedure was performed as per manufacturer's instructions. Briefly, Bovine Serum Albumin (BSA) standards (500µg/ml, 250µg/ml, 125µg/ml, 62.5µg/ml, 31.25µg/ml, 15.625µg/ml, 7.8125µg/ml and 0µg/ml) were prepared in 1X PBS for the establishment of a standard curve. The standards (25µl) were added to a maxisorp ELISA plate (Nunc, Roskilde, Denmark) in duplicate. The concentrated $gp120^{BaL}$, $gp120^{ZM651}$ and $gp140^{AncC}$ samples were diluted 5 times in 1X PBS and 25µl was added to the ELISA plate in triplicate. In addition, the blank sample (1X PBS) was added to the ELISA plate in triplicate. A developing solution containing a 50:1 ratio of reagent A and B (Appendix A2.2) was prepared and 200µl was added to each sample in the plate. The ELISA plate was then incubated for 2 hours at 37°C in the dark with

gentle shaking and subsequently read by the Microplate reader Model 680 (Bio-Rad, Hercules, CA) at an absorbance of 570nm. The absorbance readings were averaged and used to create a standard curve from which the concentration of recombinant $gp120^{BaL}$, $gp120^{ZM651}$ and $gp140^{AncC}$ was obtained.

2.6 Conformational and functional assessments of the recombinant $gp120^{BaL}$, $gp120^{ZM651}$ and $gp140^{AncC}$ Env glycoproteins

The conformational and functional integrity of the purified recombinant $gp120^{BaL}$, $gp120^{ZM651}$ and $gp140^{AncC}$ was evaluated by their ability to bind MAb's IgG1b12, 2G12 and 17b in the presence and absence of 2dWtsCD4, in capture ELISAs.

A 96-well maxisorp ELISA plate (Nunc, Roskilde, Denmark) was coated for 3 hours at room temperature with 100µl/well of an Affinity purified sheep anti-HIV-1-gp120 antibody (D7324) at a concentration of 1µg/ml in 1X PBS. The wells were emptied on paper toweling, before being blocked with 250µl/well of 1X PBS containing 0.05% Tween-20 and 10mg/ml Bovine Serum Albumin (PBS-T-BSA) (Appendix A.6) overnight at 4ºC. The blocking solution was removed by washing the plate 5 times with 1X PBS containing 0.1% Tween-20 (PBS-T) (Appendix A.6) and the wells were then incubated for 3 hours at room temperature with 100µl/well of either recombinant $gp120^{BaL}$, $gp120^{ZM651}$ or $gp140^{AncC}$ at final concentrations of 500ng/ml, 100ng/ml,

20ng/ml, and 4ng/ml (obtained by 5-fold dilutions of each recombinant protein in PBS-T).

Recombinant $gp120^{BaL}$, $gp120^{ZM651}$ or $gp140^{AncC}$ analysed for 17b binding in the presence of 2dWtsCD4 were produced at final concentrations of 1000ng/ml, 200ng/ml, 40ng/ml, and 8ng/ml (obtained by 5-fold dilutions of each recombinant protein in PBS-T) and incubated with equal volumes of 2dWtsCD4 (2µg/ml) to ensure final concentrations of 500ng/ml, 100ng/ml, 20ng/ml, and 4ng/ml. This combination was incubated at room temperature for one hour before being added to the ELISA plate. Each protein concentration was analysed in duplicate. After washing the plate 5 times with PBS-T, primary antibody probes IgG1b12, 2G12 and 17b were diluted 1000 times in PBS-T, added to the relevant wells (100µl/well) and incubated for 2 hours at room temperature. Unbound primary antibody probes were removed by washing 5 times with PBS-T. After washing, the ECL™ Anti-human IgG Horseradish peroxidase (HRP)-linked whole antibody probe was diluted 2000 times in PBS-T and 100µl was added to all the wells. The ELISA plate was then incubated for 1 hour at 4ºC. Unbound secondary antibodies were removed by washing 5 times with PBS-T and 100µl of the 1 step ™ Ultra-TMB-ELISA substrate (Thermo scientific, Rockford, IL) was then added to each well and allowed to develop in the dark for approximately 15-30 minutes. The blue reaction was terminated by the addition of 50µl of 2mM sulphuric acid (H_2SO_4) (Appendix A.6) resulting in the production of a yellow colour. The plate was read on the Microplate reader Model 680 (Biorad) at an absorbance of

450nm. This experiment was performed three times and similar results were obtained each time.

All three recombinant Env glycoproteins were purified, quantified and characterised throughout the course of the study, as required.

2.7 Confirmation that gp120^{ZM651} is able to bind CD4 efficiently

The CD4 binding function of gp120^{ZM651} was further confirmed in a CD4 binding ELISA. The 96-well maxisorp ELISA plate was coated for 3 hours at room temperature with 100µl/well of full length sCD4 at a concentration of 1µg/ml in 1X PBS. The sCD4 was removed and the wells were blocked overnight with 250µl/well of 1X PBS-T-BSA (Appendix A.6) at 4ºC. The wells were then washed 5 times with PBS-T and 100µl of gp120^{ZM651}, gp120^{BaL}, gp140^{AncC}and HIV-1$_{96ZM651}$gp120 was added to each well in triplicate at a single concentration of 500ng/ml and incubated for 2.5 hours at room temperature. After washing the plate 5 times with PBS-T the human primary antibody probe 48D was diluted 500 times with PBS-T and 100µl was added to each well and incubated for 2 hours at room temperature. Any unbound primary antibody was removed by washing 5 times with PBS-T. Thereafter, the ECL^{TM} Anti-human IgG Horseradish peroxidase (HRP)-linked whole antibody was diluted 2000 times in PBS-T, and 100µl was added to the respective wells and incubated for 1 hour at 4ºC. After washing 5 times with PBS-T, the reactions were developed and

the absorbance readings were measured using the method described in section 2.6. This experiment was performed three times and the results were consistent each time.

2.8 Recombinant $gp120^{BaL}$, $gp120^{ZM651}$ and $gp140^{AncC}$-mediated apoptosis of uninfected Jurkat T lymphocytes

2.8.1 Maintenance of Jurkat T lymphocyte cell lines

Jurkat T lymphocytes were propagated in 25cm^3 flasks (Nunc, Roskilde, Denmark) while being maintained in complete RPMI-1640 (Sigma-Aldrich; Steinheim, Germany), [RPMI-1640 supplemented with 10% heat-inactivated FCS, L- glutamine (200nM), Penicillin (1000µg/ml) and streptomycin (1000µg/ml)] (Appendix A.2). When viable Jurkat T lymphocyte densities were above $1x10^6$cells/ml, the lymphocytes were diluted and re-seeded at $2x10^5$cells/ml. Briefly, suspension Jurkat T lymphocytes were gently vortexed to disperse clumps, and the appropriate volumes of lymphocytes were subsequently transferred into new 25cm^3 flasks and made up to 10ml with fresh complete RPMI-1640 media.

2.8.2 Jurkat T lymphocyte stocks and cell counting

Jurkat T lymphocyte stocks were prepared in a filter sterilised freezing mix (Appendix A.2). The lymphocytes were centrifuged at 200xg for 10 minutes and subsequently

resuspended in freezing mix, ensuring that there was $1x10^6$ cells/ml. The protocol hereafter was performed in the exact same manner as mentioned in section 2.3.1.1. Jurkat T lymphocyte cell lines were discarded after 20 passages, and new cell lines were propagated from frozen cell stocks. Jurkat T lymphocytes were counted using trypan blue solution on a haemocytometer as explained in section 2.3.1.2.

2.8.3 Establishment of a flow cytometric protocol for the analysis of early and late apoptosis of Jurkat T lymphocytes by Annexin V and 7-AAD staining

The Cytomics FC500 (Beckman Coulter) five colour flow cytometer was used in all flow cytometric analyses. The machine was calibrated daily with fluorescently labeled beads (Beckman Coulter Inc, Fullerton, CA, USA) to ensure that the lasers were aligned properly, and washed appropriately after use, as per training instructions. Choosing the relevant parameters, a protocol to measure early and late apoptosis in Jurkat T lymphocytes using Annexin V and 7-amino-Actinomycin D (7-AAD) staining was established and optimized. The FL1 channel was used for the detection of Annexin V-FITC while 7-AAD was detected in the FL4 channel. Therefore, the protocol included a forward scatter (FSC) (measures cell size) versus side scatter (SSC) (measures cell granularity/complexity) dot plot to visualise and characterise the entire population of Jurkat T lymphocytes, an Annexin V versus 7-AAD dot plot, and corresponding histograms for the analysis of Annexin V and 7-AAD staining. The appropriate channels and voltages were established by positioning the viable Jurkat T

lymphocytes in the correct quadrant for the dot plot (which measure 2 parameters) and to ensure that the negative peaks in the histograms (which measure 1 parameter) were within the first decade. Ultimately, the total number of events acquired for 200 seconds was used as the cut off, and these settings were kept constant in all flow cytometric protocols.

Untreated and 4µM Camptothecin (Sigma-Aldrich, Steinheim, Germany) (pro-apoptotic agent used as a positive control)-treated Jurkat T lymphocytes ($1x10^6$cells/ml) were processed in order to establish baselines to which the recombinant Env glycoprotein-treated samples would be compared. Camptothecin is a highly toxic chemical compound that induces apoptosis in a dose dependent manner by inhibiting the DNA topoisomerase I enzyme during DNA synthesis [256, 257].

2.8.4 Flow Cytometric analysis of early and late apoptosis

Initially, apoptosis experiments were established using only recombinant $gp120^{BaL}$ and $gp120^{ZM651}$. Jurkat T lymphocytes ($1x10^6$cells/ml) were seeded in a 24-welled plate (Nunc, Roskilde, Denmark) and either untreated (negative control) or treated with 4µM Camptothecin (Appendix A.8), 50nM of recombinant $gp120^{BaL}$ or $gp120^{ZM651}$ and incubated in a water jacketed 37°C, 5% CO_2 incubator until sampled. Samples (500µl) were taken at 0 (baseline), 24 and 48 hours. For each batch of samples at

different time points, an untreated stained, 4µM Camptothecin-treated, $gp120^{BaL}$ and $gp120^{ZM651}$-treated samples were analysed by Annexin V and 7-AAD staining.

2.8.4.1 Annexin V and 7-AAD staining

The Annexin V-FITC/7-AAD kit (Beckman Coulter Inc, Fullerton, CA, USA) was used to measure early and late apoptosis (2 parameters), according to manufacturers' instructions. A cell that is undergoing early apoptosis is physiolocially different to a cell that is undergoing late apoptosis. Early apoptosis is characterised by externalised phosphotidyl serine residues in the phospholipid bilayer of the cell membrane while late apoptosis is characterised by DNA fragmentation and the formation of apoptotic bodies [258, 259]. Annexin V is a calcium-dependent phospholipid binding protein that is able to detect these phosphotidyl serine residues [258, 259], which can be fluorescently labeled with Annexin V that is conjugated to FITC. Seven-AAD on the other hand, is a fluorescent dye that is able to pass through cell membranes that have lost their integrity and structure and stain nucleic acids [260]. When used together, Annexin V and 7-AAD staining can be analysed simultaneously to detect early and late apoptosis/necrosis [260]. Jurkat T lymphocytes that stain positive for Annexin V only (Ann V+/7-AAD-) are undergoing early apoptosis while, those that stain positive for both Annexin V and 7-AAD (Ann V+/7-AAD+) are undergoing late apoptosis and possibly early necrosis. Viable Jurkat T lymphocytes stain negative for both Annexin V and 7-AAD (Ann V-/7-AAD-) and the completely necrotic lymphocytes stain positive

for 7-AAD only (Ann V-/7-AAD+). The analysis of early and late apoptosis assisted in defining and understanding the physical cellular state of the treated lymphocytes at the various timepoints used.

The 10X binding buffer (Appendix A.8) provided within the Annexin V-FITC/7-AAD kit was diluted 10 times in sH_2O, stored at 4°C and used in all subsequent staining procedures. For each time point, the samples were centrifuged at 500xg for 5 minutes, resuspended in 100µl of 1X binding buffer, and dual stained on ice with 10µl Annexin V-FITC and 20µl 7-AAD. Samples were left on ice in the dark for 15 minutes, followed by the addition of 400µl of 1X binding buffer. Finally, the samples were analysed by flow cytometry within an hour of staining. These experiments were performed several times to ensure consistency and representative data from a single experiment is shown later in the study.

The experiment was repeated using the same controls but different concentrations of $gp120^{BaL}$ and $gp120^{ZM651}$. Instead of using 50nM $gp120^{BaL}$ and $gp120^{ZM651}$, concentrations of 250nM and 500nM were used, to determine if $gp120^{BaL}$ and $gp120^{ZM651}$-mediated apoptosis occurred in a dose/concentration-dependent manner.

Furthermore, the flow cytometric protocol was modified by the addition of a dot plot that measured CD4 expression on the Jurkat T lymphocytes (CD4-PE versus SSC). This was to ensure that at least 80-90% of the Jurkat T lymphocytes were CD4

positive. The dot plot and histograms displaying Annexin V/7-AAD staining was gated on the CD4+ Jurkat T lymphocyte population. The staining procedures were performed as mentioned in section 2.8.3.1 with an addition of a CD4-PE antibody which was detected in the FL2 channel.

The modified protocol was used for Annexin V/7-AAD analysis of 50nM recombinant $gp120^{BaL}$, $gp120^{ZM651}$ and $gp140^{AncC}$-mediated apoptosis. The experiment was established in the same manner described in section 2.8.3 and an additional negative control (mock) was used. The mock control was prepared and purified from the supernatant of HEK293T cells transfected with an empty plasmid.This experiment was performed at least three times to ensure consistency and representative data from a single experiment is shown later in the study. In addition to Annexin V and 7-AAD analysis, the Jurkat T lymphocytes were subjected to TUNEL for the detection of chromosomal DNA fragmentation.

2.8.4.2 DNA fragmentation detection by Tdt-mediated dUTP Nick End Labeling (TUNEL)

DNA fragmentation was detected and quantified using the DeadEnd^{TM} Fluorometric TUNEL System (Promega Corporation, Madison, USA) according to the manufacturer's instructions (Technical Bulletin #TB235 at www.promega.com/tbs). The TUNEL assay measures DNA fragmentation which is a hallmark of late

apoptosis. The assay is based on the action of Terminal deoxynucleotidyl transferase (Tdt) enzyme, which functions by adding Fluorescein (FITC)-labelled-2'-deoxyuridine 5'- triphosphates (FITC-dUTPs) to the exposed 3' hydroxyl ends of the fragmented DNA [261, 262].

As with the Annexin V/7-AAD staining analysis, a protocol was set up and optimised for the TUNEL assay using untreated (negative control) or 4µM Camptothecin-treated Jurkat T lymphocytes. The protocol established was similar to that of the Annexin V and 7-AAD protocol, including a FSC versus SSC dot plot, a CD4-PE versus SSC dot plot (gating around CD4+ Jurkat T lymphocytes), and a histogram that measured TUNEL-FITC activity (DNA fragmentation). TUNEL activity was detected in the FL1 channel and the histogram was gated on the CD4+ Jurkat T lymphocytes therefore demonstrating apoptosis of CD4+ Jurkat T lymphocytes only.

Jurkat T lymphocytes ($2x10^6$cells/ml) were untreated, 4µM Camptothecin-treated, 50nM of recombinant $gp120^{BaL}$, $gp120^{ZM651}$ or $gp140^{AncC}$-treated, or mock-treated and incubated in a water jacketed 37°C, 5% CO_2 incubator until sampled at 0 and 65 hours post treatment. Initially, the TUNEL experiments were performed at 0, 24, 48, 65 hours as done previously by Arthos *et al*, 2002 on gp120-treated PBMCs [227] and 72 hours to determine the timepoint at which efficient levels of DNA fragmentation could be observed. Efficient levels of DNA fragmentation were observed post 48 hours, and it was found that apoptotic levels could be more easily measured at 65

hours compared to those observed at 72 hours (data not shown). Samples (1ml) were transferred into a 15ml tube (Nunc, Roskilde, Denmark) and washed twice with 1ml of 1X PBS by centrifuging at 300xg for 10 minutes at 4ºC in order to remove the FCS from the lymphocytes, as the serum is able to inactivate the Paraformaldehyde fixing regent. The pellets were resuspended in 500µl of 1X PBS and 5ml of 1% Paraformaldehyde (BDH Limited Poole, England) (Appendix A.8) before being incubated for 20 minutes on ice. Each sample was washed once with 1ml of 1X PBS by centrifuging at 300xg for 10 minutes at 4ºC and resuspended in 500µl of 1X PBS. The lymphocyte membranes were permeabilized overnight with 5ml of 70% ethanol (Appendix A.1) at -20ºC.

Thereafter, the lymphocytes were washed twice with 1ml of 1X PBS by centrifuging at 300xg for 10 minutes at 4ºC and during the wash, a 50µl Tdt enzyme solution (1µl of Tdt enzyme, 5µl of Nucleotide mix and 45µl of Equilibration buffer) was prepared according to the manufacturers' instructions. The pellets were equilibrated with the equilibration buffer (provided in the kit) for 5 minutes at room temperature before being centrifuged at 300xg for 10 minutes at 4ºC. Thereafter, the Tdt enzyme solution was added to the pellet and incubated at 37ºC in a water bath for one hour with minimal light exposure. The reactions were gently resuspended every 15 minutes.

After the one hour incubation, 1ml of 1X PBS containing 20mM EDTA (Appendix A.8) was added, and the sample was vortexed gently followed by centrifugation at 300xg for 10 minutes at 4ºC. The pellets were then washed in 1ml of 1X PBS-BSA

containing 0.1% Triton-100 (Appendix A.8) by centrifuging again at 300xg for 10 minutes at 4ºC. After resuspending the lymphocytes in 100µl of 1X PBS they were stained with 10µl of the CD4-PE monoclonal antibody for 15 minutes in the dark at room temperature. Finally, 400µl of 1X PBS was added to the stained cells and all the samples were analysed by flow cytometry within an hour of staining. This experiment was performed at least three times to ensure consistency and data from a single experiment are subsequently shown.

2.9 Recombinant $gp120^{BaL}$, $gp120^{ZM651}$ and $gp140^{AncC}$-mediated apoptosis of uninfected CD4+ T lymphocytes

2.9.1 Isolation of Peripheral Blood Mononuclear Cells (PBMCs) and CD4+T lymphocytes

Individual fresh HIV-1 seronegative, category C (regular donors) buffy coat blood samples were obtained from the SANBS for the isolation of PBMCs and CD4-enriched PBMCs (subsequently referred to as CD4+ T lymphocytes). All experiments were performed using single donor buffy preparations. For the isolation of CD4+ T lymphocytes, each buffy coat (10ml) was diluted in an equal volume (10ml) of 1X PBS containing 2% FCS (PBS-FCS) (Appendix A.7) after being incubated with the Human CD8+ Cell Depletion cocktail (Rosettesep; Stem Cell Technologies Inc, Catalog Number: 15663) for 20 minutes at room temperature, according to the manufacturer's instructions. The diluted blood was then divided in half and very gently layered onto

15ml of Ficoll-Paque^{TM} Plus (GE Healthcare Biosciences) within 50ml tubes (Nunc, Roskilde, Denmark). The samples were centrifuged at 350xg for 30 minutes at room temperature and the buffy layer which contained the CD4+T lymphocytes was removed. The CD4+T lymphocytes were washed 3-5 times in PBS-FCS by centrifugation at 230xg for 10 minutes at room temperature. The supernatant was discarded each time while the pellet was resuspended in PBS-FCS before every subsequent wash. Finally, the CD4+ T lymphocytes were resuspended in 5ml of complete RPMI-1640 medium, counted and seeded. The isolation of PBMCs was performed in the same manner except that the Human CD8+ Cell Depletion cocktail was not used. Although the culture looked fairly pure, we cannot exclude the possibility of monocytes, but as seen during flow cytometric analyses where monocytes, which have a different physiological appearance, would appear as a separate population, majority of monocytes have been excluded. Furthermore, the purity of each enriched fraction was assessed by CD8-ECD staining by flow cytometry, ensuring that more than 95% of the isolated and enriched fraction was CD4 positive only (data not shown).

2.9.2 Counting and maintenance of PBMCs and CD4+T lymphocytes

PBMCs and CD4+T lymphocytes were counted using trypan blue solution on a haemocytometer as explained in section 2.3.1.2 and $2x10^6$ cells were seeded in a $75cm^3$ culture flask and stimulated with Phytohaemagglutinin *Phaseolus vulgaris*

(PHA-P) (Sigma-Aldrich, Steinheim, Germany) at a concentration of 1µg/ml. Human Interleukin-2 (hIL-2) (Roche; Mannheim, Germany) was added to the lymphocytes 24 hours later at a concentration of 50U/ml. After 48 hours of hIL-2 stimulation and 72 hours of PHA treatment, the lymphocytes were ready for use in the apoptosis assays as discussed later and thereafter maintained in complete RPMI-1640 medium (Appendix A.2) containing 10U/ml of hIL-2 in a water jacketed 37ºC, 5% CO_2 incubator. This protocol is used routinely in our laboratory. Furthermore, previous work in our laboratory has established that this protocol results in activated lymphocytes. Therefore an activation marker was not used each time the experiment was repeated.

The culture flask was incubated in an upright position causing the lymphocytes to settle down at the bottom of the flask. The lymphocytes were not split or diluted, but replenished with fresh complete RPMI-1640 medium by either centrifuging the lymphocytes at 250xg for 5 minutes at 4ºC and resuspending in complete RPMI-1640 medium containing 10U/ml of hIL-2, or by simply removing a small volume of the old media and replacing it with fresh complete RPMI-1640 media containing 10U/ml of hIL-2. This was performed every 2-3 days and lymphocytes were discarded after 2 weeks.

2.9.3 The comparison of recombinant gp120-mediated apoptosis of activated PBMCs and CD4+ T lymphocytes

2.9.3.1 Establishment of a flow cytometric protocol for the analysis of early and late apoptosis by Annexin V and 7-AAD staining

The establishment of a protocol to measure early and late apoptosis of activated PBMCs and CD4+T lymphocytes was setup in a similar manner as for the Jurkat T lymphocytes. The protocol demonstrated apoptosis of CD3+CD4+ PBMCs/T lymphocytes. The FL1 channel was used for the detection of Annexin V-FITC, the FL2 channel was used for the detection of the CD4-PE, the FL3 channel was used for the detection of the CD8-ECD antibody, the FL4 channel was used for the detection of 7-AAD and the FL5 channel was used for the detection of the CD3-PC7 antibody. The protocol included a FSC versus SSC dot plot, a CD3-PC7 versus CD4-PE dot plot containing a gate around the CD3+CD4+ T lymphocytes, an Annexin V versus 7-AAD dot plot and an histogram measuring CD8-ECD staining, both of which were gated on the CD3+CD4+ T lymphocytes. Untreated and 4µM Camptothecin-treated PBMCs/CD4+T lymphocytes ($1x10^6$/ml) were processed in order to establish baselines which the treated samples were compared to.

2.9.3.2 Flow cytometric analysis of early and late apoptosis using Annexin V/7-AAD staining

Both activated PBMCs and CD4+ T lymphocytes were analysed and compared to allow for an optimal protocol set-up, and to determine which cell types allowed for optimal detection of gp120 mediated apoptotic events. For this comparison, only one of the purified recombinant Env glycoproteins ($gp120^{BaL}$) was used. Therefore, after 48 hours of hIL-2 stimulation and 72 hours of PHA treatment, the activated lymphocytes were untreated, 50nM $gp120^{BaL}$-treated, 4µM Camptothecin-treated and mock-treated. Samples were taken at 0, 5, 24 and 48 hours and the levels of early and late apoptosis were analysed by CD3-PC7, CD4-PE and Annexin V/7-AAD staining. The staining procedures were performed as mentioned in section 2.8.3.1 with an addition of 10µl of the CD4-PE and CD3-PC7 antibodies which were detected in the FL2 and FL5 channels, respectively. This experiment was performed once in duplicate and data from a single experiment is shown.

2.9.4 The analysis of early and late apoptosis of $gp120^{BaL}$, $gp120^{ZM651}$ and $gp140^{AncC}$-treated CD4+T lymphocytes

After 48 hours of hIL-2 stimulation and 72 hours of PHA treatment, the activated CD4+T lymphocytes ($1x10^6$cells/ml) were seeded in a 24-well plate (Nunc) and either untreated (negative control) or treated with 4µM Camptothecin, the mock purification

control, 50nM of either recombinant $gp120^{BaL}$, $gp120^{ZM651}$ or $gp140^{AncC}$ and incubated in a water jacketed 37°C, 5% CO_2 incubator until sampled. Samples (500µl) were taken at 0 (baseline), 24 and 48 hours. All samples at each time point were analysed by Annexin V and 7-AAD staining as mentioned in 2.8.3.1 with the addition of 10µl of the CD4-PE, CD3-PC7 and CD8-ECD antibodies which were detected in the FL2, FL5 and FL3 channels, respectively. This experiment was performed three times to ensure consistency and data from a single experiment is shown.

2.9.5 Detection of DNA fragmentation of $gp120^{BaL}$, $gp120^{ZM651}$ and $gp140^{AncC}$-treated CD4+T lymphocytes by TUNEL

The establishment of a protocol that measured DNA fragmentation within treated CD4+T lymphocytes was set up in a similar manner as the Annexin V and 7-AAD staining analysis protocol. The protocol included a FSC versus SSC dot plot, a CD3-PC7 versus CD4-PE dot plot gating around the CD3+CD4+ T lymphocytes and histograms measuring CD8-ECD staining (for the detection of CD8-ECD positive lymphocytes) and TUNEL-FITC activity both of which were gated on the CD3+CD4+ T lymphocyte. The experiment was established as mentioned in section 2.9.4. Samples were taken at 0 hours and 65 hours post treatment and the difference was analysed by TUNEL as mentioned in section 2.8.3.2 with the addition of 10µl of the CD3-PC7 and CD8-ECD antibodies. This experiment was performed three times to

ensure consistency to ensure consistency and representative data from a single experiment is shown later in the study.

2.10 Presentation and analysis of flow cytometry data

All dot plots generated were analysed using the quadstats feature offered in the CXP 2.2 software on the Cytomics FC500. The data (represented as percentages within each quadrant) obtained from the Annexin V and 7-AAD staining analysis of early and late apoptosis of untreated, 4µM Camptothecin-treated, mock-treated, $gp120^{BaL}$, $gp120^{ZM651}$ and $gp140^{AncC}$-treated Jurkat and CD4+ T lymphocytes were analysed relative to the baseline values (untreated control) obtained. The difference in percentage between the untreated samples and treated samples at 24 and 48 hours post treatment were presented in the format of Tables. The data presented for each cell type was taken from one experiment. The levels of DNA fragmentation obtained from the TUNEL assays performed on the untreated, 4µM Camptothecin-treated, mock-treated, $gp120^{BaL}$, $gp120^{ZM651}$ and $gp140^{AncC}$-treated Jurkat and CD4+ T lymphocytes were displayed as percentages on histograms and analysed relative to the baseline values (untreated control) at the two time points tested. The data presented for each cell type was taken from one experiment.

CHAPTER 3: RESULTS

3.1 Recombinant gp120^{BaL}, gp120^{ZM651} and gp140^{AncC} expression, purification and characterization

3.1.1 Large scale plasmid preparation of gp120^{BaL}, gp120^{ZM651} and gp140^{AncC} recombinant expression plasmids

Single colonies of recombinant *E.coli* DH5α transformed with gp120^{BaL}, gp120^{ZM651} and gp140^{AncC} were grown overnight and successfully used to extract sufficient quantities and qualities of each plasmid (Figure 3.1). The three purified plasmids were used in transfection experiments of HEK 293T mammalian cells and were isolated throughout the study, as required. In addition, the pcDNA 3.1 expression plasmid (with no inserts) was obtained for use in control transfections, and mock purifications.

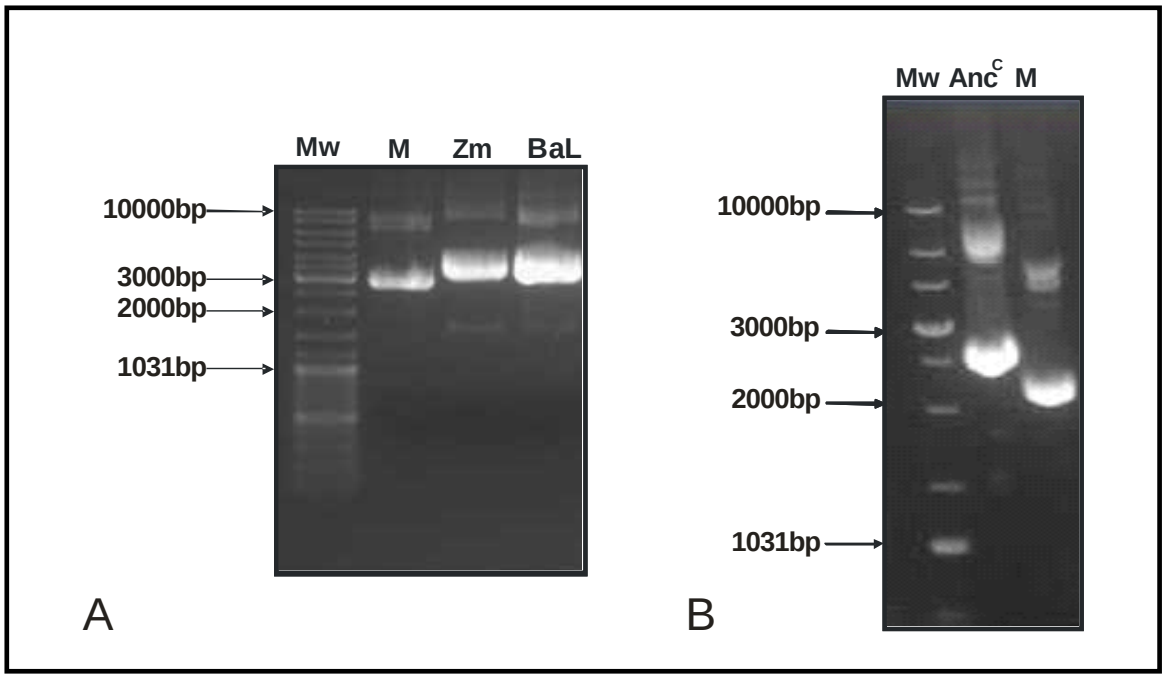

Figure 3.1: Agarose gel electrophoresis (0.8%) of (A) recombinant pciNeo-BaLgp120 (BaL), p96ZM651gp120-CD5-opt (Zm) and (B) Ancestral subtype C gp140 (Anc^C) expression plasmids extracted from recombinant *E.coli* DH5α. DNA sizes (bp - base pairs) are indicated on the left. Mw: O' GeneRuler^{TM} DNA ladder mix (range 50bp-10kb) (Fermentas), M: empty pcDNA 3.1 expression plasmid (mock).

3.1.2 Optimization of HEK 293T mammalian transfections

Comparison of the two different transfection protocols (Polyfect versus Calcium Chloride) showed that expression of $gp120^{ZM651}$ and $gp120^{BaL}$ in HEK 293T mammalian cells was more efficient with the Polyfect® reagent at 24, 48 and 72

hours post transfection (Figure 3.2A and B). It appeared that there was no or minimal expression of $gp120^{BaL}$ with the calcium chloride protocol (Figure 3.2B).

The non specific bands seen in Figure 3.2A and B are as a result of pooled HIV-1 seropositive human sera that were used as the primary antibody in the western blot analysis.

Thus, the Polyfect method was used in all subsequent transfection experiments, and supernatants were harvested at 48 hours post transfection. This is the established method used in our laboratory for the expression of $gp140^{AncC}$ (Figure 3.2C), thus all three Env glycoproteins were expressed using transient transfections of HEK 293T mammalian cells with recombinant DNA and the Polyfect® reagent.

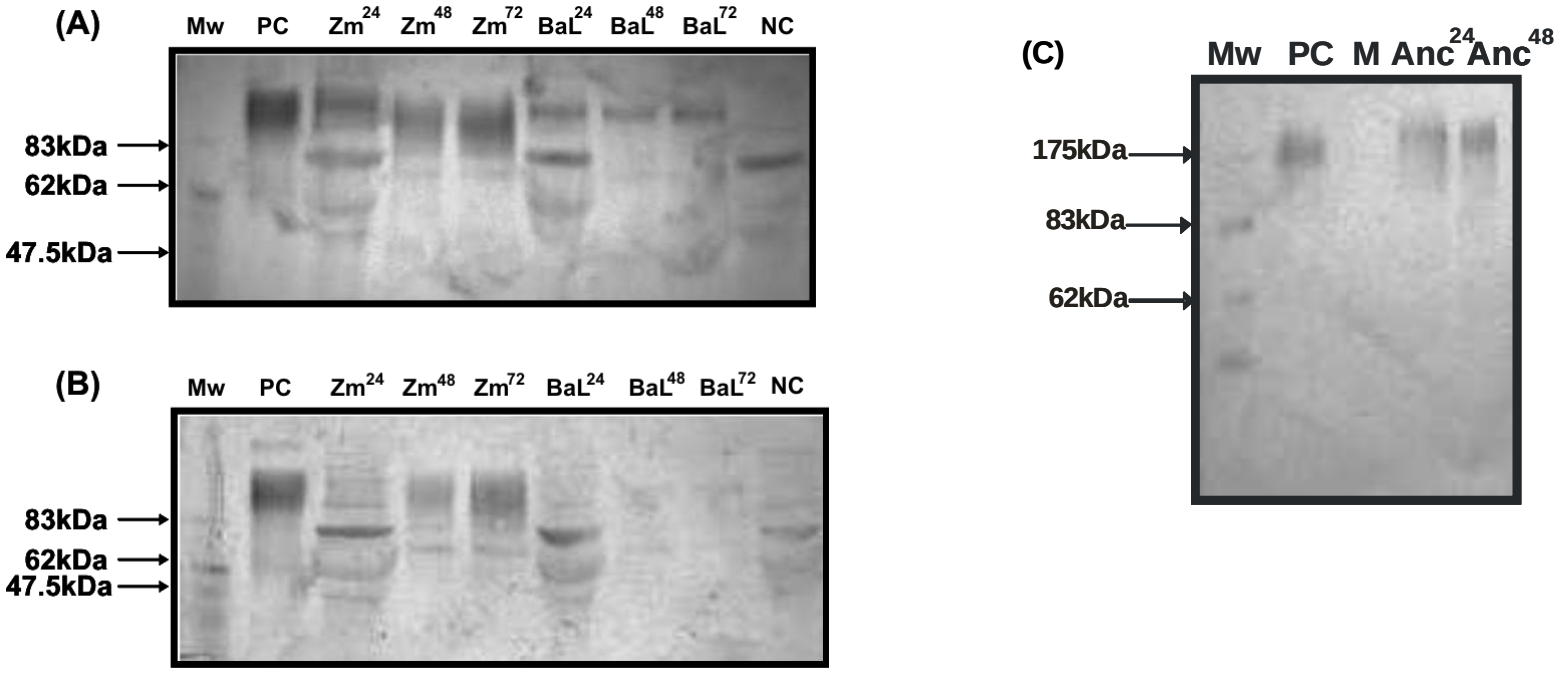

Figure 3.2: Western blot comparison of harvested supernatants from (A) Polyfect and (B) $CaCl_2$ transfections of HEK 293T cells with $gp120^{BaL}$ (BaL) and $gp120^{ZM651}$ (Zm) at 24 (Zm^{24}, BaL^{24}), 48 (Zm^{48}, BaL^{48}) and 72 (Zm^{72}, BaL^{72}) hours post transfection and (C) Polyfect transfections of HEK 293T cells with $gp120^{AncC}$ at 24 (Anc^{24}) and 48 (Anc^{28}) hours post transfection. Mw: Protein Molecular weight marker, broad range (6-175 kilodaltons;kDa) (Biolabs, New England), PC: HIV-$1_{96ZM651}$gp120 (NIH) Positive Control, NC: Negative control, supernatant harvested from non transfected HEK 293 T cells at 72 hours, M:Polyfect transfections of mock plasmid at 48 hours post transfection. Protein sizes (kDa; kilodaltons) are indicated on the left.

3.1.3 Purification of gp120^{BaL}, gp120^{ZM651} and gp140^{AncC} by lectin affinity chromatography

Recombinant gp120^{BaL}, gp120^{ZM651} and gp140^{AncC} were successfully expressed on a large scale in HEK 293T cells, and purified by lectin affinity chromatography. The expression and purification procedures of gp120^{BaL} and gp120^{ZM651} were analysed by SDS-PAGE and Western Blotting.

There was no unbound protein present in the harvested supernatants and washing buffers after being passed through the lectin column as seen in lanes FT and W of the recombinant gp140^{AncC} purification process (Figure 3.3A and B). The same result was observed in the SDS-PAGE and Western Blot analysis of the purification processes of recombinant gp120^{BaL} and gp120^{ZM651} (results not shown). All three purified and concentrated recombinant Env glycoproteins did not appear to be degraded as seen in Figure 3.3E, and were of the expected sizes of 120kDa (gp120^{BaL} and gp120^{ZM651}) and 140kDa (gp140^{AncC}).

The non-specific bands that are visible on the Western blot (left) of the mock purification process (Figure 3.3C) could be other cellular proteins that are detected by the human sera primary antibody used during Western Blot analysis.

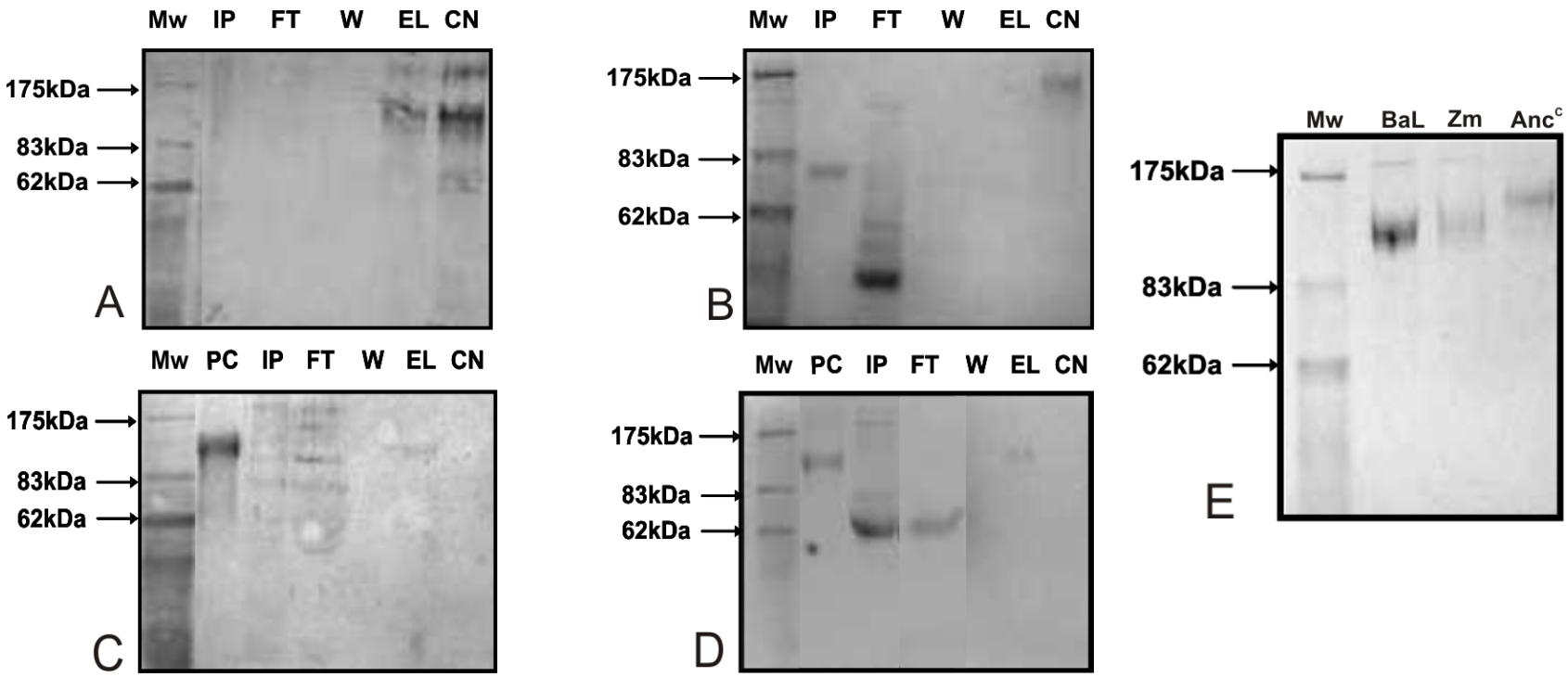

Figure 3.3: SDS-PAGE (on the right) and Western Blot analysis (on the left) of the recombinant gp140^{AncC}protein (A and B) and mock (C and D) purification procedures. (E) SDS-PAGE and Coomassie Brilliant Blue staining analysis of all three purified and concentrated recombinant proteins. PM: Molecular weight marker, broad range (6-175 kilodaltons;kDa) (Biolabs), IP: Input, FT: Flow through, W: Wash, EL: Elution, CN: Concentrated recombinant protein, PC: HIV-1$_{96ZM651}$gp120 (NIH) Positive Control. Protein sizes (kDa) are indicated on the left.

3.1.4 Quantification of purified recombinant gp120^{BaL}, gp120^{ZM651} and gp140^{AncC}

A standard curve was obtained using the absorbance readings obtained from standard concentrations of BSA protein (Figure 3.4). The straight line equation (y=0.0019x+0.1134) was used to determine the concentration of the protein by solving for the x-value. The y-value is the mean absorbance value and the R^2-value represents how well the straight line is fitted to each point of the graph. Therefore, a higher R^2 –value means a better or closer fit of each absorbance value (point) to the straight line graph. For the initial purifications, the concentrations of gp120^{BaL}, gp120^{ZM651} and gp140^{AncC} were 107.6µg/ml, 162.5µg/ml and 150µg/ml, respectively. These concentrations varied in subsequent purifications, but, overall, approximately 2mg of recombinant gp120^{BaL} and gp140^{AncC} was purified from 2L of harvested supernatant, while 1.5mg of recombinant gp120^{ZM651} was purified from 2L of harvested supernatant.

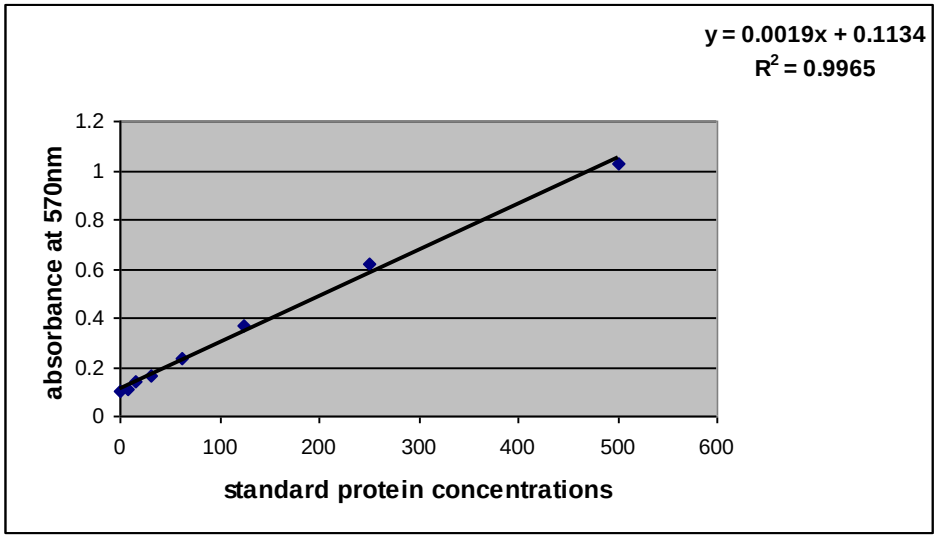

Figure 3.4: Typical standard curve graph obtained from a range of BSA concentrations. The straight line equation and R^2 value is shown on the top right corner.

3.1.5 Characterization of purified recombinant gp120^{BaL}, gp120^{ZM651} and gp140^{AncC}

Conformational studies were successfully performed on the expressed, purified and concentrated Env glycoproteins to determine that they were conformationally intact as well as functional (Figure 3.5). The binding efficiency of recombinant gp120^{ZM651}, gp120^{BaL} and gp140^{AncC} to Mabs IgG1b12, 17b, 17b post sCD4 binding, 48D and 2G12 was analysed. These Mabs bind to functionally and structurally important epitopes on gp120 (see discussion). The data shown in Figure 3.5 represents the means from duplicate analyses of single parameters which are the different antibodies that were used.

Recombinant $gp120^{ZM651}$, $gp120^{BaL}$ and $gp140^{AncC}$ were all able to bind the MAb IgG1b12 (Figures 3.5A-C), in a dose dependent manner. There were differences noted between binding of $gp120^{ZM651}$, $gp120^{BaL}$ and $gp140^{AncC}$ to 17b, 17b post sCD4 binding and 2G12 (Figures 3.5A-C). For example, only $gp120^{BaL}$ could bind 2G12 (Figures 3.5A-C). In addition, 17b was only able to bind recombinant $gp120^{BaL}$ and $gp140^{AncC}$ in the presence of sCD4 (Figures 3.5B and C).

Because the capture ELISA did not show $gp120^{ZM651}$ binding to 17b in the presence of sCD4, (which is an indirect measure of gp120-sCD4 binding), a further CD4 binding ELISA was performed (Figure 3.6). The data shown in Figure 3.6 represents the means from duplicate analyses of single parameters (48D in the presence and absence of CD4).

Results showed that in the presence of full length sCD4, 48D interacted very poorly/not at all with $gp120^{ZM651}$ and $gp140^{AncC}$, but strongly with $gp120^{BaL}$ (Figures 3.6A, B and C)

Even though $gp120^{ZM651}$ was unable to interact with 17b, it did however show efficient binding affinities for IgG1b12, whose epitopes overlap with the CD4 binding site. Overall, all three recombinant Env glycoproteins had a functional CD4 binding site, and were conformationally intact, and were used for all subsequent experiments.

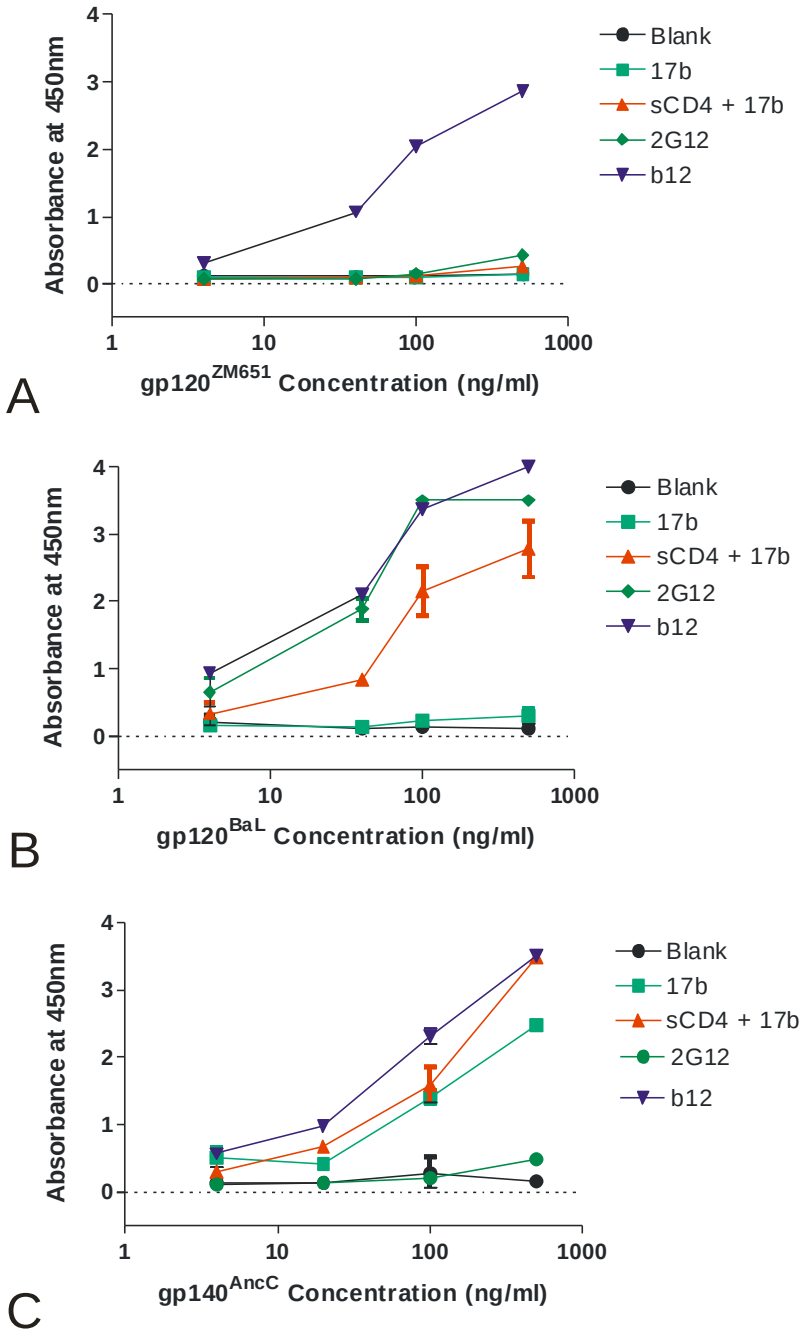

Figure 3.5: The measurement of antibody binding to purified recombinant HIV-1 gp120^{ZM651} (A), gp120^{BaL} (B) and gp140^{AncC} (C) by capture ELISAs. Error bars represent standard deviation.

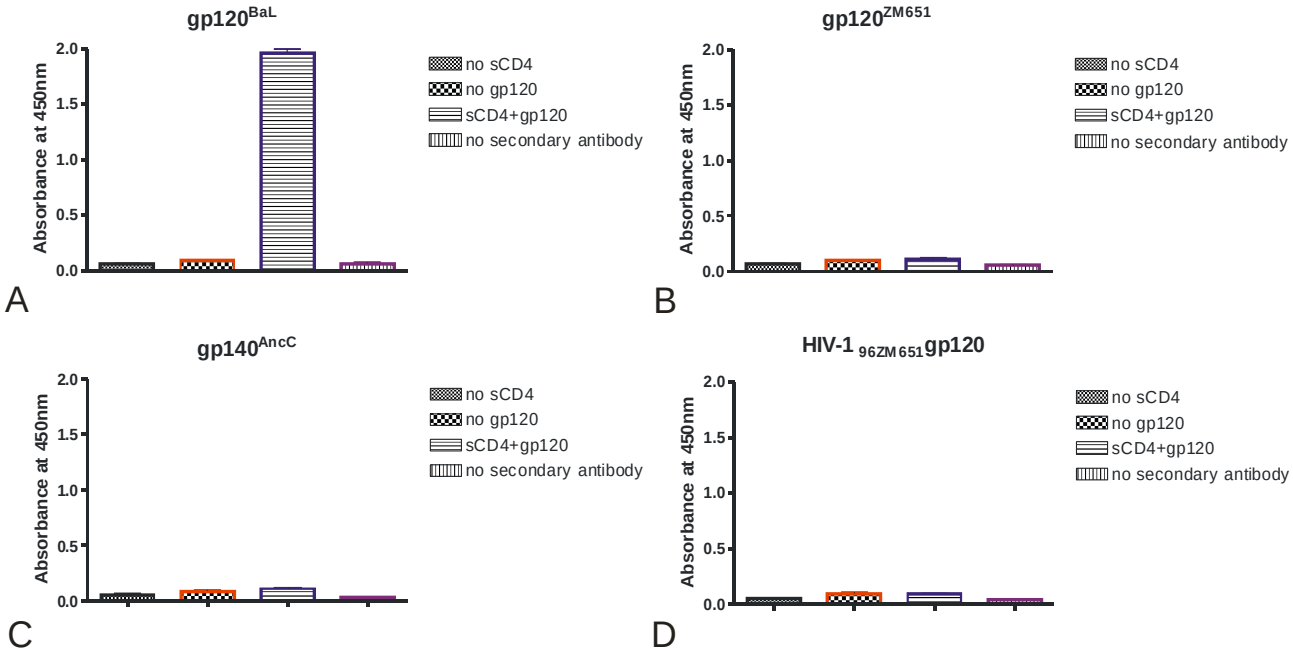

Figure 3.6: Bar charts depicting the ability of purified recombinant HIV-1 $gp120^{BaL}$ (A), $gp120^{ZM651}$ (B), $gp140^{AncC}$ (C) and HIV-$1_{96ZM651}$gp120 (NIH) (D) to interact with 48D in the presence of full length sCD4. Error bars represent standard deviation.

All three recombinant Env glycoproteins were then analysed for their ability to induce apoptosis of Jurkat T lymphocytes via gp120-CD4 interactions and of CD4+ T lymphocytes via gp120-CD4 and/ or co-receptor interactions (CCR5 in this case).

3.2 Flow cytometric analyses of $gp120^{BaL}$, $gp120^{ZM651}$ and $gp140^{AncC}$-mediated early and late apoptosis of uninfected Jurkat T lymphocytes

All the flow cytometry experiments were performed several times, and dot plots and/or histograms and associated tables from only one experiment that was considered representative of the data is depicted throughout.

3.2.1 Establishment of a flow cytometric protocol for the analysis of Annexin V and 7-AAD staining of uninfected Jurkat T lymphocytes

A protocol that could measure early and late apoptosis using Annexin V and 7-AAD staining was successfully established using untreated Jurkat T lymphocytes (Figure 3.7). The untreated lymphocytes were stained with Annexin V and 7-AAD, and the typical analysis plots selected and incorporated into the protocol (shown for each experimental run) included a forward scatter linear (FSC) and side scatter log (SSC) dot plot confirming the entire Jurkat T lymphocyte population (Figure 3.7A), and an ungated Annexin V versus 7-AAD dot plot showing the proportions of Jurkat T lymphocytes staining positive for either or both markers (Figure 3.7B). In the example shown in Figure 3.7B, the majority of Jurkat T lymphocytes were viable (94.8%; stained negative for both Annexin V and 7-AAD in quadrant A3), while 4.0% and 1.1% were undergoing early (Annexin V positive; quadrant A4) and late apoptosis (Annexin V and 7-AAD positive; quadrant A2), respectively. Completely necrotic Jurkat T

lymphocytes were detected in quadrant A1 (0.2%; 7-AAD positive). The ungated histograms in Figures 3.7C and 3.7D represent the total percentage of lymphocytes that stained positive for Annexin V and 7-AAD, respectively. Recombinant gp120^{BaL} and gp120^{ZM651} were chosen for the establishment and optimization of the Annexin V and 7-AAD staining assay. The flow cytometry protocol outlay shown in Figure 3.7 was used initially for the analysis of early and late apoptosis of gp120^{BaL} and gp120^{ZM651}-treated (using concentrations of 50nM, 250nM or 500nM) and untreated Jurkat T lymphocytes.

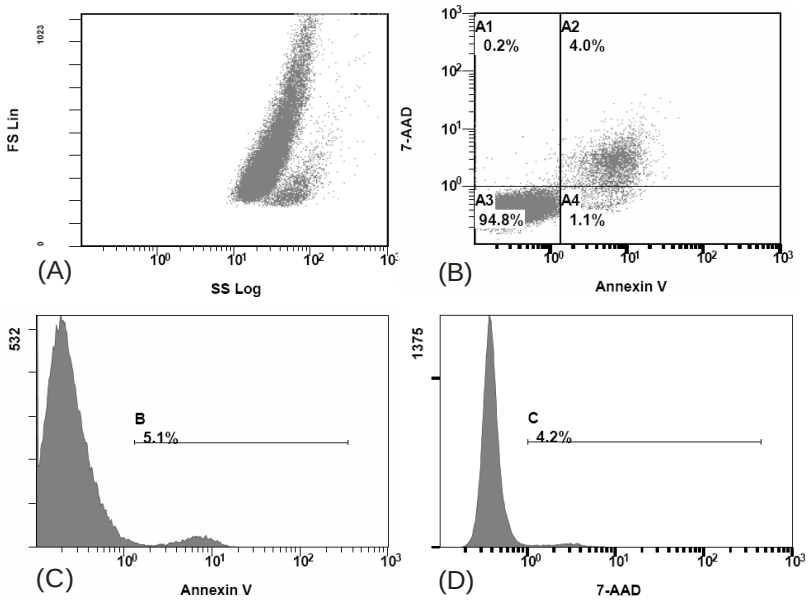

Figure 3.7: Example of Dot blots and histograms of untreated lymphocytes from the protocol established for the Annexin V and 7-AAD staining analysis of gp120^{BaL} and gp120^{ZM651}-mediated early and late apoptosis of Jurkat T lymphocytes. The entire cell population is shown in (A), and the viable cells are positioned within the first decade (10^0), as seen in (B), (C) and (D).

3.2.2 Early and late apoptosis of uninfected Jurkat T lymphocytes mediated by varying concentrations of gp120^{BaL} and gp120^{ZM651}

Data from the results obtained are shown in Figure 3.8, displaying the outcome of the staining analysis of untreated and Camptothecin-treated Jurkat T lymphocytes at 24 hours post treatment.

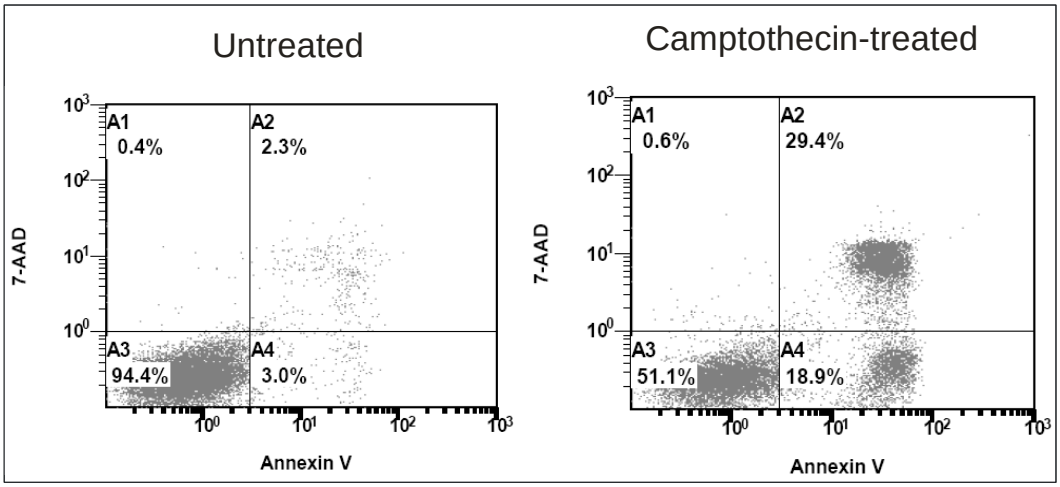

Figure 3.8: Dot plots displaying the Annexin V and 7-AAD staining analysis of untreated and 4µM Camptothecin-treated Jurkat T lymphocytes from one experiment at 24 hours post treatment.

3.2.2.1 Apoptosis of Jurkat T lymphocytes mediated by 50nM, 250nM and 500nM gp120^{BaL} and gp120^{ZM651}

The ability of 4µM Camptothecin (positive control), 50nM gp120^{BaL} and gp120^{ZM651} to induce apoptosis of Jurkat T lymphocytes over time was analysed by Annexin V and 7-AAD staining. The results from a single experiment are presented in Table 3.1. The percentages obtained in the quadrants for early (A4) and late (A2) apoptosis at 24 and 48 hours post treatment were subtracted from the untreated/baseline percentage values at the same time points and the differences are shown in Table 3.1. As expected, relative to the baseline, the Camptothecin positive control induced high levels of late apoptosis (22%) 24 hours post treatment, with 60% of the Jurkat T lymphocyte population undergoing late apoptosis and entering necrosis at 48 hours post treatment (Table 3.1).

Furthermore, the addition of 50nM gp120^{BaL} and gp120^{ZM651} induced low levels (less than 10%) of late apoptosis over time, with 6.9% and 1.9% of gp120^{BaL} and gp120^{ZM651}-treated Jurkat T lymphocytes expressing late apoptosis markers at 48 hours post treatment, respectively (Table 3.1). There were higher levels of early apoptosis after 24 and 48 hours of exposure to 50nM gp120^{ZM651} in comparison to 50nM gp120^{BaL}. However, gp120^{BaL} induced the highest levels of late apoptosis after 48 hours of exposure (Table 3.1). Overall, 50nM gp120^{BaL} and gp120^{ZM651}-treated

Jurkat T lymphocytes displayed low levels of early and late apoptosis after 48 hours of treatment.

Table 3.1: Percentages of early and late apoptosis of Jurkat T lymphocytes from individual experiments mediated by 50nM, 250nM and 500nM $gp120^{BaL}$and $gp120^{ZM651}$ at 24 and 48 hours post exposure.

Lymphocyte Treatments (Jurkat T lymphocytes)	Percentage of Early Apoptosis (Ann V+/7-AAD-) (%)		Percentage of Late Apoptosis (Ann V+/7-AAD+) (%)	
	24 hours	48 hours	24 hours	48 hours
4µM Camptothecin	19.8	2.6	22.0	60.0
Untreated	**2.2**	**3.9**	**2.0**	**4.3**
50nM $gp120^{ZM651}$	1.2	1.0	0.7	1.9
Untreated	**3.0**	**1.5**	**2.3**	**2.5**
250nM $gp120^{ZM651}$	1.6	1.6	-	0.4
500nM $gp120^{ZM651}$	-	3.9	0.3	-
Untreated	**2.2**	**3.9**	**2.0**	**4.3**
50nM $gp120^{BaL}$	-	0.4	0.9	6.9
Untreated	**3.0**	**1.5**	**2.3**	**2.5**
250nM $gp120^{BaL}$	-	7.4	1.7	2.2
500nM $gp120^{BaL}$	-	9.3	1.5	2.5

Given that 50nM gp120^{BaL} and gp120^{ZM651} induced low levels of apoptosis, Jurkat T lymphocytes were treated with 250nM and 500nM gp120^{BaL} and gp120^{ZM651} to determine if there was a dose response effect (Table 3.1).

Relative to the baseline, a small percentage of 250nM and 500nM gp120^{BaL}-treated Jurkat T lymphocytes were undergoing late apoptosis (Table 3.1). At 48 hours post treatment, 250nM gp120^{ZM651} induced 1.6% of early apoptosis while 500nM gp120^{ZM651} induced 3.9% early apoptosis. Even though there seems to be a concentration effect on early apoptosis at 48 hours post exposure, both concentrations (250nM and 500nM) of gp120^{ZM651} used were unable to induce increased levels of late apoptosis at this same time point (Table 3.1).

Similarly, gp120^{BaL} seemed to induce a concentration effect on the levels of early apoptosis after 48 hours of exposure i.e. the addition of 250nM gp120^{BaL} induced up to 7.4% early apoptosis while 500nM gp120^{BaL} induced 9.3% of early apoptosis (Table 3.1). Interestingly, the levels of late apoptosis induced by 250nM and 500nM gp120^{BaL} after 48 hours of exposure were lower than the early levels observed at the same time point (Table 3.1). Furthermore, at 24 hours post treatment, 250nM gp120^{BaL} was able to induce levels of late apoptosis (1.7%) that were similar to that induced by 500nM gp120^{BaL} (1.5%) (Table 3.1).

Therefore, due to the low levels of apoptosis observed even in the presence of higher recombinant Env glycoprotein concentrations; 50nm $gp120^{BaL}$, $gp120^{ZM651}$ and $gp140^{AncC}$ was used in all subsequent experiments. In an attempt to improve the low levels of apoptosis being obtained, and to ensure that low levels of CD4 expression on the Jurkat T lymphocytes was not responsible, the established flow cytometric protocol was modified to confirm the presence of CD4 on the Jurkat T lymphocytes tested.

3.2.3 Flow cytometric analysis of apoptosis mediated by 50nM $gp120^{BaL}$, $gp120^{ZM651}$ and $gp140^{AncC}$ using a modified protocol

The settings of the previously established flow cytometric protocol were modified and a new protocol was set up in the exact same manner as mentioned in section 3.2.1. Protocol modifications included the addition of a CD4-PE versus SSC dot plot that measured CD4-PE staining on the Jurkat T lymphocytes (Gate C) (Figure 3.9B). The Annexin V versus 7-AAD dot plot (Figure 3.9C) was gated on Gate C, therefore displaying early and late apoptosis of CD4-PE positive Jurkat T lymphocytes only.

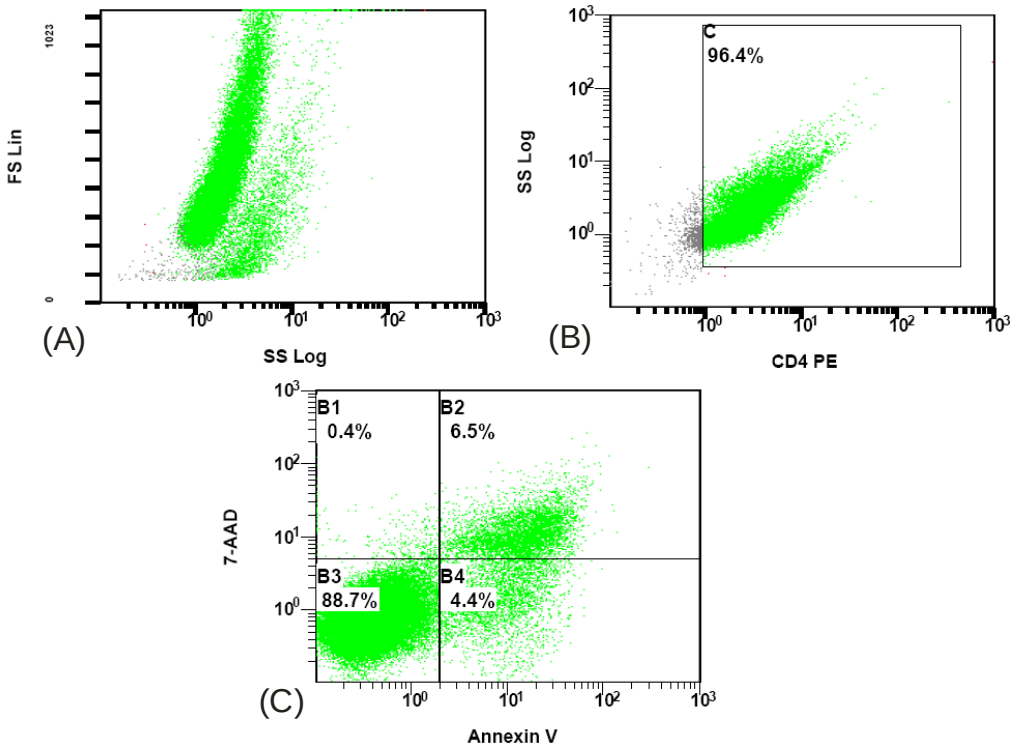

Figure 3.9: Example of dot blots of untreated lymphocytes from the modified flow cytometric protocol established for Annexin V and 7-AAD staining analysis of $gp120^{BaL}$, $gp120^{ZM651}$ and $gp140^{AncC}$-mediated early and late apoptosis of Jurkat T lymphocytes.

3.2.3.1 Early and late apoptosis mediated by 50nM $gp120^{BaL}$, $gp120^{ZM651}$ and $gp140^{AncC}$

Dot plots demonstrating Annexin V and 7-AAD analysis of untreated and Camptothecin-treated Jurkat T lymphocytes after 24 hours using the modified flow cytometric protocol are shown in Figure 3.10.

The results shown in Figure 3.11, Figure 3.12 and Table 3.2 were obtained from one experiment, and are representative of at least three independent experiments and showed comparable results (this applies to all the subsequent dot plots and associated Tables shown throughout the rest of the dissertation).

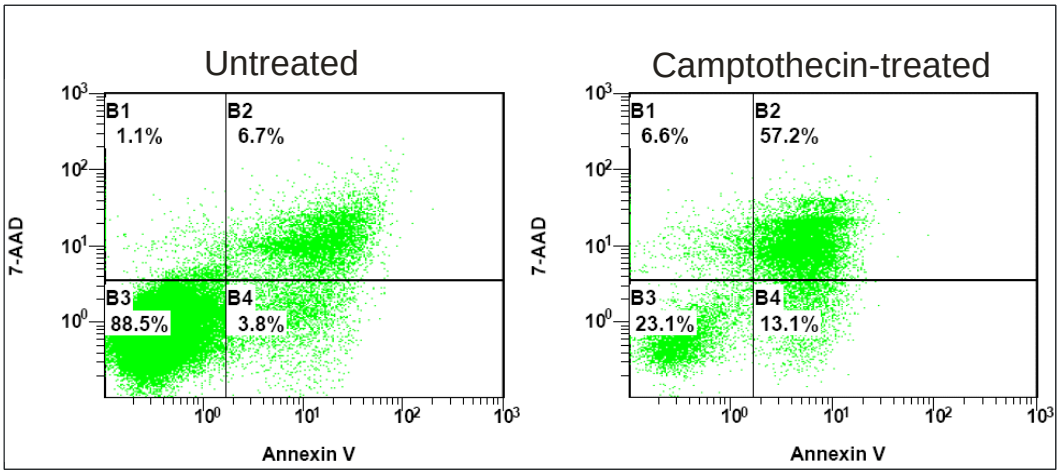

Figure 3.10: Dot plots displaying the Annexin V and 7-AAD staining analysis of untreated and 4µM Camptothecin-treated Jurkat T lymphocytes from one experiment post 24 hours using the modified protocol.

In comparison to the initial protocol, the selected dot plot for the modified protocol showed higher levels of baseline apoptosis, and this can be attributed to a higher passage number of the cell lines used. Relative to the untreated Jurkat T lymphocytes, 50nm $gp120^{BaL}$, $gp120^{ZM651}$ and $gp140^{AncC}$-treated Jurkat T lymphocytes displayed higher levels of late apoptosis at 24 hours than at 48 hours post treatment (Figure 3.11 and 3.12 and Table 3.2). Furthermore, relative to the

untreated control, the percentage of $gp120^{BaL}$, $gp120^{ZM651}$ and $gp140^{AncC}$-treated Jurkat T lymphocytes undergoing early apoptosis increases (3.5%, 4.1% and 2.8%, respectively) with a simultaneous decrease in Jurkat T lymphocytes undergoing late apoptosis at 48 hours post treatment (Figure 3.12 and Table 3.2). This was not observed in the untreated Jurkat T lymphocytes (Figure 3.11 and Table 3.2).

In addition, the mock-treated (negative control) Jurkat T lymphocytes displayed early and late apoptosis levels that were insignificantly higher than untreated Jurkat T lymphocytes (Figure 3.11 and Table 3.2). This was a consistent observation throughout all of the apoptosis assay experiments.

Overall, these results indicate that the interaction of recombinant gp120 with CD4 is able to trigger low levels of apoptosis in Jurkat T lymphocytes. In addition, the induction of apoptosis seems to be reversible. To confirm that the Jurkat T lymphocytes were undergoing apoptosis, the occurrence of chromosomal DNA fragmentation, which is a marker of late apoptosis, was analysed.

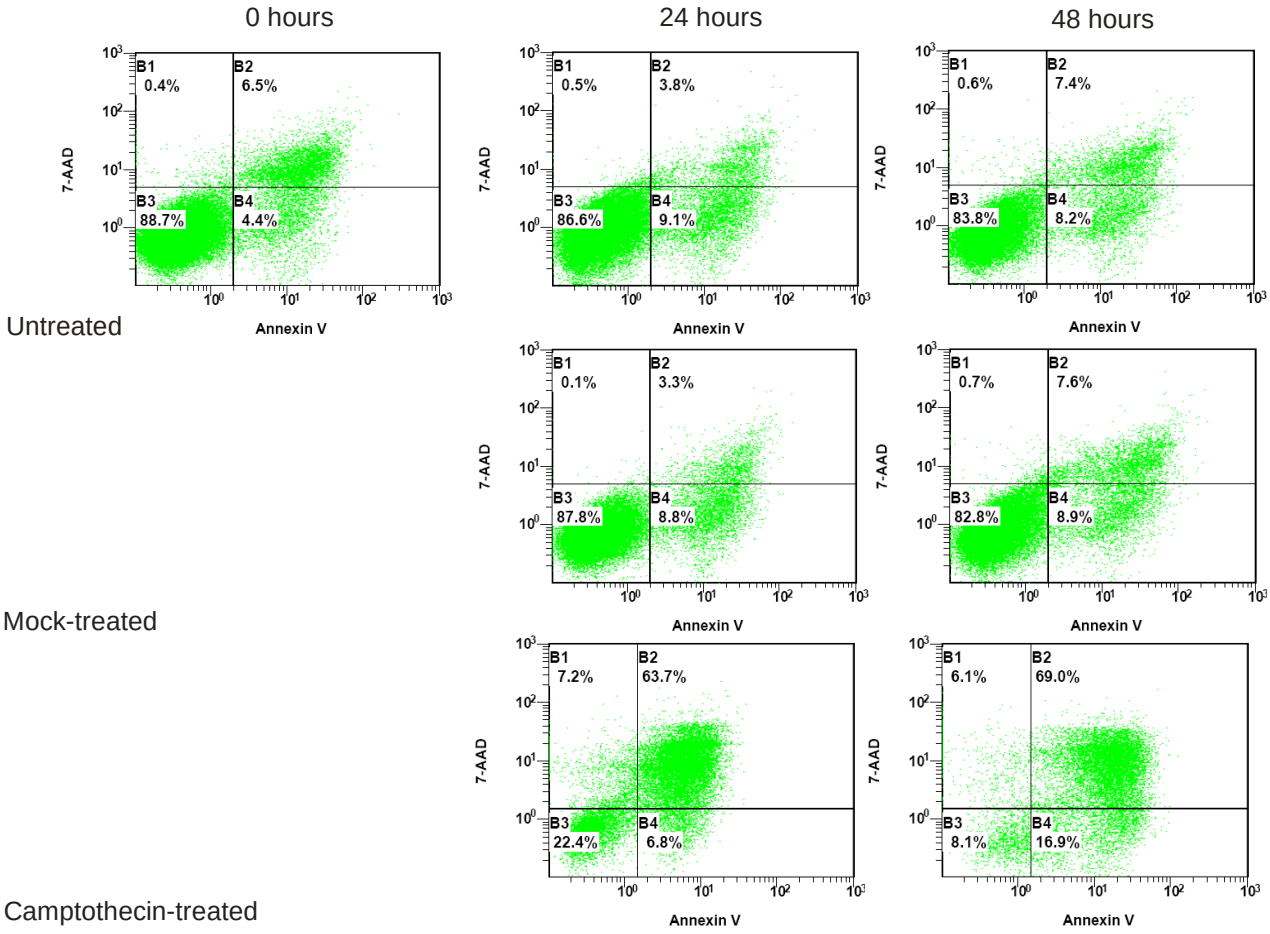

Figure 3.11: Annexin V and 7-AAD analysis of untreated, mock-treated and 4µM Camptothecin-treated Jurkat T lymphocytes from one experiment at 24 and 48 hours post treatment. The Annexin V/7-AAD analysis of the untreated Jurkat T lymphocytes at 0 hours is included for comparative purposes.

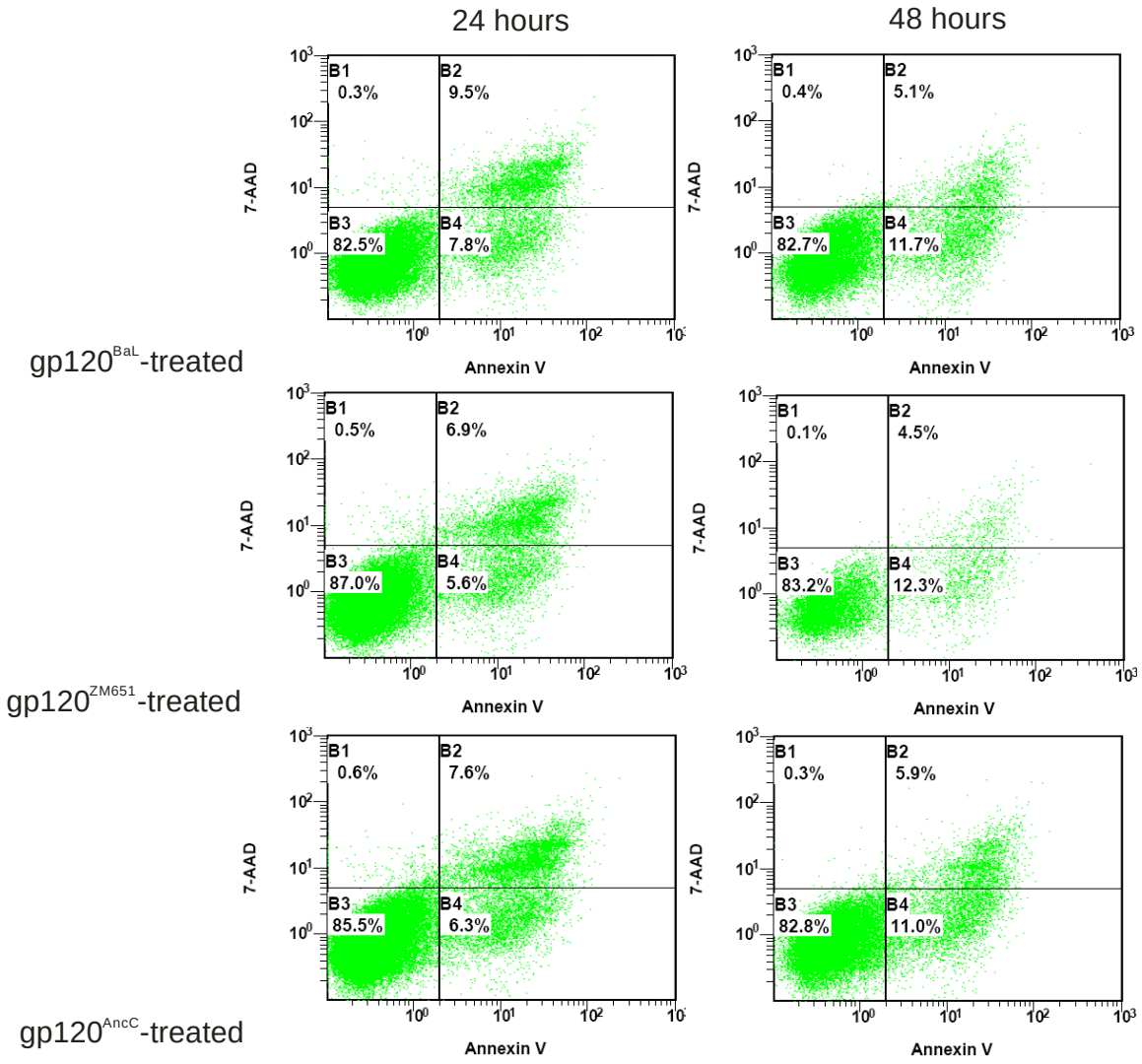

Figure 3.12: Annexin V and 7-AAD analysis of 50nM gp120^{BaL}, gp120^{ZM651} and gp140^{AncC}-treated Jurkat T lymphocytes from one experiment at 24 and 48 hours post treatment.

The percentages obtained in the quadrants for early (B4) and late (B2) apoptosis of Jurkat T lymphocytes at 24 and 48 hours post treatment with gp120^{BaL}, gp120^{ZM651} and gp140^{AncC} were subtracted from the untreated/baseline percentage values at the same time points and the differences are shown in Table 3.2.

Table 3.2: Percentages of early and late apoptosis of Jurkat T lymphocytes from one experiment mediated by 50nM gp120^{BaL}, gp120^{ZM651}and gp140^{AncC} after 24 and 48 hours of exposure.

Lymphocyte Treatments (Jurkat T lymphocytes)	Percentage of Early Apoptosis (Ann V+/7-AAD-) (%)		Percentage of Late Apoptosis (Ann V+/7-AAD+) (%)	
	24 hours	48 hours	24 hours	48 hours
Untreated	**9.1**	**8.2**	**3.8**	**7.4**
4µM Camptothecin	2.3	8.7	59.9	61.6
50nM gp120^{BaL}	-	3.5	5.7	-
50nM gp120^{ZM651}	-	4.1	3.1	-
50nM gp140^{AncC}	-	2.8	3.8	-

3.2.3.2 Detection of DNA fragmentation within 50nM gp120^{BaL}, gp120^{ZM651} and gp140^{AncC}-treated uninfected Jurkat T lymphocytes

A protocol measuring chromosomal DNA fragmentation within Jurkat T lymphocytes using TUNEL was successfully established using untreated Jurkat T lymphocytes

(protocol not shown). The protocol included the same parameters as the Annexin V and 7-AAD staining protocol, except that the Annexin V versus 7-AAD dot plot was replaced with a histogram measuring TUNEL activity. The histogram was gated on CD4+ Jurkat T lymphocytes (protocol not shown).

Untreated, 4µM Camptothecin-treated, 50nm $gp120^{BaL}$, $gp120^{ZM651}$, $gp140^{AncC}$-treated and mock-treated Jurkat T lymphocytes were analyzed by TUNEL at 0 and 65 hours post treatment (Figure 3.13). The percentage of DNA fragmentation observed in the $gp120^{BaL}$, $gp120^{ZM651}$, $gp140^{AncC}$-treated Jurkat T lymphocytes was higher than the untreated (6.1%, 5.0% and 6.8%, respectively) and mock-treated (4.9%, 3.8% and 5.6%, respectively) Jurkat T lymphocytes at 65 hours post treatment (Figure 3.13). As expected and relative to the untreated control, Camptothecin induced DNA fragmentation in approximately 84.6% of the lymphocyte population (Figure 3.13).

Overall, these results demonstrate low levels of DNA fragmentation that are higher than the levels of apoptosis obtained from the Annexin V and 7-AAD staining analysis (Figure 3.12 and Table 3.2), possibly due to being treated with the Env glycoproteins for up to 65 hours instead of 48 hours.

The results shown in Figure 3.13 were obtained from one experiment, and are representative of at least two independent experiments that demonstrated similar results (this applies to subsequent TUNEL data shown later in the dissertation).

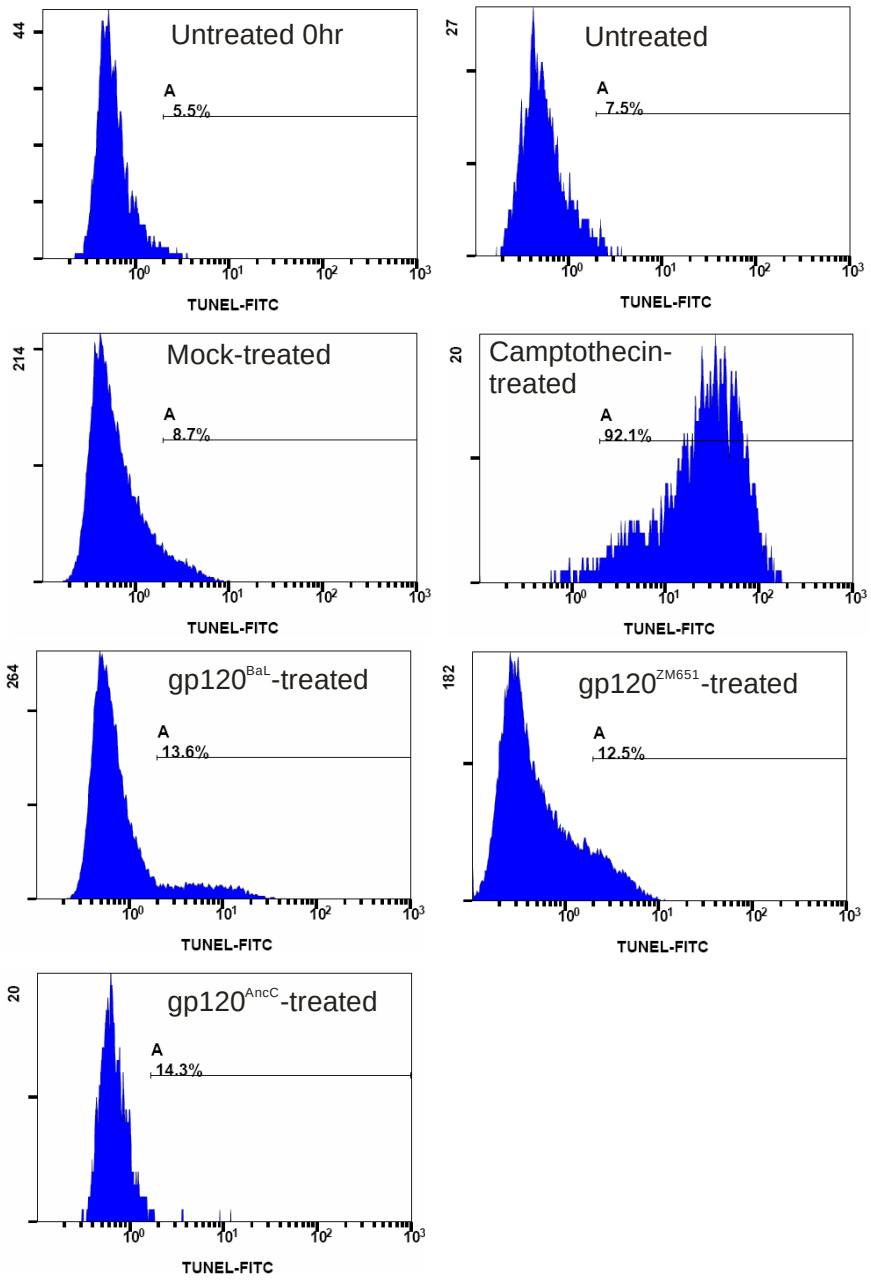

Figure 3.13: TUNEL analysis of DNA fragmentation in Jurkat T lymphocytes from one experiment induced by the addition of 50nM recombinant gp120^{BaL}, gp120^{ZM651} and gp140^{AncC} post 65 hours. The histogram of the untreated Jurkat T lymphocytes at 0 hours is included for comparative purposes. The percentage of TUNEL positive Jurkat T lymphocytes is presented on each histogram. The data was taken from one experiment.

3.3 Flow cytometric analyses of $gp120^{BaL}$, $gp120^{ZM651}$ and $gp140^{AncC}$-mediated early and late apoptosis of activated CD4+ T lymphocytes

3.3.1 Establishment of a flow cytometric protocol for the analysis of Annexin V and 7-AAD staining of activated CD4+ T lymphocytes

A protocol measuring early and late apoptosis using Annexin V and 7-AAD staining was successfully established using untreated PBMCs and CD4-enriched PBMCs (subsequently called CD4+ T lymphocytes). Although the dot plots and protocol shown in Figure 3.14 were used for the Annexin V/7-AAD staining analysis of CD4+ T lymphocytes, the same parameters and settings were used for Annexin V/7-AAD staining analysis of PBMCs (data not shown). The entire cell population was confirmed in a FSC versus SSC dot plot (Figure 3.13A) and a dot plot measuring CD3-PC7 and CD4-PE staining was used to identify the majority CD3+CD4+ population (Gate H) (Figure 3.13B). The Annexin V versus 7-AAD staining dot plot was gated on Gate H, thereby displaying early and late apoptosis of CD3+CD4+ T lymphocytes only (Figure 3.14C). In addition, the depletion of CD8+ T lymphocytes was confirmed in a histogram measuring CD8-ECD staining (Figure 3.14D). Using various gating strategies, the unstained cells that produced a tail-like appearance around the well defined lymphocyte population in Figure 3.14B were established as non-specific staining through various gating strategies and were therefore not

included in the gate. An optimum gating strategy was used to develop optimal experiments.

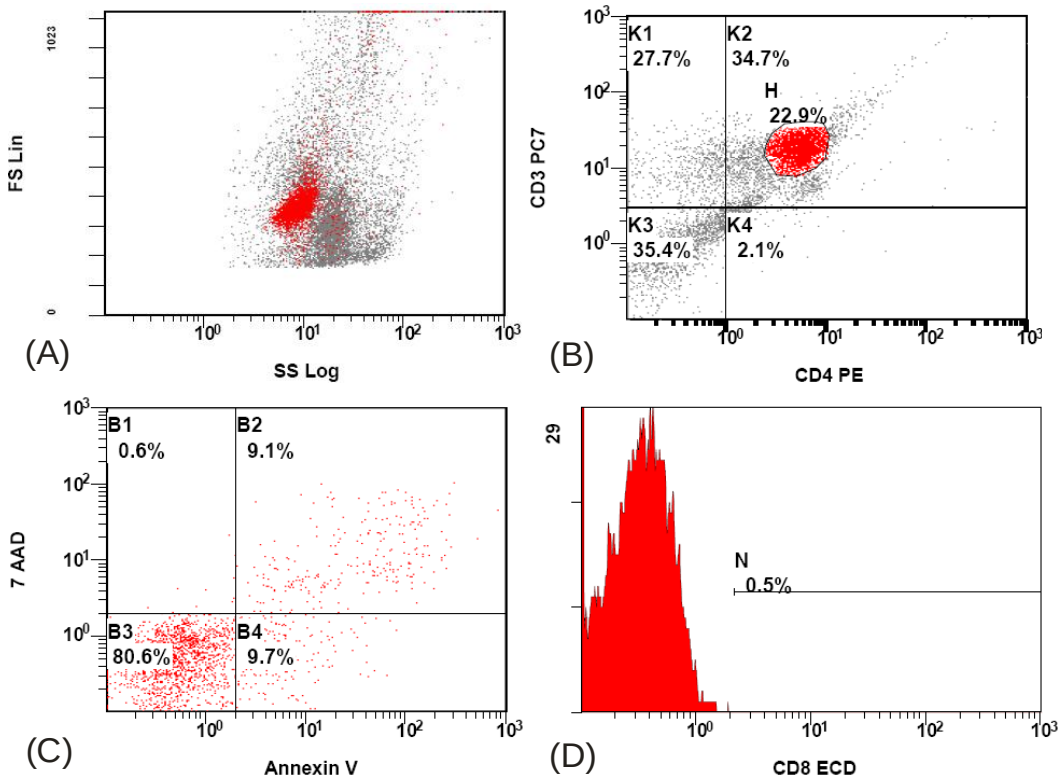

Figure 3.14: Annexin V and 7-AAD staining analysis of activated CD4+ T lymphocytes. (A) The entire CD8 depleted lymphocyte population, (B) the CD3-PC7 and CD4-PE positive lymphocytes shown in Gate H from the entire population shown in A, (C) Annexin V and 7-AAD staining analysis of the CD3+CD4+ T lymphocytes within Gate H and (D) an histogram showing CD8-ECD positive T lymphocytes. The viable CD4+ T lymphocytes are positioned within 10^0 as shown in (C).

To determine the difference between the use of PBMCs or CD4+ T lymphocytes, both types were activated and treated with recombinant $gp120^{BaL}$ followed by the flow cytometric analysis of early and late apoptosis by Annexin V/7-AAD staining, using the established protocol (Figure 3.14).

3.3.2 Apoptosis of PBMCs and CD4+ T lymphocytes mediated by 50nM $gp120^{BaL}$

The $gp120^{BaL}$-treated PBMCs and CD4+ T lymphocytes were subjected to Annexin V and 7-AAD staining analysis after 5, 24 and 48 hours post treatment and levels of early and late apoptosis were monitored. There was no apoptosis detected in the $gp120^{BaL}$-treated PBMCs or CD4+ T lymphocytes after 5 hours, but apoptosis levels increased at 24 and 48 hours post treatment, and were similar in both PBMCs and CD4+ T lymphocytes (results not shown). However, the dot plots and analyses were cleaner and more reproducible using the CD4+ T lymphocyte populations, thus, the CD4+ T lymphocytes were used in all subsequent apoptosis assays.

3.3.3 Detection of early and late apoptosis of uninfected CD4+ T lymphocytes mediated by 50nM and 100nM $gp120^{BaL}$, $gp120^{ZM651}$ and $gp140^{AncC}$

CD4+ T lymphocytes were treated with either a 50nM or 100nM concentration of recombinant $gp120^{BaL}$, $gp120^{ZM651}$ and $gp140^{AncC}$ to determine if the recombinant Env glycoproteins would have a dose-response effect on the induction of apoptosis. Dot

plots from the results obtained are shown in Figure 3.15, displaying the outcome of the staining analysis of untreated and Camptothecin-treated CD4+ T lymphocytes post 24 hours (Figure 3.15).

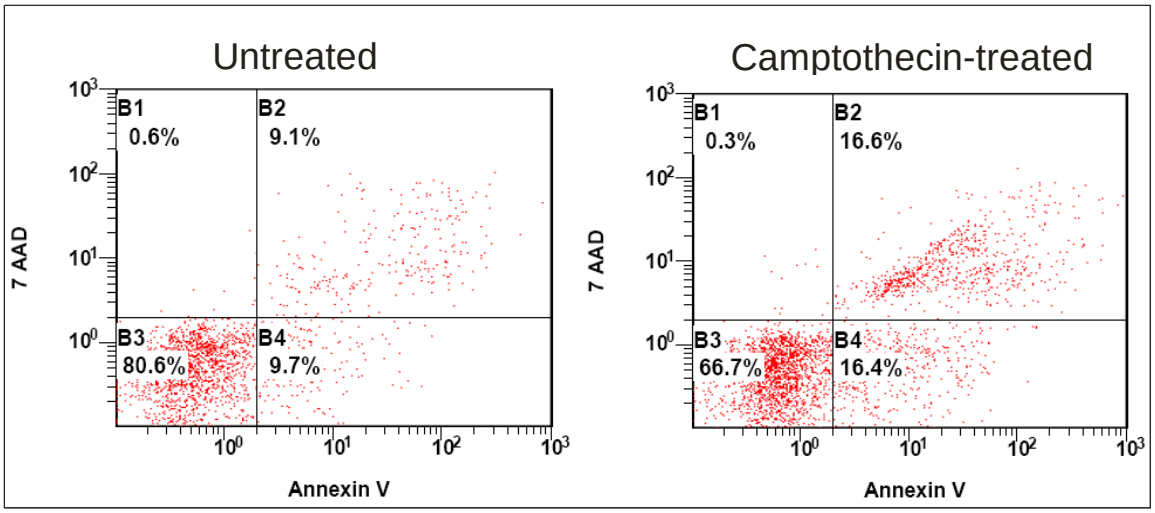

Figure 3.15: Dot plots demonstrating Annexin V and 7-AAD analysis of untreated and 4µM Camptothecin-treated CD4+ T lymphocytes from a single donor at 24 hours post treatment.

Interestingly, all recombinant Env glycoprotein-treated CD4+ T lymphocytes retained their abilities to stain positive for CD3-PC7 but displayed a decrease in CD4-PE staining after 24 hours of treatment (Figures 3.16D-F). This could be attributed to Env binding to all available molecules of surface CD4, or to CD4 downregulation post gp120 binding. Owing to this occurrence, Gate H surrounding the CD3+CD4+ T lymphocytes was extended during all Annexin V and 7-AAD staining (Figure 3.16) and TUNEL (dot plots not shown) analyses of the $gp120^{BaL}$, $gp120^{ZM651}$ and $gp140^{AncC}$-treated CD4+ T lymphocytes so to include all of the CD4+ T lymphocytes.

CD3-PC7 versus CD4-PE dot plots taken from the Annexin V and 7-AAD analysis protocol are shown in Figure 3.16, demonstrating the shift in the CD3+CD4+ T lymphocyte population.

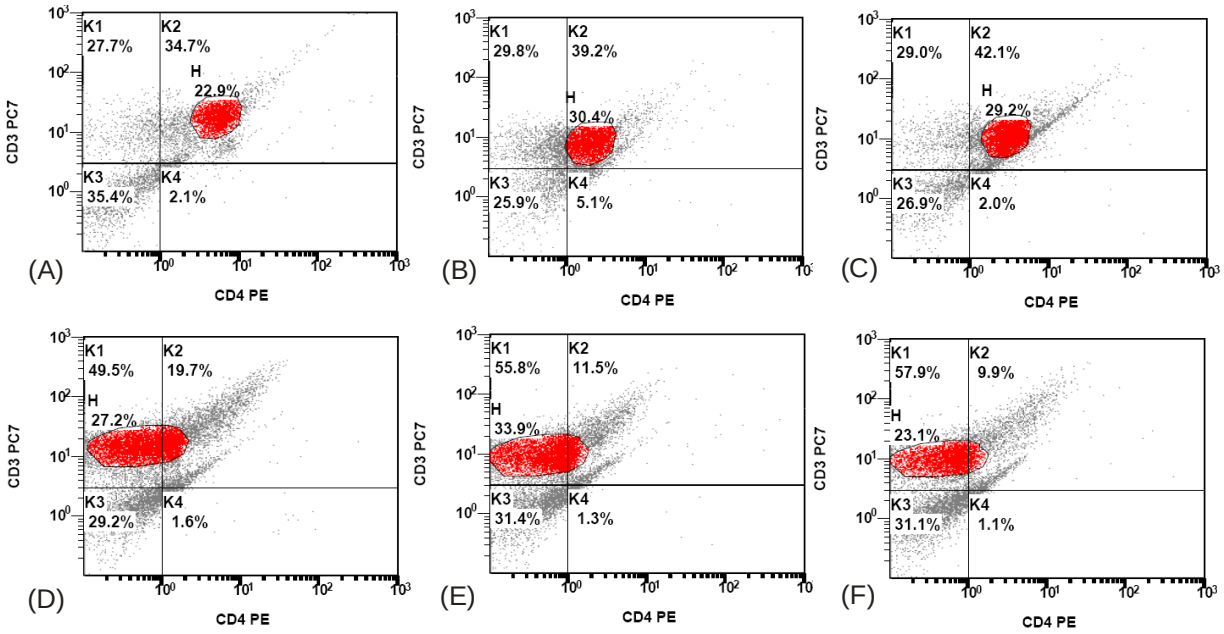

Figure 3.16: Changes in CD4-PE binding observed in CD4+ T lymphocytes after 24 hours of (D) $gp120^{BaL}$, (E) $gp120^{ZM651}$ and (F) $gp140^{AncC}$ treatment which did not occur in the (A) untreated, (B) mock-treated and (C) Camptothecin-treated CD4+ T lymphocytes during the Annexin V and 7-AAD staining analyses.

Relative to the baseline and after 48 hours of treatment, the 50nM concentrations of $gp120^{BaL}$, $gp120^{ZM651}$ and $gp140^{AncC}$ were able to induce an approximate 12.2%, 10.3% and 14.5% increase in late apoptosis of the CD4+ T lymphocytes, respectively (Figure 3.18). However, the increase in concentration of all three recombinant Env

glycoproteins to 100nM did not produce a dose response effect. After 48 hours of exposure to 100nM $gp120^{BaL}$, $gp120^{ZM651}$ and $gp140^{AncC}$, 9.7%, 7.3% and 10.4% of the CD4+ T lymphocytes were undergoing late apoptosis, respectively (Figure 3.19).

After being exposed to Camptothecin for 48 hours, 38.1% of the CD4+ T lymphocyte population was undergoing late apoptosis and entering necrosis (Figure 3.17). As mentioned before, the mock-treated CD4+ T lymphocytes demonstrated levels of late apoptosis that were higher at 24 and 48 hours post treatment in comparison to the untreated CD4+ T lymphocytes (Figure 3.17).

Overall, the results show an increase in the levels of late apoptosis in CD4+ T lymphocytes over time, attributed to the addition of recombinant $gp120^{BaL}$, $gp120^{ZM651}$ and $gp140^{AncC}$. Furthermore, higher levels of apoptosis were observed in the treated CD4+ T lymphocytes in comparison to the Jurkat T lymphocytes.

Apoptosis of $gp120^{BaL}$, $gp120^{ZM651}$ and $gp140^{AncC}$-treated CD4+ T lymphocytes was further confirmed by TUNEL analysis of chromosomal DNA fragmentation.

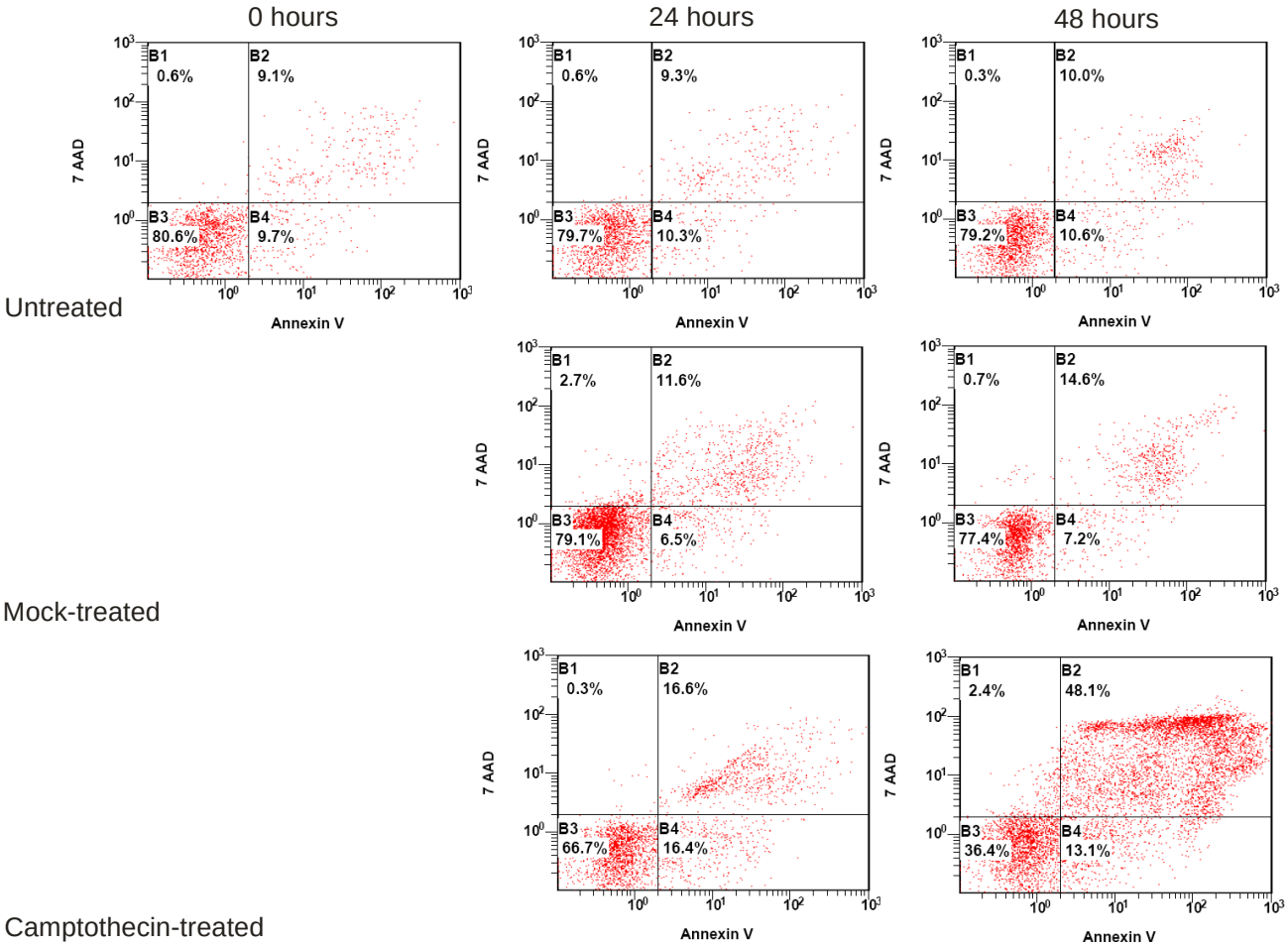

Figure 3.17: Annexin V and 7-AAD analysis of untreated, mock-treated and 4µM Camptothecin-treated CD4+ T lymphocytes from one donor at 24 and 48 hours post treatment. The Annexin V/7-AAD staining analysis of untreated CD4+ T lymphocytes at 0 hours are included for comparative purposes.

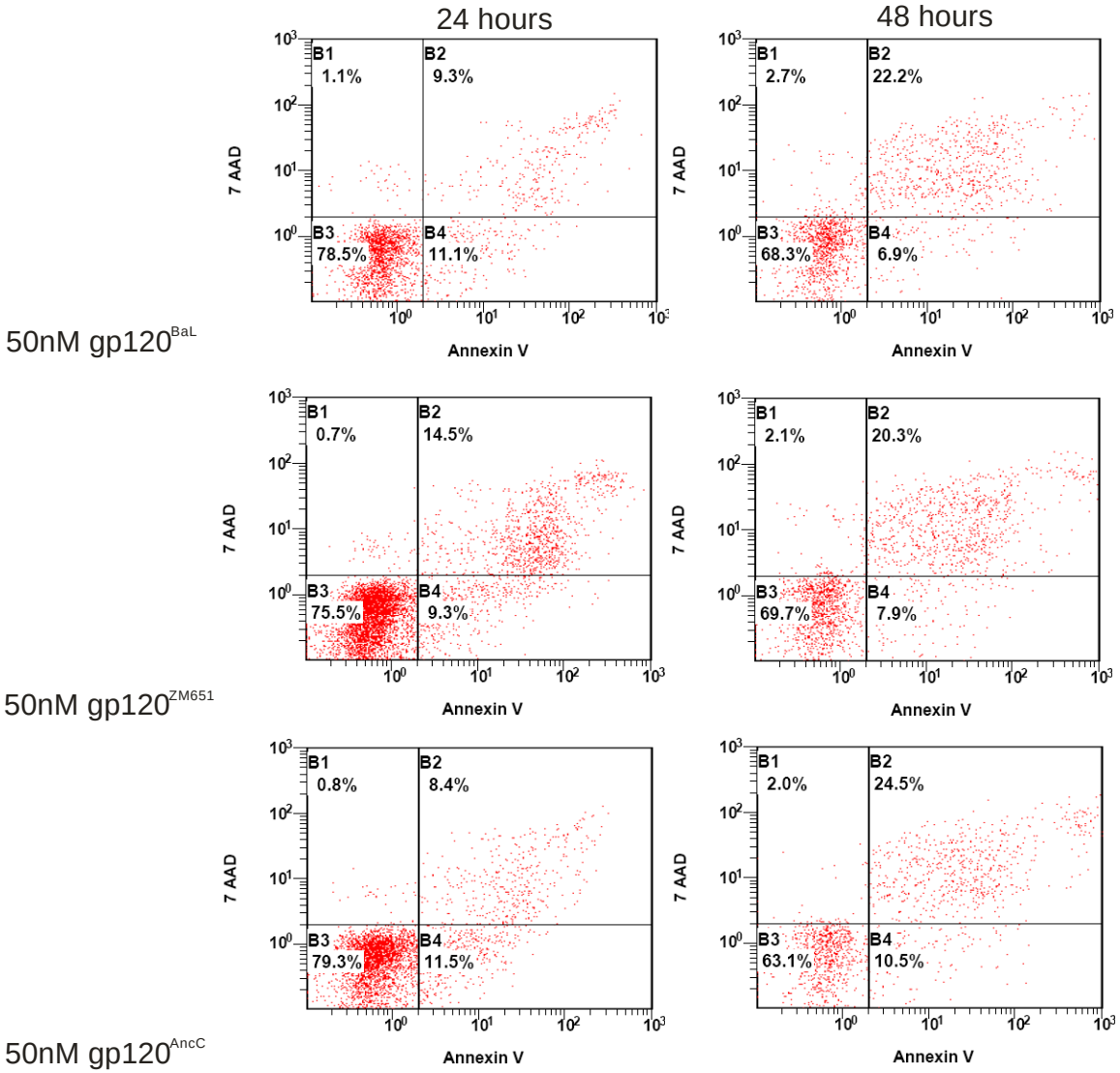

Figure 3.18: Annexin V and 7-AAD analysis of 50nM gp120^{BaL}, gp120^{ZM651} and gp140^{AncC}-treated CD4+ T lymphocytes from one donor at 24 and 48 hours post treatment.

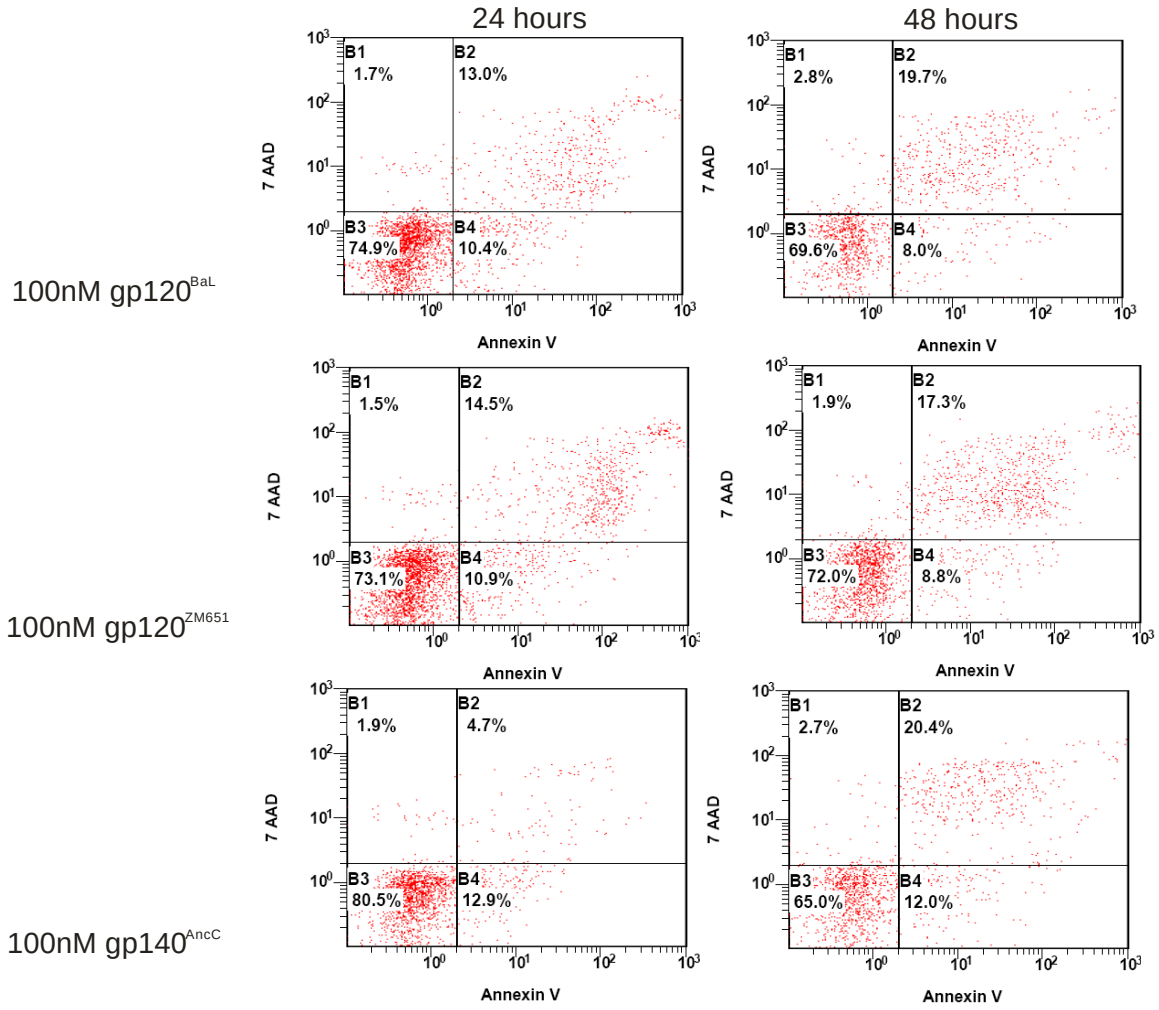

Figure 3.19: Annexin V and 7-AAD analysis of 100nM gp120^{BaL}, gp120^{ZM651} and gp140^{AncC}-treated CD4+ T lymphocytesfrom one donor at 24 and 48 hours post treatment.

The percentages of early and late apoptosis post 24 and 48 hours of 50nM and 100nM gp120^{BaL}, gp120^{ZM651} and gp140^{AncC} were subtracted from the baseline percentages at the same time points, and the differences are shown in Table 3.3. The data shown in the table are from an individual experiment that was performed using PBMC-derived CD4+ T lymphocytes from an individual donor.

Table 3.3: Percentages of early and late apoptosis of CD4+ T lymphocytes from a single donor mediated by 50nM and 100nM $gp120^{BaL}$, $gp120^{ZM651}$and $gp140^{AncC}$ after 24 and 48 hours of exposure.

Lymphocyte Treatments (CD4+ T lymphocytes)	Percentage of Early Apoptosis (Ann V+/7-AAD-) (%)		Percentage of Late Apoptosis (Ann V+/7-AAD+) (%)	
	24 hours	48 hours	24 hours	48 hours
Untreated	**10.3**	**10.6**	**9.3**	**10.0**
4µM Camptothecin	6.1	2.5	7.2	38.1
50nM $gp120^{BaL}$	0.8	-	-	12.2
100nM $gp120^{BaL}$	0.1	-	3.7	9.7
50nM $gp120^{ZM651}$	-	-	5.2	10.3
100nM $gp120^{ZM651}$	0.6	-	5.2	7.3
50nM $gp140^{AncC}$	1.2	-	-	14.5
100nM $gp140^{AncC}$	2.6	1.4	-	10.4

3.3.4 The analysis of DNA fragmentation in 50nM gp120^{BaL}, gp120^{ZM651} and gp140^{AncC}-treated CD4+ T lymphocytes

A protocol measuring chromosomal DNA fragmentation in untreated, 4µM Camptothecin-treated, mock-treated, gp120^{BaL}, gp120^{ZM651} and gp140^{AncC}-treated CD4+ T lymphocytes using TUNEL was successfully established using untreated CD4+ T lymphocytes (protocol not shown). The protocol was set up in the exact same manner used for the analysis of Annexin V and 7-AAD staining of CD4+ T lymphocytes, with the exception of a histogram, gated on CD3+CD4+ T lymphocytes, that measured TUNEL activity (protocol not shown).

The level of DNA fragmentation in untreated and Camptothecin-treated, mock-treated, 50nM gp120^{BaL}, gp120^{ZM651} and gp140^{AncC}-treated CD4+ T lymphocytes was analyzed by TUNEL after 0 and 65 hours of exposure (Figure 3.20). Relative to the untreated (0 and 65 hour) CD4+ T lymphocytes, gp120^{BaL}, gp120^{ZM651} and gp140^{AncC} induced up to 13.3%, 15.6% and 11.5% DNA fragmentation in the CD4+ T lymphocytes, respectively (Figure 3.20). Camptothecin-treated CD4+ T lymphocytes demonstrated 50.9% of DNA fragmentation while the mock-treated CD4+ T lymphocytes showed a slightly higher percentage (2.1% higher) of DNA fragmentation in comparison to the untreated control (Figure 3.20).

Interestingly, the Jurkat T lymphocytes seem to be more susceptible to camptothecin that the CD4+ T lymphocytes. The higher susceptibility observed in the Jurkat T lymphocytes may be attributed to the fact that they are immortalized. Overall, in comparison to the Jurkat T lymphocytes, $gp120^{BaL}$, $gp120^{ZM651}$ and $gp140^{AncC}$ were able to induce higher levels of apoptosis of CD4+ T lymphocytes during both the Annexin V/7-AAD and TUNEL analyses. Furthermore, $gp140^{AncC}$ demonstrated the highest level of late apoptosis post 48 hours during the Annexin V/7-AAD analysis (Figure 3.18) while $gp120^{ZM651}$ displayed the highest level of DNA fragmentation post 65 hours during the TUNEL analysis (Figure 3.20).

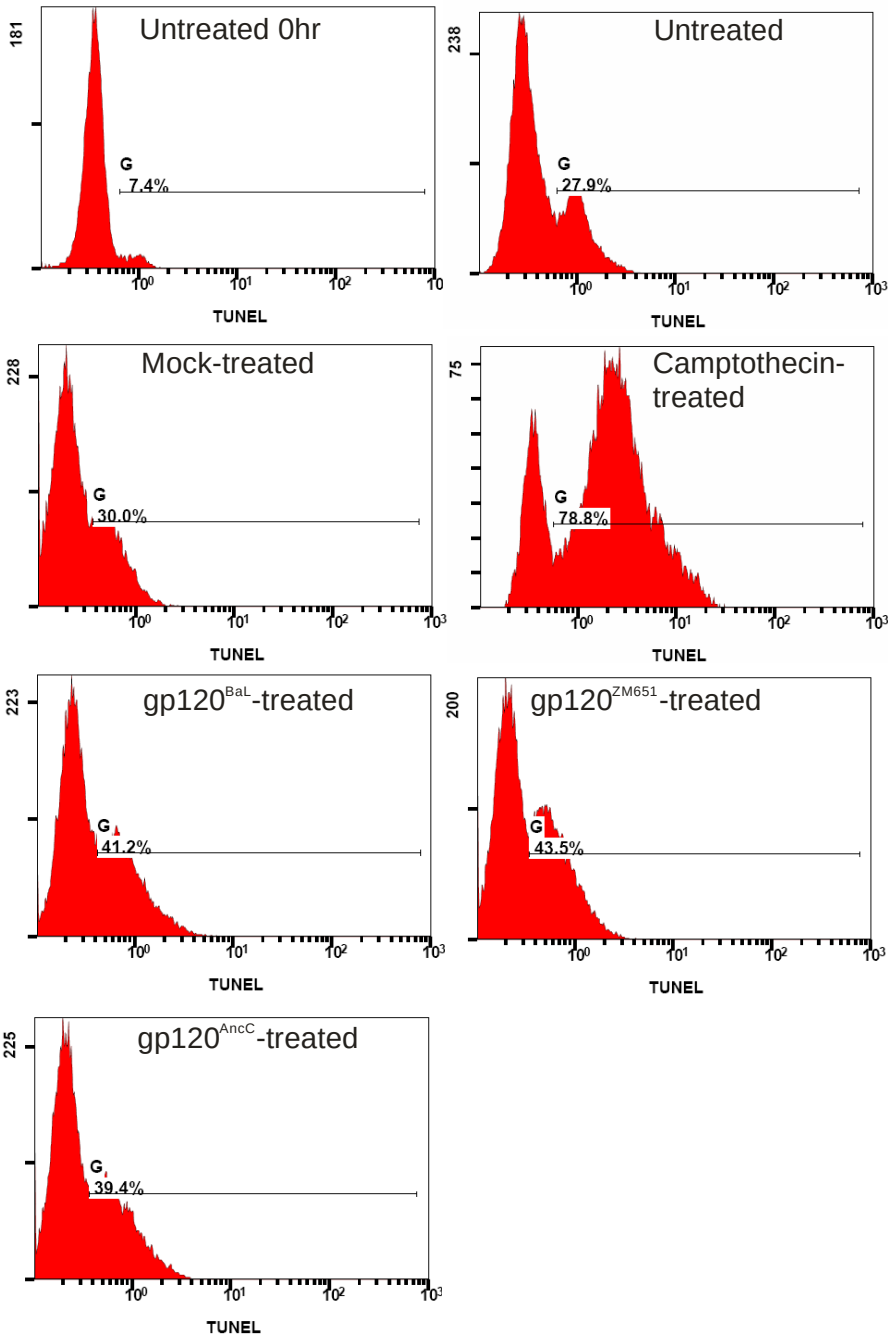

Figure 3.20: TUNEL analysis of DNA fragmentation in CD4+ T lymphocytes from a single donor induced by the addition of $gp120^{BaL}$, $gp120^{ZM651}$ and $gp140^{AncC}$ post 65 hours. The histogram of the untreated CD4+ T lymphocytes at 0 hours is included for comparative purposes. The percentage of TUNEL positive lymphocytes is presented on each histogram.

CHAPTER 4: DISCUSSION

Apoptosis of uninfected CD4+ T lymphocytes due to aberrant signalling initiated from the binding of HIV-1 gp120 to the CD4 receptor as well as co-receptors, CCR5 and CXCR4 has been described as a contributing mechanism to the depletion of CD4+ T lymphocytes which in turn correlates with disease progression to AIDS [192, 219, 263, 264]. The true mechanisms however, leading to uninfected CD4+ T lymphocyte death remain unclear and controversial. This study addressed the ability of recombinant HIV-1 $gp120^{BaL}$, $gp120^{ZM651}$ and $gp140^{AncC}$ (all CCR5-utilizing) to mediate apoptosis of Jurkat T lymphocytes and activated CD4+ T lymphocytes via interactions with CD4 only and CD4 and/or CCR5, respectively. .

The recombinant subtype B $gp120^{BaL}$ and subtype C $gp120^{ZM651}$ and $gp140^{AncC}$ glycoproteins used throughout the course of this study were successfully expressed in mammalian HEK 293T cells (Figure 3.2) [265, 266], purified using lectin affinity chromatography (Figure 3.3) [232, 267] and quantified (Figure 3.4). Previous studies have employed *Spodoptera frugiperda* (Sf9) insect cells (baculovirus expression system) [255, 268, 269] and other mammalian cell lines such as Chinese hamster ovary (CHO) cells [83, 227, 270] for the expression of functional Env glycoproteins. Mammalian cell expression systems are advantageous for Env glycoprotein expression, as they possess the necessary machinery required for post translational modifications such as glycosylation, which is imperative for the stability and proper folding of Env glycoproteins [83, 271, 272]. The insect glycosylation pathway is reportedly less complex than that of mammalian cells, consequently recombinant gp120 expressed in insect cells has been shown to contain carbohydrates with a high-mannose variety compared to the more complex carbohydrates found on gp120

expressed in mammalian cells [273, 274]. Therefore, the expression of our recombinant Env glycoproteins in a mammalian cell system was expected to produce correctly glycosylated and folded recombinant Env glycoproteins.

Expression in HEK 293T cells yielded approximately 1mg of purified $gp120^{BaL}$, $gp120^{ZM651}$ and $gp140^{AncC}$ per litre of culture supernatant, which was then estimated to be >90% pure through Coomassie Brilliant Blue staining analysis (Figure 3.3E). Using the same cell line and similar purification procedure, Varadarajan *et al*. (2005) were able to obtain yields of recombinant gp120 that ranged between 1-2mg per litre of culture supernatant [275]. Thus, the expression and purification protocol used in this study was relatively efficient, comparable to others and adequately addressed the needs of this project.

The purified recombinant $gp120^{ZM651}$, $gp120^{BaL}$ and $gp140^{AncC}$ Env glycoproteins were shown to be conformationally intact and functional in capture ELISA's (Figure 3.5A, B and C, respectively), and thus used in all subsequent apoptosis experiments. The MAb IgG1b12 was able to bind to all three glycoproteins in a dose dependent manner (Figures 3.5A, B and C). These results agree with previous studies that demonstrate significant binding of IgG1b12 to recombinant subtype C Env glycoproteins [9], primary virus isolates [276, 277] as well as cross-clade reactivity [278]. MAb IgG1b12, is known to have a high affinity for a highly conserved epitope that overlaps the CD4 binding site on gp120 [279]. The V1/V2 loops of gp120 have also been implicated in the IgG1b12-gp120 interaction [280]. The subtype B gp120 amino acid residues reported to be involved in the IgG1b12-gp120 interaction include S365,

D368, I371, Y384 and V430 [281]. Overall, binding of all three purified recombinant Env glycoproteins to IgG1b12 implied that their CD4 binding sites were conformationally intact.

Recombinant $gp120^{BaL}$ and $gp140^{AncC}$ showed enhanced binding affinities for 17b in the presence of sCD4 (Figures 3.5B and C) whereas extremely low binding activity was observed for $gp120^{ZM651}$ (Figure 3.5A). The 17b epitope overlaps the V1/V2 shielded CCR5 binding site [91, 98] and the amino acid residues that have been implicated in gp120 binding include K121, R419, I420, K421, Q422, I423 and Y435 [71, 282]. Since IgG1b12 was able to bind efficiently to $gp120^{ZM651}$, it can be suggested that the CD4 binding site of $gp120^{ZM651}$ is conformationally intact, but does not seem to undergo the conformational rearrangements required for the exposure of the co-receptor binding site which includes the overlapping 17b epitope. Alternatively, the 17b epitope is absent on $gp120^{ZM651}$. Since $gp120^{BaL}$ and $gp140^{AncC}$ showed enhanced binding to 17b in the presence of sCD4, the conformational integrity of their CD4 binding sites were further confirmed.

The ability of recombinant $gp120^{ZM651}$ to interact with CD4 was further corroborated in CD4 binding ELISA's (Figure 3.6). Like 17b, 48D binds to a highly conserved region on HIV-1 gp120 that becomes more accessible following the gp120-CD4 interaction [283, 284]. Our results showed that in the presence of sCD4, 48D was unable to interact with $gp120^{ZM651}$ as efficiently as it did with $gp120^{BaL}$ (Figure 3.6B and A, respectively). Comparably, 48D showed no binding activity against $gp140^{AncC}$ and $HIV\text{-}1_{96ZM651}gp120$ (Figure 3.6C and D, respectively). These results agree with a

previous finding that had demonstrated 48D binding to $gp120^{BaL}$, but showed poor reactivity against subtype C isolates [283, 284]. Therefore, it is clear that 48D is not a suitable antibody for the characterization of recombinant subtype C Env glycoproteins.

Since both 48D and 17b interact with CD4 induced epitopes, it has been suggested that these two antibodies share a common binding site [284]. It is possible that the amino acid residues required for a successful 48D-gp120 binding are similar, or overlap with those in the 17b-gp120 interaction. Well conserved gp120 regions, such as the ring structure linking the C3 and C4 regions, the base of the stem loop structure in the V1 and V2 loops, a ten amino acid sequence in the C2 region and the C5 region, have been implicated in 17b and 48D binding [284]. In addition, most of the gp120 residues implicated in 17b and 48D binding are hydrophobic [284], providing a potential explanation for the restricted accessibility of their epitopes prior to the gp120-CD4 interaction [284].

As expected, 2G12 showed a high affinity for $gp120^{BaL}$ but bound poorly to $gp120^{ZM651}$ and $gp140^{AncC}$ (Figures 3.5A, B and C). MAb 2G12 recognizes a cluster of high mannose sugars composed of external α 1-2 terminal mannose residues on gp120 [285, 286]. Mutational studies have demonstrated the importance of N-linked glycans at positions 295, 332 and 392 on gp120 in 2G12 binding [285-287]. A probable explanation for the poor binding activity of 2G12 to $gp120^{ZM651}$ and $gp140^{AncC}$ is that subtype C Env glycoproteins often lack the Asparagine residue at glycosylation site 295, and contain a valine residue instead [276, 288, 289]. More recently, it was

shown that glycosylation site 295 is not the sole determinant of 2G12 binding resistance and that glycosylation sites, 442 and 448 play a major role in the binding of 2G12 to subtype C viruses [287]. The ability of 2G12 to bind $gp120^{BaL}$ confirms that it is properly folded and glycosylated, while its inability to bind $gp120^{ZM651}$ and $gp140^{AncC}$ suggests differences in the structure and pattern of glycosylation between recombinant subtype B and C Env glycoproteins.

The initial Annexin V and 7-AAD staining protocol was used for the analysis of 50nM, 250nM and 500nM soluble recombinant $gp120^{BaL}$ and $gp120^{ZM651}$-mediated apoptosis and showed low levels of early and late apoptosis of uninfected Jurkat T lymphocytes. In addition, a dose dependent response effect on the levels of late apoptosis was not observed in the Jurkat T lymphocytes when treated with 250nM and 500nM recombinant $gp120^{BaL}$ and $gp120^{ZM651}$ post 48 hours (Table 3.1), as shown previously by Ullrich *et al.* (2000) in human umbilical vein endothelial cells using X4 gp120 and gp160 and by Hesselgesser *et al.* (1998) in Human hNT neurons in the absence of CD4 and through co-receptor signalling [237, 247].

Ullrich *et al.* (2000) utilized gp120 and gp160 at concentrations of 0.1µg/ml and 1 µg/ml and observed a dose dependent response at 10 hours post treatment through gp120-CXCR4 signalling [237]. Therefore, it is possible that complete saturation of the CD4 receptors with recombinant $gp120^{BaL}$ and $gp120^{ZM651}$ Env glycoproteins at concentrations of 30µg/ml (250nM) and 60µg/ml (500nM) after 24 and 48 hours of exposure, could have contributed to the lack of a dose dependent response observed in our study. Soluble gp120 concentrations within the lymph nodes of HIV-1 infected

patients reportedly range between 120-960ng/ml (~1nM-8nM) [290, 291] while the concentrations of gp120 within the serum of HIV-1 infected patients reportedly range from 12-92ng/ml (~0.1nM-0.76nM) [292]. Ideally, future work should investigate the apoptotic ability of a range of lower soluble Env glycoprotein concentrations that are similar to those reported in HIV-1 infected individuals. Furthermore, there seems to be a concentration effect of 50nM, 250nM and 500nM $gp120^{BaL}$ and $gp120^{ZM651}$ on early apoptosis of Jurkat T lymphocytes post 48 hours (Table 3.1). Forthcoming experiments should monitor apoptosis for more than 48 hours to determine if an optimal dose response effect can be attained.

Nevertheless, a higher level of early apoptosis and a lower level of late apoptosis was observed in the 250nM (7.4% early; 2.2% late) and 500nM (9.3% early; 2.5% late) $gp120^{BaL}$-treated Jurkat T lymphocytes in comparison to that of the 50nM $gp120^{BaL}$ (0.4% early; 6.9% late) treatment at 48 hours post exposure. A similar effect was observed in the $gp120^{ZM651}$-treated Jurkat T lymphocytes i.e. demonstrated a higher level of late apoptosis after 48 hours of exposure to 50nM $gp120^{ZM651}$ in comparison to the higher concentrations used (Table 3.1). This may be attributed to a dose dependent apoptotic response seen between the 50nM, 250nM and 500nM $gp120^{BaL}$ and $gp120^{ZM651}$ concentrations. A large proportion of the susceptible Jurkat T lymphocytes treated with the 250nM and 500nM concentrations of $gp120^{BaL}$ and $gp120^{ZM651}$ may have already undergone late apoptosis and necrosis at 48 hours post treatment (no staining), hence the detection of lower levels of late apoptosis. Future work could determine whether there is an Env-mediated dose dependent apoptotic response in Jurkat T lymphocytes by monitoring apoptosis more frequently, and for a

longer time period. In addition, the impact of ongoing Jurkat T lymphocyte cell division should be elucidated.

Using the modified protocol, higher levels of early than late apoptosis were observed after 48 hours of exposure to 50nM $gp120^{BaL}$, $gp120^{ZM651}$ and $gp140^{AncC}$ (Table 3.2 and Figure 3.12). Furthermore, there were higher levels of late apoptosis observed after 24 hours of exposure compared to those observed at 48 hours post treatment of all three Env glycoproteins. This phenomenon could be attributed to Jurkat T lymphocytes 'recovering' from late apoptosis. The apoptotic signalling via a gp120-CD4 interaction seems to be weak and consequently reversible as some Jurkat T lymphocytes were able to recover from late apoptotic events (Table 3.2 and Figure 3.12). It is likely that early apoptotic events are reversible as well, however that was not observed in this study or to our knowledge in previous studies of this type, and therefore cannot be confirmed. The weak signalling could be attributed to unstable interactions formed between $gp120^{BaL}$, $gp120^{ZM651}$ and $gp140^{AncC}$ and the CD4 receptor causing the recombinant Env glycoproteins to attach and then detach shortly thereafter. As a result, the apoptotic signals transduced were possibly incomplete or partially lost along the pathway resulting in the low levels of early and late apoptosis that were observed.

Since Jurkat T lymphocytes express CD4 receptors only, the apoptosis levels observed are presumably due to signalling cascades initiated solely by the interaction of recombinant $gp120^{BaL}$, $gp120^{ZM651}$ and $gp140^{AncC}$ with CD4. Apoptotic signalling via gp120-CD4 interactions has been reported previously in PBMCs and CD4+ T

lymphocytes [227, 231, 293]. Since CD4 is associated with $p56^{Lck}$, a T lymphocyte specific tyrosine kinase (also expressed in Jurkat and CEM T lymphocytes) [294], its involvement in CD4 signalling has been suggested [61, 295]. The cross linking of CD4 with gp120 reportedly upregulates CD4 associated $p56^{Lck}$ kinase activity which then decreases over long periods of time [296]. Decreased $p56^{Lck}$ activity is characterised by the dissociation of $p56^{Lck}$ from the CD4 receptor which can be caused by the interaction of gp120 with CD4 [296, 297].

Ultimately, several differences in the levels of apoptosis obtained after 48 hours of 50nM $gp120^{BaL}$ and $gp120^{ZM651}$ treatment were observed between the initial and modified flow cytometric protocols. Firstly, using the modified flow protocol, 50nM $gp120^{BaL}$ demonstrated similar levels of late apoptosis compared to those obtained using the initial flow protocol by 250nM and 500nM $gp120^{BaL}$ at 48 hours post treatment (Table 3.1 and 3.2 or Figure 3.12). Furthermore, using the initial protocol, 50nM $gp120^{BaL}$ induced higher levels of late apoptosis (6.9%) at 48 hours post treatment (Table 3.1 and 3.2 or Figure 3.12). In contrast, using the modified protocol, 50nM $gp120^{ZM651}$ was able to induce higher levels of early and late apoptosis compared to all three concentrations of $gp120^{ZM651}$ tested using the initial protocol (Table 3.1 and 3.2 or Figure 3.12). The introduction of the gating strategy used in the modified protocol may be responsible for these differences; however, the results obtained from the modified protocol are probably more reliable since the population of Jurkat T lymphocytes analysed was confirmed to be CD4 positive, suggesting that any levels of apoptosis detected were mediated via CD4 (Figure 3.9B).

In a similar study conducted by Wang *et al.* (2009), through lactate dehydrogenase (LDH) assays, 10nM recombinant IIIB gp120 was shown to significantly reduce the viability of non-activated Jurkat T lymphocytes after 24 and 48 hours of treatment [298]. To further verify that the reduction in cell viability was a product of pro-apoptotic signals, the active form of caspase 3, DISC formation as well as Bax expression were successfully detected within the gp120-treated Jurkat T lymphocytes after just 24, 6 and 3 hours, respectively [298]. In this study, the detection of DNA fragmentation by TUNEL analysis of the treated Jurkat T lymphocytes further validated that soluble recombinant $gp120^{BaL}$, $gp120^{ZM651}$ and $gp140^{AncC}$ were able to successfully induce low levels of apoptosis via CD4 signalling only (Figure 3.13).

Apoptosis induced by gp120 can also be analysed by utilizing a model in which gp120 is cross-linked with an anti-gp120 antibody and exposed to an anti-CD3 antibody [235, 299]. Using this model, Anand and Ganju, (2006) demonstrated gp120-mediated DNA fragmentation, indicative of apoptosis in Jurkat T lymphocytes via TUNEL analysis [235]. Furthermore, gp120-mediated apoptosis was analysed in the presence and absence of anti-CD3 and anti-gp120 antibodies, demonstrating ~5% apoptosis of Jurkat T lymphocytes treated with only gp120 and a five-fold increase in the percentage of apoptosis of the Jurkat T lymphocytes treated with gp120, anti-gp120 and anti-CD3 [235]. The percentage of apoptosis obtained when treated with gp120 only, agrees with those obtained in our study (Table 3.2 and Figures 3.12 and 3.13). However, since immune activation has been suggested in the regulation of HIV-1-mediated apoptosis [235], the model of cross-linking gp120 better simulates

the *in vivo* situation in HIV-1 infected individuals and should be further evaluated in future Env-mediated apoptosis studies.

The details of the binding kinetics between gp120, CD4 and co-receptors are not well understood. However, through single molecule analysis, Chang *et al.* (2005) were able to directly analyse the binding kinetics of a single gp120 molecule to single CD4 and CCR5 molecules [300]. In agreement with the possibility that $gp120^{BaL}$, $gp120^{ZM651}$ and $gp140^{AncC}$ form weak or unstable interactions with CD4, it was shown that the gp120-CD4 interaction is of a low strength, short-lived and unless CCR5 (or CXCR4 in the case of X4 isolates) is within close proximity to CD4, gp120 will detach rapidly from CD4 [300]. It was further suggested that gp120 prepares to form a bond with its co-receptor soon after it forms a bond with CD4 [300]. Additionally, the force required to break the gp120-co-receptor interaction is supposedly larger than that required to break the gp120-CD4 interaction [300].

Interestingly, it has been suggested that if the relevant co-receptor is not within close proximity of the CD4 receptor, gp120 presumably scans the cell membrane for a co-receptor during the short-lived gp120-CD4 interaction [301]. However, previous studies have shown that gp120 induces the actin-dependent co-localization of CD4 and its specific co-receptor during entry [302]. Once gp120 interacts with its co-receptor, it is unclear if it remains bound to CD4 [301]. Since CCR5 is absent on the Jurkat T lymphocytes, it is possible that the CCR5-utilizing $gp120^{BaL}$, $gp120^{ZM651}$ and $gp140^{AncC}$ remained bound to the CD4 receptors for a short and limited period of time, resulting in low levels of apoptosis and recovery of lymphocytes due to weak or short-

lived CD4 signalling. Similarly and more recently, Dobrowsky *et al.* (2008) proposed that the destabilization of the gp120-CD4 interaction over time and advancement to co-receptor interactions could be a viral mechanism that ensures efficient fusion and entry into the host cell [301].

CD4 has been shown to be expressed as monomers and covalently linked homodimers on T lymphocytes, monocytes and macrophages, with the monomeric form prevailing on monocytes and lymphocytes [303, 304]. The organization of CD4 and co-receptors on the lymphocyte surface appears to play a significant role during Env-mediated apoptosis, and this may vary with cell types [305]. Therefore, in addition to a short-lived gp120-CD4 interaction in the absence of a co-receptor, the organization of CD4 receptor molecules on the Jurkat T lymphocytes could be a contributing factor to the low levels of apoptosis that were detected.

In comparison to the non-activated Jurkat T lymphocytes, higher levels of apoptosis were observed in the 50nM soluble recombinant $gp120^{BaL}$, $gp120^{ZM651}$ and $gp140^{AncC}$-treated, activated and uninfected CD4+ T lymphocytes (Table 3.3 and Figures 3.18). Contrary to several other findings which demonstrated soluble recombinant CCR5-utilizing gp120-mediated apoptosis after 5 [227] and 16 hours in PBMCs [239] and 6 hours and 10 hours in HUVEC cells [237], insignificant levels of apoptosis of CD4+ T lymphocytes were observed after 5 hours of exposure to 50nM $gp120^{BaL}$ (data not shown). Consequently, 50nM $gp120^{BaL}$, $gp120^{ZM651}$ and $gp140^{AncC}$-mediated apoptosis of CD4+ T lymphocytes was analysed at 24 and 48 hours post treatment. The levels of apoptosis observed in our study agree with previous findings that

demonstrate 10-15% of apoptosis mediated by gp120 [220, 231]. Roggero *et al.* (2001) observed similar levels of apoptosis even though gp120 was presented in a membrane-bound form, suggesting that soluble and membrane-bound Env glycoproteins are able to induce similar levels of apoptosis. Arthos *et al*. (2002) demonstrated approximately 4% and 7% apoptosis of 50nM R5 gp120-treated activated PBMCs via Annexin V/propidium iodide staining (post 5 hours) and TUNEL analysis (post 65 hours), respectively [227]. These apoptotic percentages are slightly lower than those obtained in our study; however it is possible that if a longer incubation period was allowed, the levels of apoptosis obtained would have been similar to ours. As observed previously and in our study, incubation times of 24 hours or more with soluble recombinant gp120 appear to be required to achieve low levels of bystander apoptosis [229].

Since the CD4+ T lymphocytes express CD4 and co-receptor molecules, the apoptotic signalling observed could be attributed to both gp120-CD4 and gp120-CCR5 signalling. Only a few primary CD4+ T lymphocytes express detectable levels of CCR5 [306, 307], however in support of the present study, R5 viruses have been shown to induce a significant decline in infected and uninfected CD4+ T lymphocytes via apoptosis by inducing expression of Fas and caspase 8 [224, 263, 306, 308].

Differences between the Jurkat and CD4+ T lymphocytes that explain the variable results obtained could possibly include activation states and the presence of a co-receptor on the cell surface. Kinet *et al.* (2002) demonstrated the importance of the activation state of CD4+ T lymphocytes in gp120-mediated signalling via CD4 and co-

receptors CXCR4 or CCR5 [309]. The mitogen-activated protein kinase (MAPK) pathway was shown to be activated by gp120 in CD4+ T lymphocytes that had been activated via their T-cell receptors (TCR) via CD4 and co-receptors, and this was not observed in non-stimulated T lymphocytes [309]. Furthermore, gp120 has been shown to activate the MAPK pathway in activated CD4+ Jurkat T lymphocytes [309, 310].

Since the CD4+ T lymphocytes used in the current study were activated with PHA and pre-stimulated with hIL-2 before treatment with recombinant $gp120^{BaL}$, $gp120^{ZM651}$ and $gp140^{AncC}$, they were in a highly activated state. Therefore, the heightened state of immune activation is probably associated with the higher levels of apoptosis observed and the presence of co-receptors on the activated CD4+ T lymphocytes possibly provides additional apoptotic signals through gp120 interactions. Because different levels of PHA activation could impact on results obtained, this should be addressed in future studies. In addition, future work including the analysis of the contribution of the CCR5 co-receptor in subtype C R5 gp120-mediated apoptosis would be beneficial. These studies could be conducted in the presence and absence of the CCR5 inhibitor, TAK-779 [311] or by using CD4+ T lymphocytes that do not express CCR5 [312]. Dissecting out the important steps that follow gp120-CD4 and gp120-CCR5 interactions would assist in understanding the processes involved in the culmination of apoptotic signals that are activated by these interactions on CD4+ T lymphocytes.

The role of the CD4 receptor and co-receptors CCR5 and CXCR4 in Env-mediated apoptosis of activated PBMCs have been investigated previously. Arthos *et al.* (2002) confirmed that the Env-CD4 interaction is able to induce significant levels of apoptosis in the absence of a co-receptor [227]. Moreover, the levels of apoptosis were enhanced in the presence of co-receptors with X4 gp120 inducing higher levels of apoptosis than the R5 gp120 [227].

Interestingly, analogous signalling cascades appear to be initiated by gp120 and the natural ligands for CXCR4 and CCR5 upon binding [310, 313]. The interaction of HIV-1 gp120 with CCR5 on macrophages seems to activate ion channels for the transport of K^+, Cl^- and Ca^{2+} resulting in elevated levels of intracellular Ca^{2+} [232]. In addition, there have been implications for the involvement of CXCR4 in the induction of CD95-independent apoptosis in CD4+ T cells [314]. Evidently, important signals are transduced after the interaction of HIV-1 gp120 with CCR5/CXCR4.

The ability of monomeric $gp120^{BaL}$ and $gp120^{ZM651}$ and trimeric/oligomeric $gp140^{AncC}$ to induce apoptosis was compared in the Jurkat T lymphocytes and CD4+ T lymphocytes. Annexin V/7-AAD staining (analysed using the modified flow cytometric protocol) and TUNEL analysis revealed that the levels of Jurkat T lymphocyte apoptosis induced by trimeric/oligomeric $gp140^{AncC}$ were similar to those induced by monomeric $gp120^{BaL}$ and $gp120^{ZM651}$. Furthermore, the levels of apoptosis induced were very similar between the subtype B and C Env glycoproteins. These findings agree with those of Machuca *et al.* (2004) who showed inconsequential differences in the degree of apoptosis of PBMCs and CEM.NKR-CCR5 cells induced between

several HIV-1 group M viral isolates [315]. This suggests that recombinant R5 monomeric $gp120^{BaL}$, monomeric $gp120^{ZM651}$ and trimeric/oligomeric $gp140^{AncC}$ were able to induce similar levels of apoptosis in Jurkat T lymphocytes in a conformation and subtype independent manner. Similarly, Zhang *et al.* (2001) reported comparable affinities between trimeric and monomeric HIV-1 gp140 for sCD4 [316] while, Bardi *et al.* (2006) demonstrated comparable levels of apoptosis of human neuroblastoma cells and mouse pre-B 300-19 cells, induced between monomeric and oligomeric IIIB gp120 even in the absence of CD4 [317].

It can therefore be suggested that monomeric and oligomeric Env glycoproteins are able to induce comparable levels of apoptosis in Jurkat T lymphocytes, human neuroblastoma cells and mouse pre-B 300-19 cells. It is worth noting that subtype B gp120 demonstrated higher levels of apoptosis compared to subtype C gp120 during the Annexin V/7-AAD analysis using the initial flow cytometric protocol (Table 3.1). Because of our contrasting findings regarding the differences in apoptosis based on different Env glycoprotein subtypes, further investigation is required to confirm whether there is a significant difference in apoptosis induced between subtype B and C Env glycoproteins.

A huge difference in the degree of apoptosis induced between the subtype B and C Env glycoproteins was not observed during the Annexin V/7-AAD and TUNEL analyses of the treated CD4+ T lymphocytes, but rather between the different forms i.e. monomeric versus oligomeric. During the Annexin V/7-AAD analysis, the oligomeric $gp140^{AncC}$ at a concentration of 50nM seemed to induce higher levels of

apoptosis in comparison to monomeric gp120^{BaL} and gp120^{ZM651} (Figure 3.18), while during the TUNEL analysis, gp120^{ZM651} induced higher levels of DNA fragmentation in comparison to gp120^{BaL} and gp140^{AncC} (Figure 3.20). Moreover, when used at a concentration of 100nM, slight variations in the levels of apoptosis induced by all three Env glycoproteins was observed. Interestingly, and similarly to Arthos *et al*. (2002) who utilized X4 gp120 (HIV-1 92UG21-9) [227], an increase in the levels of apoptosis was not observed when CD4+ T lymphocytes were treated with 100nM gp120^{BaL}, gp120^{ZM651} and gp140^{AncC} (Figure 3.19). However, a dose dependent effect of gp120 on apoptosis has been observed previously in CD4+ [251, 299] and CD8+ T lymphocytes [318]. Different forms of gp120 (monomeric, trimeric and oligomeric) exist in an infected individual, possibly in varying proportions; however the concentrations of each *in vivo* are unclear and would vary with patients' viral loads.

Since our experiments were performed using CD4+ T lymphocytes from different donors, the discrepancies in the results obtained could be due to donor variability or the different methodologies used. For example, Accornero *et al.* (1997) used the model in which the CD4+ T lymphocytes were treated with gp120 cross-linked with anti-gp120 and anti-CD3 antibodies [299]. Since slight variations in the levels of apoptosis induced by 50nM and 100nM monomeric gp120^{BaL} and gp120^{ZM651} and trimeric/oligomeric gp140^{AncC} were observed during both the Annexin V/7-AAD (Figure 3.18 and 3.19) and TUNEL analyses (Figure 3.20), the difference in apoptosis induced between monomeric and trimeric/oligomeric Env glycoproteins is unclear and additional studies are required to clarify whether a difference may exist. Furthermore,

forthcoming experiments should employ a single donor to limit any inconsistencies due to donor variation.

In a recent study, HIV-1 subtype C Vpr was found to induce lower levels of apoptosis of 293T cells in comparison to subtype B Vpr [319]. Presumably, the effect of other pro-apoptotic HIV-1 proteins on the level of apoptosis induced may vary between subtypes. Moreover, differences in apoptosis induced by different HIV-1 subtypes during HIV-1 infection are possibly influenced by a collective contribution from each pro-apoptotic HIV-1 protein.

An interesting observation during both the Annexin V/7-AAD and TUNEL analysis of the recombinant R5 $gp120^{BaL}$, $gp120^{ZM651}$ and $gp140^{AncC}$-treated CD4+ T lymphocytes, was the shifting of the CD4+ CD3+ lymphocyte population into the CD4-CD3+ quadrant after just 24 hours of exposure (Figure 3.15). The inability of the CD4-PE antibody to stain the lymphocytes could be because $gp120^{BaL}$, $gp120^{ZM651}$ and $gp140^{AncC}$ have remained bound to the CD4 receptors. If this is the case, then it can be suggested that the CD4-PE antibody $gp120^{BaL}$, $gp120^{ZM651}$ and $gp140^{AncC}$ share a common binding site. Another explanation for this phenomenon could be the down regulation of CD4 receptors post Env glycoprotein treatment. Long and short term exposure of CEM cells to gp120 has been investigated previously by Juszczak *et al.* (1991), demonstrating that 20 hours of gp120 exposure resulted in a 35% decrease of cell surface expressed CD4 [296]. Moreover, the down regulation of CD4 receptors occurs subsequent to the dissociation of CD4-$p56^{Lck}$ complex which is thought to be caused by gp120 binding [296]. This phenomenon was not observed in

the recombinant $gp120^{BaL}$, $gp120^{ZM651}$ and $gp140^{AncC}$-treated Jurkat T lymphocytes, possibly due to the absence of the CCR5 co-receptor which reportedly establishes a stronger interaction with gp120 post CD4 receptor binding. This interesting observation warrants further investigation into the expression levels of CD4 molecules on the surface of Jurkat and CD4+ T lymphocytes.

During the course of HIV-1 infection, CCR5-utilizing viruses switch to CXCR4-utilizing viruses which in turn correlates with the progression to AIDS which is defined by a progressive decline in CD4+ T lymphocytes [76]. Therefore, since apoptosis is one of the main contributors to CD4+ T lymphocyte depletion, it can be hypothesized that R5 gp120 induces low levels of apoptosis throughout the course of HIV-1 infection, however, upon increased incidence of X4 gp120, the levels of apoptosis intensify. Furthermore, R5 viruses are preferentially transmitted; therefore, intense rates of apoptosis induced by these viruses would not be beneficial for their survival. Previously, it was shown that both X4 and R5 viruses are very similar in terms of active viral replication and cytopathicity, however, X4 viruses tend to induce a more rapid decline in CD4+ T lymphocytes due to the fact that CXCR4 is expressed more extensively than CCR5 [320, 321].

Overall, the levels of apoptosis seen in this study are not extremely high but probably correlate with those occurring in typical progressor patients i.e. a gradual turnover of CD4+ T lymphocytes and depletion over approximately 10 years. Apoptosis of immune cells during the early stages of in HIV-1 infection is believed to be involved in the disruption of the anti-HIV immune response which ultimately affects disease

progression [322]. To assist in understanding the role of Env-mediated-apoptosis in disease progression, it would be beneficial to evaluate and compare the difference in the levels of apoptosis induced between subtype C R5 and X4-utilizing Env glycoproteins relative to the different stages of HIV-1 infection. These studies could be conducted *in vitro*, through the comparison of subtype C R5 and X4 Env glycoprotein induced apoptosis of PBMC's from HIV-1, subtype C positive donors at different clinical stages of infection.

In summary, the present study demonstrated that recombinant $gp120^{BaL}$, $gp120^{ZM651}$ and $gp140^{AncC}$ were able to induce pro-apoptotic signals in uninfected Jurkat T lymphocytes as well as in uninfected activated CD4+ T lymphocytes. Apoptotic signalling in the Jurkat T lymphocytes can be attributed to signalling via the CD4 receptor, while the apoptotic signalling in the CD4+ T lymphocytes were likely transduced via CD4 and co-receptor engagement, potentially with additional contributing signals from the activated TCR. Elucidating the apoptotic events induced by HIV-1 gp120 could assist in understanding HIV-1 disease progression and CD4+ T lymphocyte depletion in AIDS patients and could lead to novel therapeutic strategies and antiretroviral drug discoveries. Therapeutic developments that could possibly block or inhibit apoptotic signal transduction at early or late stages of the pathway could drastically affect patient outcomes and CD4+ T lymphocyte counts.

APPENDICES

APPENDIX A: Laboratory Recipes

A.1 Solutions for bacterial cell culture, production of competent *E. coli* DH5α cells and transformation of competent *E. coli* DH5α cells

Luria-Bertani (LB) Broth

10g of tryptone powder (Oxoid, Hampshire, England), 5g of yeast extract powder (Biolab, Wadeville, Gauteng, South Africa) and 5g of NaCl (Sigma-Aldrich, Steinheim, Germany) was dissolved in sH_2O (Dismed Criticare, Midrand, South Africa) and made up to a final volume of 1L. The broth was autoclaved (121ºC, 20 minutes) and stored at room temperature until use.

LB Agar plates

3g of agar powder (Biolab, Wadeville, Gauteng, South Africa) was dissolved in 200ml of LB broth. The agar was autoclaved and cooled before the ampicillin (100µg/ml) (Roche, Mannheim, Germany) was added (Ex: 200ml of broth or agar = 200µl ampicillin). Thereafter, the agar was poured into 90mm Petri dishes under sterile conditions and allowed to set at room temperature.

70% (v/v) Ethanol (1L)

1.4L >99.9% Ethanol (Merck, Hohenbrunn, Germany) was made up to a final volume of 2L with sH_2O (Dismed Criticare).

Ampicillin (100mg/ml)

1g Ampicillin (Roche) was dissolved in 10ml of 70% Ethanol (Merck). The stock solutions were stored at -20^{o}C in 1ml aliquots until required.

Transformation Buffer (100mM $CaCl_2$, 10mM PIPES-HCl, 15% Glycerol, pH 7.0)

1.4702 g of $CaCl_2.2H_2O$ (Sigma-Aldrich, Steinheim, Germany), 0.3024 g of PIPES (Boehringer Mannheim, GmbH, Germany) and 15ml of glycerol (Merck, Hohenbrunn, Germany) were made up to a final volume of 100 ml with sH_20 (Dismed Criticare). The pH of the solution was adjusted to 7.0 using 10M NaOH (Merck, Darmstadt, Germany), and the buffer was autoclaved and stored at -20 ºC until use.

A.1.2 Isolation of plasmid DNA (Protocol obtained from the QIAfilter Plasmid Purification Handbook, Qiagen)

All buffers were provided in the Qiagen QIAfilter™ Plasmid Maxi Kit (Qiagen, Maryland, USA).

Composition of Resuspension Buffer P1 (50mM Tris-Cl, 10mM EDTA, 100µg/ml RNase A)

6.06g of Tris base powder

3.72g $Na_2EDTA.2H_2O$

The pH of the solution was adjusted to 8.0 with HCl before being made up to a final volume of 1L with sH_2O. For every litre of P1 buffer, 100mg of RNase A was added. Stored at 4ºC after the addition of RNase A.

Composition of Lysis Buffer P2 (200mM NaOH, 1% SDS)

8.0g NaOH pellets

50ml of 20% Sodium Dodecyl Sulphate (SDS) (w/v) solution

Made up to 1L in sH_2O and stored at room temperature

Composition of Neutralization Buffer P3 (3.0M Potassium acetate)

294.5g Potassium Acetate

The pH was adjusted to 5.5 with glacial acetic acid before the final volume was adjusted to 1L with sH_2O. This solution was stored at room temperature.

Composition of Buffer QBT ((750mM NaCl, 50mM MOPS, 15% isopropanol, 0.15% Triton X-100)

43.83g NaCl

10.46g MOPS (free acid)

The pH was adjusted to 7.0 with NaOH before 150ml of pure isopropanol and 15ml of 10% Triton X-100 solution (v/v) was added. The final volume was adjusted to 1L with sH_2O and stored at room temperature.

Composition of Buffer QC (1.0M NaCl, 50mM MOPS, 15% isopropanol)

58.44g NaCl

10.46g MOPS (free acid)

The pH was adjusted to 7.0 with NaOH before 150ml of pure isopropanol was added. The final volume was adjusted to 1L with sH_2O and stored at room temperature.

Composition of Buffer QF (1.25M NaCl, 50mM Tris-Cl, 15% isopropanol)

73.05g NaCl

6.06g Tris base powder

The pH was adjusted to 8.5 with HCl before 150ml of pure isopropanol was added. The final volume was adjusted to 1L with sH_2O and stored at room temperature.

A.1.3 Agarose Gel Electrophoresis

0.5M Ethylenediamine tetraacetic acid (EDTA) (pH 8.0)

93.05 g of EDTA powder (Calbiochem, CA, USA) was dissolved in sH_20 (Dismed Criticare) to a final volume of 500 ml. The pH of the solution was adjusted to 8.0 using 10M NaOH and subsequently autoclaved and stored at room temperature until use. The EDTA was only soluble once the pH had reached 8.0.

50X Tris Acetate EDTA (TAE) Buffer

242 g of Tris (hydroxymethyl)-aminoethane (Sigma-Aldrich, Steinheim, Germany), 57.1 ml of glacial acetic acid (Merck, Hohenbrunn, Germany) and 100 ml of 0.5 M EDTA (Calbiochem) were mixed with sH_20 (Dismed Criticare) to a final volume of 1 L

and stored at room temperature until use. Immediately before use, the solution was diluted to 1X TAE by mixing 20ml of 50X TAE with 980ml of sH_20 (Dismed Criticare).

6X DNA Loading Buffer

0.25% Bromophenol Blue (Merck Chemicals, Saarchem, Wadeville, South Africa) and 30% glycerol (Merck) was made up in 10ml of sH_2O (Dismed Criticare). The buffer was stored in 1ml aliquots at -20^oC until required.

0.8% Agarose gel

0.8g of agarose powder (Sigma-Aldrich, Steinheim, Germany) was added to 100ml of 1X TAE buffer and heated until the agarose powder had dissolved completely. The agarose solution was cooled slightly before 7.5µl of Ethidium Bromide (Promega Corporation, Madison, USA) was added to it (used at a concentration of 0.5µg/ml). Finally the solution was poured into a Bio-Rad Gel Chamber System (Bio-Rad, Hercules, CA) and allowed to set.

A.2 Mammalian Cell culture

Complete culture media

50ml Heat-inactivated (56^oC water bath for 30 min) Fetal Calf Serum/Bovine serum (Gibco; Grand Island, USA), 5ml 200mM 100X stock L-glutamine (Gibco; Grand Island, USA), 2.5ml 10000µg/ml Penicillin-Streptomycin (Gibco; Grand Island, USA) was added to 500ml RPMI 1640 without L-glutamine (Sigma-Aldrich; Steinheim, Germany) in the case of Jurkat T lymphocytes and CD4+ T lymphocytes or 500ml DMEM (Sigma-Aldrich; Steinheim, Germany) in the case of HEK 293T cells.

Freezing Mix

50% of heat-inactivated FCS, 40% RPMI/DMEM and 10% filter sterilized (0.2 µM Acrodisc® 25 mm syringe filters; Pall Corporation, Ann Arbor, MI, USA) Dimethyl-sulphoxide (DMSO) ((Fluka Biochemika, Steinheim, Germany) was made up to the

volume required and 1ml of the freezing mix was added per $1x10^6$ cells. The freezing stocks were aliquoted in 1 ml quantities into autoclaved cryovials (Nunc, Roskilde, Denmark) and stored in a nest box overnight at -80ºC, and moved into liquid nitrogen storage until required.

A2.1 Solutions for Calcium Chloride ($CaCl_2$) transfections

2.5M $CaCl_2$

91,85g $CaCl_2.H_2O$ (Sigma-Aldrich) was dissolved in sH_2O (Dismed Criticare) to a final volume of 250ml. The solution was filter sterilized using 0.2 µM Acrodisc® 25 mm syringe filters (Pall Corporation) and stored at -20^{o}C in 10ml aliquots until required.

2x HEPES (280mM NaCl, 50mM Hepes, 1.5mM $Na_2HPO_4.2H_2O$)

0.817g NaCl (Sigma-Aldrich), 0.6g Hepes (Sigma-Aldrich, Steinheim, Germany) and 0.013g $Na_2HPO_4.2H_2O$ (Sigma-Aldrich, Steinheim, Germany) was dissolved in sH_2O to a final volume of 50ml. The pH was adjusted to 7.7 using 10M NaOH and the solution was filter sterilized and stored in 5ml aliquots at -20^{o}C until required.

A2.2 Solutions for Protein Purification

1M NaCl in 1X PBS

29.22g of NaCl (Sigma-Aldrich) was dissolved in ice-cold 1X Dulbecco's Phosphate Buffered Saline (without $CaCl_2$) (PBS) (Sigma-Aldrich, Steinheim, Germany) to a final volume of 500ml. This solution was stored at 4ºC until required.

0.75M Methyl α-D-mannopyranoside (MMP)

7.4g of MMP (Sigma-Aldrich, Steinheim, Germany) was dissolved in ice-cold 1X PBS to a final volume of 50ml. This solution was prepared fresh every time before required.

0.01% Sodium Azide

0.01g of Sodium Azide (extremely neurotoxic) (Sigma-Aldrich, Steinheim, Germany) was weighed out in a fume hood and dissolved in 100ml of sH_20. This solution was stored at room temperature until required.

BSA Protein Assay Kit (Thermo Scientific)

Reagent A contains sodium carbonate, sodium bicarbonate, bicinchonic acid and sodium tartrate in 0.1M NaOH.

Reagent B contains 4% cupric sulfate

A.3 Solutions for SDS-PAGE

10X Tank Buffer pH 8.3

30.3g of Tris (hydroxymethyl)-aminoethane (Sigma-Aldrich, Steinheim, Germany), 144.1g of Glycine (Merck, Darmstadt, Germany) and 10g of SDS (Merck, Darmstadt, Germany) was dissolved in 1000ml of sH_20. The solution was diluted 10 times before use and stored at room temperature.

4X Stacking Gel Buffer pH 6.8

30.2g of 0.5M Tris was dissolved in 100ml of sH_20. The pH was adjusted to 6.8 using 1M HCl and the solution was made up to a final volume of 500ml and subsequently stored at 4^oC until required

4X Resolving Gel Buffer pH 8.8

90.8g 1.5M Tris was dissolved in 100ml of sH_20. The pH was adjusted to 8.8 using 1M HCl and the solution was made up to a final volume of 500ml and subsequently stored at 4^oC until required.

10% SDS

10g of SDS (Merck) was dissolved in sH_20 to a final volume of 100ml and stored at room temperature until required.

10% Ammonium Persulphate (APS)

0.1g of APS (Sigma-Aldrich, Steinheim, Germany) was dissolved in sH_20 to a final volume of 1ml. This solution was prepared fresh each time before use.

8% Resolving Gels (2 gels)

11.83ml of sH_20, 6.25ml of the 4X Resolving gel buffer, 6.67ml of the Acrylamide/bis-Acrylamide 30% Monomer solution (Sigma-Aldrich; Steinheim, Germany, Catalogue number: A3449) and 250µl of 10% SDS were mixed together and just before casting the gel solutions, 250µl of 10% APS and 15µl of Tetramethylethylene-diamine (TEMED) (Sigma-Aldrich; Steinheim, Germany) was added to the solution and gently mixed.

Stacking Gel (2 gels)

5.73ml of sH_20, 2.5ml of the 4X Stacking gel buffer, 1.67ml of the Acrylamide/bis-Acrylamide 30% Monomer solution and 100µl of 10% SDS were mixed together and just before casting the gel solutions, 100µl of 10% APS and 10µl of TEMED was added to the solution and gently mixed.

2X Loading Buffer

2.5ml of the 4X Stacking gel buffer, 4ml of 10% SDS, 2ml Glycerol (Merck, Darmstadt, Germany), 100µl β-mercaptoethanol (Sigma-Aldrich; Steinheim, Germany) and a 2mg of Bromophenol Blue (Saarchem) was dissolved in sH_20 and made up to a final volume of 20ml. The solution was stored at -20ºC until required.

A.4 Solutions for Western Blotting

Transfer Buffer pH 9.2

200ml of methanol (Merck Chemicals, Saarchem, Wadeville, South Africa), 100 ml of 10X Tank Buffer and 700ml of sH_20 were mixed and stored at room temperature until required.

10X Tris-Buffered Saline (TBS) (pH 7.4)

160g of NaCl, 4g of KCl (Sigma-Aldrich; Steinheim, Germany) and 60g of Tris pH 8.0 were dissolved in sH_20 to a final volume of 2L. The pH was adjusted to 7.4 using HCl and the solution was then autoclaved and stored at room temperature until required.

TBS containing 0.1% Tween-20 (T-TBS)

The 10X TBS stock solution was diluted 1:10 times with sH_20 and Tween 20 (Saarchem, Midrand, South Africa) was added at a concentration of 0.1% (v/v). This solution was prepared fresh each time before use.

5% Skimmed milk (Blocking Buffer)

5g of Blotting Grade Blocker (non-fat dry milk) (Biorad, Hercules, CA) was dissolved on 100ml of T-TBS. This solution was prepared fresh each time before required.

1X T-PBS containing 0.5% Bovine Serum Albumin (BSA) (T-PBS-BSA)

0.5g of BSA was dissolved in 100ml of 1X T-PBS. This solution was prepared fresh each time before required.

NBT/BCIP Solution

A quarter of a NBT/BCIP tablet (Roche, Mannheim, Germany) was dissolved in 2.5ml of sH_20 with minimal light exposure. This solution was prepared fresh each time before use.

A.5 Solutions for Coomassie Staining

Coomassie Blue Staining

0.25g of Coomassie® Brilliant Blue R250 (Sigma-Aldrich; Steinheim, Germany) was dissolved in 500ml of methanol, 100ml of acetic acid and 400ml of sH_20. This solution was stored at room temperature until required.

Destaining Solution 1 (40% Methanol, 7% Acetic Acid)

400ml of methanol, 70ml of acetic acid (Merck, Darmstadt, Germany) and 530ml of sH_20 were mixed and stored at room temperature until required.

A.6 Solutions for ELISA's

2M Sulphuric Acid (H_2SO_4)

54,3ml of H_2SO_4 (98% H_2SO_4; Molarity=18, 4) was mixed with 445.7ml of sH_20 and stored at room temperature until required.

1X PBS containing 0.05% Tween 20 (T-PBS)

A solution of 10X PBS was diluted 1:10 times with sH_20 and Tween-20 was added at a concentration of 0.05% (v/v). This solution was prepared fresh each time before required.

1X T-PBS containing 10mg/ml Bovine Serum Albumin (BSA) (T-PBS-BSA) (Blocking Buffer)

BSA (Roche; Mannheim, Germany) was mixed with 1X T-PBS at a concentration of 10mg/ml. This solution was prepared fresh each time before required.

A.7 Solutions for the isolation of CD4+ T lymphocytes

1X PBS containing 2% FCS (PBS-FCS)

10ml of heat-inactivated FCS (Gibco; Grand Island, USA) was added to 500ml of 1X PBS and stored at 4ºC until required for use.

A.8 Flow Cytometry Solutions

Composition of 10X Binding Buffer (provided in the Annexin V/7-AAD kit) (Beckman Coulter, USA)

0.1M Hepes pH 7.4, 1.4M NaCl and 25mM $CaCl_2$ was dissolved in sH_20 and stored at 4ºC. This solution was diluted ten times with sH_20 and stored at 4ºC until required for use.

Camptothecin Stock Solution at 10mg/ml

25mg of Camptothecin (Sigma-Aldrich; Steinheim, Germany) (weighed out in a fume hood as it is extremely toxic) was dissolved in 2.5ml of filter sterilized DMSO. The solution was stored in the dark at 4ºC and thawed in a 37ºC water bath before use.

4µM Camptothecin

0.14µl of the 10mg/ml stock solution was added to each 1ml culture of Jurkat T lymphocytes or CD4+ T lymphocytes.

4% Paraformaldehyde (PFA) Stock Solution (10ml)

4g of PFA (weighed out in a fume hood as it is extremely toxic) ((BDH Limited Poole, England) and 5µl of 1M NaOH was added to 8ml of sH_20 before being heated for 10 minutes at 59ºC while vigorously shaking. The volume of solution was adjusted to 9ml with sH_20 followed by the addition of 1ml of 10X PBS. The solution was mixed and stored at -20ºC in 1ml aliquots for a maximum period of one month. Before use, the 4% PFA stock solution was diluted 1:4 times in 1X PBS and used at room

temperature as 1% PFA. This solution was stored at 4ºC for a maximum period of a week.

20mM EDTA

4ml of 0.5M EDTA was added to 96ml of sH_20 and stored at room temperature until required.

1X PBS containing 0.1% Triton X-100 and 5mg/ml BSA (50ml)

5µl of Triton X-100 (Merck, Darmstadt, Germany) and 0.25g of BSA was dissolved in 50ml of 1X PBS. The solution was stored at 4ºC until required.

APPENDIX B: Ethics Waiver

University
of the Witwatersrand,
Johannesburg

Human Research Ethics Committee (Medical)
(formerly Committee for Research on Human Subjects (Medical))

Secretariat: Research Office, Room SH10005, 10th floor, Senate House • Telephone: +27 11 717-1234 • Fax: +27 11 339-5708
Private Bag 3, Wits 2050, South Africa

Ref: W-CJ-090526-1
26/05/2009

TO WHOM IT MAY CONCERN:

Waiver: This certifies that the following research does not require clearance from the Human Research Ethics Committee (Medical).

Investigator: **Ms Natasha Pillay**

Project title: **HIV-1 Subtype C envelope glycoprotein-mediated apoptosis in bystander CD4+T lymphocytes.**

Reason: This is a wholly laboratory study using commercial Jurkat T cell lines, peripheral blood mononuclear cells and existing HIV-1 envelope glycoprotein plasmid constructs. There are no humans involved.

UNIVERSITY OF THE WITWATERSRAND
PROF PE CLEATON-JONES
HREC (MEDICAL)
2009 -05- 26
JOHANNESBURG

Professor Peter Cleaton-Jones
Chair: Human Research Ethics Committee (Medical)

copy: Anisa Keshav, Research Office, Senate House, Wits

REFERENCES

1. *Update on acquired immune deficiency syndrome (AIDS)--United States.* MMWR Morb Mortal Wkly Rep, 1982. **31**(37): p. 507-8, 513-4.
2. Gottlieb, M.S., et al., *Pneumocystis carinii pneumonia and mucosal candidiasis in previously healthy homosexual men: evidence of a new acquired cellular immunodeficiency.* N Engl J Med, 1981. **305**(24): p. 1425-31.
3. *Kaposi's sarcoma and Pneumocystis pneumonia among homosexual men--New York City and California.* MMWR Morb Mortal Wkly Rep, 1981. **30**(25): p. 305-8.
4. Kahn, J.O. and B.D. Walker, *Acute human immunodeficiency virus type 1 infection.* N Engl J Med, 1998. **339**(1): p. 33-9.
5. Barre-Sinoussi, F., et al., *Isolation of a T-lymphotropic retrovirus from a patient at risk for acquired immune deficiency syndrome (AIDS).* Science, 1983. **220**(4599): p. 868-71.
6. Gallo, R.C., et al., *Isolation of human T-cell leukemia virus in acquired immune deficiency syndrome (AIDS).* Science, 1983. **220**(4599): p. 865-7.
7. Coffin, J., et al., *What to call the AIDS virus?* Nature, 1986. **321**(6065): p. 10.
8. CDC, *Update on acquired immune deficiency syndrome (AIDS)--United States.* MMWR Morb Mortal Wkly Rep, 1982. **31**(37): p. 507-8, 513-4.
9. Gao, F., et al., *Origin of HIV-1 in the chimpanzee Pan troglodytes troglodytes.* Nature, 1999. **397**(6718): p. 436-41.
10. Reeves, J.D. and R.W. Doms, *Human immunodeficiency virus type 2.* J Gen Virol, 2002. **83**(Pt 6): p. 1253-65.
11. Robertson, D.L., et al., *HIV-1 nomenclature proposal.* Science, 2000. **288**(5463): p. 55-6.
12. Plantier, J.C., et al., *A new human immunodeficiency virus derived from gorillas.* Nat Med, 2009. **15**(8): p. 871-2.
13. Robertson, D.L., B.H. Hahn, and P.M. Sharp, *Recombination in AIDS viruses.* J Mol Evol, 1995. **40**(3): p. 249-59.
14. McCutchan, F.E., *Global epidemiology of HIV.* J Med Virol, 2006. **78 Suppl 1**: p. S7-S12.
15. Hemelaar, J., et al., *Global and regional distribution of HIV-1 genetic subtypes and recombinants in 2004.* AIDS, 2006. **20**(16): p. W13-23.
16. Osmanov, S., et al., *Estimated global distribution and regional spread of HIV-1 genetic subtypes in the year 2000.* J Acquir Immune Defic Syndr, 2002. **29**(2): p. 184-90.
17. UNAIDS. *Report on the global AIDS epidemic 2010*. 2010 [cited 2010 10 January]; Available from: www.unaids.org.
18. Turpin, J.A., *The next generation of HIV/AIDS drugs: novel and developmental antiHIV drugs and targets.* Expert Rev Anti Infect Ther, 2003. **1**(1): p. 97-128.
19. Barbaro, G., et al., *Highly active antiretroviral therapy: current state of the art, new agents and their pharmacological interactions useful for improving therapeutic outcome.* Curr Pharm Des, 2005. **11**(14): p. 1805-43.
20. Palella, F.J., Jr., et al., *Declining morbidity and mortality among patients with advanced human immunodeficiency virus infection. HIV Outpatient Study Investigators.* N Engl J Med, 1998. **338**(13): p. 853-60.
21. Hammer, S.M., et al., *Treatment for adult HIV infection: 2006 recommendations of the International AIDS Society-USA panel.* JAMA, 2006. **296**(7): p. 827-43.
22. Adamson, C.S. and E.O. Freed, *Anti-HIV-1 therapeutics: from FDA-approved drugs to hypothetical future targets.* Mol Interv, 2009. **9**(2): p. 70-4.
23. Roberts, J.D., K. Bebenek, and T.A. Kunkel, *The accuracy of reverse transcriptase from HIV-1.* Science, 1988. **242**(4882): p. 1171-3.
24. Chazal, N. and D. Gerlier, *Virus entry, assembly, budding, and membrane rafts.* Microbiol Mol Biol Rev, 2003. **67**(2): p. 226-37, table of contents.

25. Aloia, R.C., H. Tian, and F.C. Jensen, *Lipid composition and fluidity of the human immunodeficiency virus envelope and host cell plasma membranes.* Proc Natl Acad Sci U S A, 1993. **90**(11): p. 5181-5.
26. Raulin, J., *Human immunodeficiency virus and host cell lipids. Interesting pathways in research for a new HIV therapy.* Prog Lipid Res, 2002. **41**(1): p. 27-65.
27. Wyatt, R. and J. Sodroski, *The HIV-1 envelope glycoproteins: fusogens, antigens, and immunogens.* Science, 1998. **280**(5371): p. 1884-8.
28. Takasaki, T., et al., *Electron microscopic study of human immunodeficiency virus type 1 (HIV-1) core structure: two RNA strands in the core of mature and budding particles.* Arch Virol, 1997. **142**(2): p. 375-82.
29. You, J.C. and C.S. McHenry, *HIV nucleocapsid protein. Expression in Escherichia coli, purification, and characterization.* J Biol Chem, 1993. **268**(22): p. 16519-27.
30. Vaishnav, Y.N. and F. Wong-Staal, *The biochemistry of AIDS.* Annu Rev Biochem, 1991. **60**: p. 577-630.
31. Goto, T., M. Nakai, and K. Ikuta, *The life-cycle of human immunodeficiency virus type 1.* Micron, 1998. **29**(2-3): p. 123-38.
32. Gelderblom, H.R., *Assembly and morphology of HIV: potential effect of structure on viral function.* AIDS, 1991. **5**(6): p. 617-37.
33. Gelderblom, H.R., et al., *Fine structure of human immunodeficiency virus (HIV) and immunolocalization of structural proteins.* Virology, 1987. **156**(1): p. 171-6.
34. Molling, K., et al., *Association of viral reverse transcriptase with an enzyme degrading the RNA moiety of RNA-DNA hybrids.* Nat New Biol, 1971. **234**(51): p. 240-3.
35. Gelderblom, H.R., M. Ozel, and G. Pauli, *Morphogenesis and morphology of HIV. Structure-function relations.* Arch Virol, 1989. **106**(1-2): p. 1-13.
36. Muesing, M.A., et al., *Nucleic acid structure and expression of the human AIDS/lymphadenopathy retrovirus.* Nature, 1985. **313**(6002): p. 450-8.
37. Gallo, R., et al., *HIV/HTLV gene nomenclature.* Nature, 1988. **333**(6173): p. 504.
38. Ratner, L., et al., *Complete nucleotide sequence of the AIDS virus, HTLV-III.* Nature, 1985. **313**(6000): p. 277-84.
39. Wain-Hobson, S., et al., *Nucleotide sequence of the AIDS virus, LAV.* Cell, 1985. **40**(1): p. 9-17.
40. Sanchez-Pescador, R., et al., *Nucleotide sequence and expression of an AIDS-associated retrovirus (ARV-2).* Science, 1985. **227**(4686): p. 484-92.
41. Frankel, A.D. and J.A. Young, *HIV-1: fifteen proteins and an RNA.* Annu Rev Biochem, 1998. **67**: p. 1-25.
42. Varmus, H., *Regulation of HIV and HTLV gene expression.* Genes Dev, 1988. **2**(9): p. 1055-62.
43. Gottlinger, H.G., J.G. Sodroski, and W.A. Haseltine, *Role of capsid precursor processing and myristoylation in morphogenesis and infectivity of human immunodeficiency virus type 1.* Proc Natl Acad Sci U S A, 1989. **86**(15): p. 5781-5.
44. Cannon, P.M., et al., *Structure-function studies of the human immunodeficiency virus type 1 matrix protein, p17.* J Virol, 1997. **71**(5): p. 3474-83.
45. Freed, E.O., *HIV-1 gag proteins: diverse functions in the virus life cycle.* Virology, 1998. **251**(1): p. 1-15.
46. Jacks, T., et al., *Characterization of ribosomal frameshifting in HIV-1 gag-pol expression.* Nature, 1988. **331**(6153): p. 280-3.
47. Cohen, E.A., et al., *Identification of a protein encoded by the vpu gene of HIV-1.* Nature, 1988. **334**(6182): p. 532-4.
48. Cohen, E.A., et al., *Human immunodeficiency virus vpr product is a virion-associated regulatory protein.* J Virol, 1990. **64**(6): p. 3097-9.

49. Klatzmann, D., et al., *T-lymphocyte T4 molecule behaves as the receptor for human retrovirus LAV.* Nature, 1984. **312**(5996): p. 767-8.
50. Sattentau, Q.J., et al., *Conformational changes induced in the envelope glycoproteins of the human and simian immunodeficiency viruses by soluble receptor binding.* J Virol, 1993. **67**(12): p. 7383-93.
51. Trkola, A., et al., *CD4-dependent, antibody-sensitive interactions between HIV-1 and its co-receptor CCR-5.* Nature, 1996. **384**(6605): p. 184-7.
52. Alkhatib, G., et al., *CC CKR5: a RANTES, MIP-1alpha, MIP-1beta receptor as a fusion cofactor for macrophage-tropic HIV-1.* Science, 1996. **272**(5270): p. 1955-8.
53. Deng, H., et al., *Identification of a major co-receptor for primary isolates of HIV-1.* Nature, 1996. **381**(6584): p. 661-6.
54. Hart, T.K., et al., *Binding of soluble CD4 proteins to human immunodeficiency virus type 1 and infected cells induces release of envelope glycoprotein gp120.* Proc Natl Acad Sci U S A, 1991. **88**(6): p. 2189-93.
55. Chan, D.C. and P.S. Kim, *HIV entry and its inhibition.* Cell, 1998. **93**(5): p. 681-4.
56. Clark, S.J., et al., *Peptide and nucleotide sequences of rat CD4 (W3/25) antigen: evidence for derivation from a structure with four immunoglobulin-related domains.* Proc Natl Acad Sci U S A, 1987. **84**(6): p. 1649-53.
57. Maddon, P.J., et al., *The isolation and nucleotide sequence of a cDNA encoding the T cell surface protein T4: a new member of the immunoglobulin gene family.* Cell, 1985. **42**(1): p. 93-104.
58. Doyle, C. and J.L. Strominger, *Interaction between CD4 and class II MHC molecules mediates cell adhesion.* Nature, 1987. **330**(6145): p. 256-9.
59. Robey, E. and R. Axel, *CD4: collaborator in immune recognition and HIV infection.* Cell, 1990. **60**(5): p. 697-700.
60. Dianzani, U., et al., *Physical association of CD4 with the T cell receptor.* J Immunol, 1992. **148**(3): p. 678-88.
61. Veillette, A., et al., *Signal transduction through the CD4 receptor involves the activation of the internal membrane tyrosine-protein kinase p56lck.* Nature, 1989. **338**(6212): p. 257-9.
62. Dalgleish, A.G., et al., *The CD4 (T4) antigen is an essential component of the receptor for the AIDS retrovirus.* Nature, 1984. **312**(5996): p. 763-7.
63. Maddon, P.J., et al., *The T4 gene encodes the AIDS virus receptor and is expressed in the immune system and the brain.* Cell, 1986. **47**(3): p. 333-48.
64. Lasky, L.A., et al., *Delineation of a region of the human immunodeficiency virus type 1 gp120 glycoprotein critical for interaction with the CD4 receptor.* Cell, 1987. **50**(6): p. 975-85.
65. Arthos, J., et al., *Identification of the residues in human CD4 critical for the binding of HIV.* Cell, 1989. **57**(3): p. 469-81.
66. Moebius, U., et al., *The human immunodeficiency virus gp120 binding site on CD4: delineation by quantitative equilibrium and kinetic binding studies of mutants in conjunction with a high-resolution CD4 atomic structure.* J Exp Med, 1992. **176**(2): p. 507-17.
67. Samson, M., et al., *Molecular cloning and functional expression of a new human CC-chemokine receptor gene.* Biochemistry, 1996. **35**(11): p. 3362-7.
68. Feng, Y., et al., *HIV-1 entry cofactor: functional cDNA cloning of a seven-transmembrane, G protein-coupled receptor.* Science, 1996. **272**(5263): p. 872-7.
69. Murphy, P.M., *The molecular biology of leukocyte chemoattractant receptors.* Annu Rev Immunol, 1994. **12**: p. 593-633.
70. Dragic, T., et al., *HIV-1 entry into CD4+ cells is mediated by the chemokine receptor CC-CKR-5.* Nature, 1996. **381**(6584): p. 667-73.

71. Rizzuto, C.D., et al., *A conserved HIV gp120 glycoprotein structure involved in chemokine receptor binding.* Science, 1998. **280**(5371): p. 1949-53.
72. Lu, Z., et al., *Evolution of HIV-1 coreceptor usage through interactions with distinct CCR5 and CXCR4 domains.* Proc Natl Acad Sci U S A, 1997. **94**(12): p. 6426-31.
73. Alkhatib, G., et al., *CC chemokine receptor 5-mediated signaling and HIV-1 Co-receptor activity share common structural determinants. Critical residues in the third extracellular loop support HIV-1 fusion.* J Biol Chem, 1997. **272**(32): p. 19771-6.
74. Coakley, E., C.J. Petropoulos, and J.M. Whitcomb, *Assessing chemokine co-receptor usage in HIV.* Curr Opin Infect Dis, 2005. **18**(1): p. 9-15.
75. Moore, J.P., A. Trkola, and T. Dragic, *Co-receptors for HIV-1 entry.* Curr Opin Immunol, 1997. **9**(4): p. 551-62.
76. Connor, R.I., et al., *Change in coreceptor use correlates with disease progression in HIV-1--infected individuals.* J Exp Med, 1997. **185**(4): p. 621-8.
77. Valentin, A., et al., *Dual tropism for macrophages and lymphocytes is a common feature of primary human immunodeficiency virus type 1 and 2 isolates.* J Virol, 1994. **68**(10): p. 6684-9.
78. Cecilia, D., et al., *Absence of coreceptor switch with disease progression in human immunodeficiency virus infections in India.* Virology, 2000. **271**(2): p. 253-8.
79. Tscherning, C., et al., *Differences in chemokine coreceptor usage between genetic subtypes of HIV-1.* Virology, 1998. **241**(2): p. 181-8.
80. Connell, B.J., et al., *Emergence of X4 usage among HIV-1 subtype C: evidence for an evolving epidemic in South Africa.* AIDS, 2008. **22**(7): p. 896-9.
81. van Rensburg, E.J., et al., *Change in co-receptor usage of current South African HIV-1 subtype C primary isolates.* AIDS, 2002. **16**(18): p. 2479-80.
82. Stein, B.S. and E.G. Engleman, *Intracellular processing of the gp160 HIV-1 envelope precursor. Endoproteolytic cleavage occurs in a cis or medial compartment of the Golgi complex.* J Biol Chem, 1990. **265**(5): p. 2640-9.
83. Leonard, C.K., et al., *Assignment of intrachain disulfide bonds and characterization of potential glycosylation sites of the type 1 recombinant human immunodeficiency virus envelope glycoprotein (gp120) expressed in Chinese hamster ovary cells.* J Biol Chem, 1990. **265**(18): p. 10373-82.
84. Pinter, A., et al., *Oligomeric structure of gp41, the transmembrane protein of human immunodeficiency virus type 1.* J Virol, 1989. **63**(6): p. 2674-9.
85. Chan, D.C., et al., *Core structure of gp41 from the HIV envelope glycoprotein.* Cell, 1997. **89**(2): p. 263-73.
86. Allan, J.S., et al., *Major glycoprotein antigens that induce antibodies in AIDS patients are encoded by HTLV-III.* Science, 1985. **228**(4703): p. 1091-4.
87. Helseth, E., et al., *Human immunodeficiency virus type 1 gp120 envelope glycoprotein regions important for association with the gp41 transmembrane glycoprotein.* J Virol, 1991. **65**(4): p. 2119-23.
88. Starcich, B.R., et al., *Identification and characterization of conserved and variable regions in the envelope gene of HTLV-III/LAV, the retrovirus of AIDS.* Cell, 1986. **45**(5): p. 637-48.
89. Wyatt, R., et al., *Functional and immunologic characterization of human immunodeficiency virus type 1 envelope glycoproteins containing deletions of the major variable regions.* J Virol, 1993. **67**(8): p. 4557-65.
90. Moore, J.P., et al., *Probing the structure of the human immunodeficiency virus surface glycoprotein gp120 with a panel of monoclonal antibodies.* J Virol, 1994. **68**(1): p. 469-84.

91. Wyatt, R., et al., *Involvement of the V1/V2 variable loop structure in the exposure of human immunodeficiency virus type 1 gp120 epitopes induced by receptor binding.* J Virol, 1995. **69**(9): p. 5723-33.
92. Spenlehauer, C., et al., *Study of the V3 loop as a target epitope for antibodies involved in the neutralization of primary isolates versus T-cell-line-adapted strains of human immunodeficiency virus type 1.* J Virol, 1998. **72**(12): p. 9855-64.
93. Huang, C.C., et al., *Structure of a V3-containing HIV-1 gp120 core.* Science, 2005. **310**(5750): p. 1025-8.
94. Shimizu, N., et al., *Changes in and discrepancies between cell tropisms and coreceptor uses of human immunodeficiency virus type 1 induced by single point mutations at the V3 tip of the env protein.* Virology, 1999. **259**(2): p. 324-33.
95. Hwang, S.S., et al., *Identification of the envelope V3 loop as the primary determinant of cell tropism in HIV-1.* Science, 1991. **253**(5015): p. 71-4.
96. Kuiken, C.L., et al., *Increasing antigenic and genetic diversity of the V3 variable domain of the human immunodeficiency virus envelope protein in the course of the AIDS epidemic.* Proc Natl Acad Sci U S A, 1993. **90**(19): p. 9061-5.
97. Peterson, A. and B. Seed, *Genetic analysis of monoclonal antibody and HIV binding sites on the human lymphocyte antigen CD4.* Cell, 1988. **54**(1): p. 65-72.
98. Kwong, P.D., et al., *Structure of an HIV gp120 envelope glycoprotein in complex with the CD4 receptor and a neutralizing human antibody.* Nature, 1998. **393**(6686): p. 648-59.
99. Marcon, L., et al., *Utilization of C-C chemokine receptor 5 by the envelope glycoproteins of a pathogenic simian immunodeficiency virus, SIVmac239.* J Virol, 1997. **71**(3): p. 2522-7.
100. Earl, P.L. and B. Moss, *Mutational analysis of the assembly domain of the HIV-1 envelope glycoprotein.* AIDS Res Hum Retroviruses, 1993. **9**(7): p. 589-94.
101. Kowalski, M., et al., *Functional regions of the envelope glycoprotein of human immunodeficiency virus type 1.* Science, 1987. **237**(4820): p. 1351-5.
102. Kwong, P.D., et al., *Oligomeric modeling and electrostatic analysis of the gp120 envelope glycoprotein of human immunodeficiency virus.* J Virol, 2000. **74**(4): p. 1961-72.
103. Weissenhorn, W., et al., *Atomic structure of the ectodomain from HIV-1 gp41.* Nature, 1997. **387**(6631): p. 426-30.
104. Liu, S., Q. Zhao, and S. Jiang, *Determination of the HIV-1 gp41 fusogenic core conformation modeled by synthetic peptides: applicable for identification of HIV-1 fusion inhibitors.* Peptides, 2003. **24**(9): p. 1303-13.
105. Markosyan, R.M., F.S. Cohen, and G.B. Melikyan, *HIV-1 envelope proteins complete their folding into six-helix bundles immediately after fusion pore formation.* Mol Biol Cell, 2003. **14**(3): p. 926-38.
106. Melikyan, G.B., et al., *Evidence that the transition of HIV-1 gp41 into a six-helix bundle, not the bundle configuration, induces membrane fusion.* J Cell Biol, 2000. **151**(2): p. 413-23.
107. Grewe, C., A. Beck, and H.R. Gelderblom, *HIV: early virus-cell interactions.* J Acquir Immune Defic Syndr, 1990. **3**(10): p. 965-74.
108. Freed, E.O., *HIV-1 replication.* Somat Cell Mol Genet, 2001. **26**(1-6): p. 13-33.
109. Miller, M.D., C.M. Farnet, and F.D. Bushman, *Human immunodeficiency virus type 1 preintegration complexes: studies of organization and composition.* J Virol, 1997. **71**(7): p. 5382-90.
110. Bukrinsky, M.I., et al., *Association of integrase, matrix, and reverse transcriptase antigens of human immunodeficiency virus type 1 with viral nucleic acids following acute infection.* Proc Natl Acad Sci U S A, 1993. **90**(13): p. 6125-9.

111. Bukrinsky, M. and A. Adzhubei, *Viral protein R of HIV-1.* Rev Med Virol, 1999. **9**(1): p. 39-49.
112. Bowerman, B., et al., *A nucleoprotein complex mediates the integration of retroviral DNA.* Genes Dev, 1989. **3**(4): p. 469-78.
113. Farnet, C.M. and W.A. Haseltine, *Integration of human immunodeficiency virus type 1 DNA in vitro.* Proc Natl Acad Sci U S A, 1990. **87**(11): p. 4164-8.
114. Pollard, V.W. and M.H. Malim, *The HIV-1 Rev protein.* Annu Rev Microbiol, 1998. **52**: p. 491-532.
115. Saad, J.S., et al., *Structural basis for targeting HIV-1 Gag proteins to the plasma membrane for virus assembly.* Proc Natl Acad Sci U S A, 2006. **103**(30): p. 11364-9.
116. Varmus, H., *Retroviruses.* Science, 1988. **240**(4858): p. 1427-35.
117. Goto, T., et al., *The budding of defective human immunodeficiency virus type 1 (HIV-1) particles from cell clones persistently infected with HIV-1.* Arch Virol, 1990. **111**(1-2): p. 87-101.
118. Morgan, D., et al., *HIV-1 infection in rural Africa: is there a difference in median time to AIDS and survival compared with that in industrialized countries?* Aids, 2002. **16**(4): p. 597-603.
119. Roger, M., *Influence of host genes on HIV-1 disease progression.* FASEB J, 1998. **12**(9): p. 625-32.
120. Fellay, J., et al., *A whole-genome association study of major determinants for host control of HIV-1.* Science, 2007. **317**(5840): p. 944-7.
121. Shankarappa, R., et al., *Consistent viral evolutionary changes associated with the progression of human immunodeficiency virus type 1 infection.* J Virol, 1999. **73**(12): p. 10489-502.
122. Clark, S.J., et al., *High titers of cytopathic virus in plasma of patients with symptomatic primary HIV-1 infection.* N Engl J Med, 1991. **324**(14): p. 954-60.
123. Alimonti, J.B., T.B. Ball, and K.R. Fowke, *Mechanisms of CD4+ T lymphocyte cell death in human immunodeficiency virus infection and AIDS.* J Gen Virol, 2003. **84**(Pt 7): p. 1649-61.
124. Ford, E.S., C.E. Puronen, and I. Sereti, *Immunopathogenesis of asymptomatic chronic HIV Infection: the calm before the storm.* Curr Opin HIV AIDS, 2009. **4**(3): p. 206-14.
125. Haase, A.T., *Population biology of HIV-1 infection: viral and CD4+ T cell demographics and dynamics in lymphatic tissues.* Annu Rev Immunol, 1999. **17**: p. 625-56.
126. Pantaleo, G., C. Graziosi, and A.S. Fauci, *New concepts in the immunopathogenesis of human immunodeficiency virus infection.* N Engl J Med, 1993. **328**(5): p. 327-35.
127. Jin, X., et al., *Dramatic rise in plasma viremia after CD8(+) T cell depletion in simian immunodeficiency virus-infected macaques.* J Exp Med, 1999. **189**(6): p. 991-8.
128. Ameisen, J.C. and A. Capron, *Cell dysfunction and depletion in AIDS: the programmed cell death hypothesis.* Immunol Today, 1991. **12**(4): p. 102-5.
129. Meyaard, L., et al., *Programmed death of T cells in HIV-1 infection.* Science, 1992. **257**(5067): p. 217-9.
130. Gougeon, M.L., et al., *Programmed cell death in peripheral lymphocytes from HIV-infected persons: increased susceptibility to apoptosis of CD4 and CD8 T cells correlates with lymphocyte activation and with disease progression.* J Immunol, 1996. **156**(9): p. 3509-20.
131. Cotton, M.F., et al., *Apoptosis of CD4+ and CD8+ T cells isolated immediately ex vivo correlates with disease severity in human immunodeficiency virus type 1 infection.* Pediatr Res, 1997. **42**(5): p. 656-64.
132. Badley, A.D., et al., *Dynamic correlation of apoptosis and immune activation during treatment of HIV infection.* Cell Death Differ, 1999. **6**(5): p. 420-32.

133. Bohler, T., et al., *Early effects of antiretroviral combination therapy on activation, apoptosis and regeneration of T cells in HIV-1-infected children and adolescents.* AIDS, 1999. **13**(7): p. 779-89.
134. Cossarizza, A., *Apoptosis and HIV infection: about molecules and genes.* Curr Pharm Des, 2008. **14**(3): p. 237-44.
135. Finkel, T.H., et al., *Apoptosis occurs predominantly in bystander cells and not in productively infected cells of HIV- and SIV-infected lymph nodes.* Nat Med, 1995. **1**(2): p. 129-34.
136. Debatin, K.M., et al., *High expression of APO-1 (CD95) on T lymphocytes from human immunodeficiency virus-1-infected children.* Blood, 1994. **83**(10): p. 3101-3.
137. Miura, Y., et al., *Critical contribution of tumor necrosis factor-related apoptosis-inducing ligand (TRAIL) to apoptosis of human CD4+ T cells in HIV-1-infected hu-PBL-NOD-SCID mice.* J Exp Med, 2001. **193**(5): p. 651-60.
138. Monceaux, V., et al., *Extensive apoptosis in lymphoid organs during primary SIV infection predicts rapid progression towards AIDS.* AIDS, 2003. **17**(11): p. 1585-96.
139. Dockrell, D.H., et al., *Activation-induced CD4+ T cell death in HIV-positive individuals correlates with Fas susceptibility, CD4+ T cell count, and HIV plasma viral copy number.* AIDS Res Hum Retroviruses, 1999. **15**(17): p. 1509-18.
140. Ellis, R.E., J.Y. Yuan, and H.R. Horvitz, *Mechanisms and functions of cell death.* Annu Rev Cell Biol, 1991. **7**: p. 663-98.
141. Meier, P., A. Finch, and G. Evan, *Apoptosis in development.* Nature, 2000. **407**(6805): p. 796-801.
142. Lockshin, R.A. and Z. Zakeri, *Programmed cell death and apoptosis: origins of the theory.* Nat Rev Mol Cell Biol, 2001. **2**(7): p. 545-50.
143. Arends, M.J. and A.H. Wyllie, *Apoptosis: mechanisms and roles in pathology.* Int Rev Exp Pathol, 1991. **32**: p. 223-54.
144. Cohen, G.M., *Caspases: the executioners of apoptosis.* Biochem J, 1997. **326 (Pt 1)**: p. 1-16.
145. Nicholson, D.W. and N.A. Thornberry, *Caspases: killer proteases.* Trends Biochem Sci, 1997. **22**(8): p. 299-306.
146. Wyllie, A.H., *Glucocorticoid-induced thymocyte apoptosis is associated with endogenous endonuclease activation.* Nature, 1980. **284**(5756): p. 555-6.
147. Miura, Y. and Y. Koyanagi, *Death ligand-mediated apoptosis in HIV infection.* Rev Med Virol, 2005. **15**(3): p. 169-78.
148. Ashkenazi, A., *Targeting death and decoy receptors of the tumour-necrosis factor superfamily.* Nat Rev Cancer, 2002. **2**(6): p. 420-30.
149. Pan, G., et al., *An antagonist decoy receptor and a death domain-containing receptor for TRAIL.* Science, 1997. **277**(5327): p. 815-8.
150. Pan, G., et al., *The receptor for the cytotoxic ligand TRAIL.* Science, 1997. **276**(5309): p. 111-3.
151. Suda, T., et al., *Molecular cloning and expression of the Fas ligand, a novel member of the tumor necrosis factor family.* Cell, 1993. **75**(6): p. 1169-78.
152. Yang, Y., et al., *Monocytes treated with human immunodeficiency virus Tat kill uninfected CD4(+) cells by a tumor necrosis factor-related apoptosis-induced ligand-mediated mechanism.* J Virol, 2003. **77**(12): p. 6700-8.
153. Zhang, M., et al., *Identification of a potential HIV-induced source of bystander-mediated apoptosis in T cells: upregulation of trail in primary human macrophages by HIV-1 tat.* J Biomed Sci, 2001. **8**(3): p. 290-6.
154. Nitsch, R., et al., *Human brain-cell death induced by tumour-necrosis-factor-related apoptosis-inducing ligand (TRAIL).* Lancet, 2000. **356**(9232): p. 827-8.

155. Katsikis, P.D., et al., *Fas antigen stimulation induces marked apoptosis of T lymphocytes in human immunodeficiency virus-infected individuals.* J Exp Med, 1995. **181**(6): p. 2029-36.
156. Dockrell, D.H., et al., *The expression of Fas Ligand by macrophages and its upregulation by human immunodeficiency virus infection.* J Clin Invest, 1998. **101**(11): p. 2394-405.
157. Medrano, F.J., et al., *Tumor necrosis factor beta and soluble APO-1/Fas independently predict progression to AIDS in HIV-seropositive patients.* AIDS Res Hum Retroviruses, 1998. **14**(10): p. 835-43.
158. Petrovas, C., Y.M. Mueller, and P.D. Katsikis, *HIV-specific CD8+ T cells: serial killers condemned to die?* Curr HIV Res, 2004. **2**(2): p. 153-62.
159. Gross, A., J.M. McDonnell, and S.J. Korsmeyer, *BCL-2 family members and the mitochondria in apoptosis.* Genes Dev, 1999. **13**(15): p. 1899-911.
160. Kroemer, G., *The proto-oncogene Bcl-2 and its role in regulating apoptosis.* Nat Med, 1997. **3**(6): p. 614-20.
161. Green, D.R. and J.C. Reed, *Mitochondria and apoptosis.* Science, 1998. **281**(5381): p. 1309-12.
162. van Loo, G., et al., *The role of mitochondrial factors in apoptosis: a Russian roulette with more than one bullet.* Cell Death Differ, 2002. **9**(10): p. 1031-42.
163. Martinou, J.C. and D.R. Green, *Breaking the mitochondrial barrier.* Nat Rev Mol Cell Biol, 2001. **2**(1): p. 63-7.
164. Marzo, I., et al., *The permeability transition pore complex: a target for apoptosis regulation by caspases and bcl-2-related proteins.* J Exp Med, 1998. **187**(8): p. 1261-71.
165. Zamzami, N., et al., *Subcellular and submitochondrial mode of action of Bcl-2-like oncoproteins.* Oncogene, 1998. **16**(17): p. 2265-82.
166. Shedlock, D.J., et al., *HIV-1 viral genes and mitochondrial apoptosis.* Apoptosis, 2008. **13**(9): p. 1088-99.
167. Bernardi, P., et al., *Mitochondria and cell death. Mechanistic aspects and methodological issues.* Eur J Biochem, 1999. **264**(3): p. 687-701.
168. Loeffler, M. and G. Kroemer, *The mitochondrion in cell death control: certainties and incognita.* Exp Cell Res, 2000. **256**(1): p. 19-26.
169. Quignon, F., et al., *PML induces a novel caspase-independent death process.* Nat Genet, 1998. **20**(3): p. 259-65.
170. Susin, S.A., et al., *Molecular characterization of mitochondrial apoptosis-inducing factor.* Nature, 1999. **397**(6718): p. 441-6.
171. Li, H., et al., *Cleavage of BID by caspase 8 mediates the mitochondrial damage in the Fas pathway of apoptosis.* Cell, 1998. **94**(4): p. 491-501.
172. Luo, X., et al., *Bid, a Bcl2 interacting protein, mediates cytochrome c release from mitochondria in response to activation of cell surface death receptors.* Cell, 1998. **94**(4): p. 481-90.
173. Wei, M.C., et al., *Proapoptotic BAX and BAK: a requisite gateway to mitochondrial dysfunction and death.* Science, 2001. **292**(5517): p. 727-30.
174. Wei, M.C., et al., *tBID, a membrane-targeted death ligand, oligomerizes BAK to release cytochrome c.* Genes Dev, 2000. **14**(16): p. 2060-71.
175. Griffiths, G.J., et al., *Cell damage-induced conformational changes of the pro-apoptotic protein Bak in vivo precede the onset of apoptosis.* J Cell Biol, 1999. **144**(5): p. 903-14.
176. Gross, A., et al., *Enforced dimerization of BAX results in its translocation, mitochondrial dysfunction and apoptosis.* EMBO J, 1998. **17**(14): p. 3878-85.

177. Eskes, R., et al., *Bid induces the oligomerization and insertion of Bax into the outer mitochondrial membrane.* Mol Cell Biol, 2000. **20**(3): p. 929-35.
178. Zamzami, N. and G. Kroemer, *The mitochondrion in apoptosis: how Pandora's box opens.* Nat Rev Mol Cell Biol, 2001. **2**(1): p. 67-71.
179. Castedo, M., et al., *Mitochondrial perturbations define lymphocytes undergoing apoptotic depletion in vivo.* Eur J Immunol, 1995. **25**(12): p. 3277-84.
180. Cossarizza, A., et al., *Mitochondria alterations and dramatic tendency to undergo apoptosis in peripheral blood lymphocytes during acute HIV syndrome.* AIDS, 1997. **11**(1): p. 19-26.
181. Ferri, K.F., et al., *Apoptosis control in syncytia induced by the HIV type 1-envelope glycoprotein complex: role of mitochondria and caspases.* J Exp Med, 2000. **192**(8): p. 1081-92.
182. Hsu, H., J. Xiong, and D.V. Goeddel, *The TNF receptor 1-associated protein TRADD signals cell death and NF-kappa B activation.* Cell, 1995. **81**(4): p. 495-504.
183. Re, M., et al., *High levels of HIV-1 replication show a clear correlation with downmodulation of Bcl-2 protein in peripheral blood lymphocytes of HIV-1-seropositive subjects.* J Med Virol, 1998. **56**(1): p. 66-73.
184. Genini, D., et al., *HIV induces lymphocyte apoptosis by a p53-initiated, mitochondrial-mediated mechanism.* FASEB J, 2001. **15**(1): p. 5-6.
185. Sastry, K.J., et al., *Expression of human immunodeficiency virus type I tat results in down-regulation of bcl-2 and induction of apoptosis in hematopoietic cells.* Oncogene, 1996. **13**(3): p. 487-93.
186. Chen, D., et al., *HIV-1 Tat targets microtubules to induce apoptosis, a process promoted by the pro-apoptotic Bcl-2 relative Bim.* EMBO J, 2002. **21**(24): p. 6801-10.
187. Macho, A., et al., *Mitochondrial dysfunctions in circulating T lymphocytes from human immunodeficiency virus-1 carriers.* Blood, 1995. **86**(7): p. 2481-7.
188. Miyashita, T. and J.C. Reed, *Tumor suppressor p53 is a direct transcriptional activator of the human bax gene.* Cell, 1995. **80**(2): p. 293-9.
189. Pearson, A.S., et al., *Up-regulation of the proapoptotic mediators Bax and Bak after adenovirus-mediated p53 gene transfer in lung cancer cells.* Clin Cancer Res, 2000. **6**(3): p. 887-90.
190. Knudson, C.M., et al., *Bax accelerates tumorigenesis in p53-deficient mice.* Cancer Res, 2001. **61**(2): p. 659-65.
191. Gougeon, M.L., *Apoptosis as an HIV strategy to escape immune attack.* Nat Rev Immunol, 2003. **3**(5): p. 392-404.
192. Ahr, B., et al., *Apoptosis of uninfected cells induced by HIV envelope glycoproteins.* Retrovirology, 2004. **1**: p. 12.
193. Campbell, G.R., et al., *The glutamine-rich region of the HIV-1 Tat protein is involved in T-cell apoptosis.* J Biol Chem, 2004. **279**(46): p. 48197-204.
194. McCloskey, T.W., et al., *Dual role of HIV Tat in regulation of apoptosis in T cells.* J Immunol, 1997. **158**(2): p. 1014-9.
195. Westendorp, M.O., et al., *Sensitization of T cells to CD95-mediated apoptosis by HIV-1 Tat and gp120.* Nature, 1995. **375**(6531): p. 497-500.
196. Li, C.J., et al., *Induction of apoptosis in uninfected lymphocytes by HIV-1 Tat protein.* Science, 1995. **268**(5209): p. 429-31.
197. Gibellini, D., et al., *HIV-1 Tat protein concomitantly down-regulates apical caspase-10 and up-regulates c-FLIP in lymphoid T cells: a potential molecular mechanism to escape TRAIL cytotoxicity.* J Cell Physiol, 2005. **203**(3): p. 547-56.
198. Bartz, S.R. and M. Emerman, *Human immunodeficiency virus type 1 Tat induces apoptosis and increases sensitivity to apoptotic signals by up-regulating FLICE/caspase-8.* J Virol, 1999. **73**(3): p. 1956-63.

199. Zauli, G., et al., *The human immunodeficiency virus type-1 Tat protein upregulates Bcl-2 gene expression in Jurkat T-cell lines and primary peripheral blood mononuclear cells.* Blood, 1995. **86**(10): p. 3823-34.
200. Schwartz, O., et al., *Endocytosis of major histocompatibility complex class I molecules is induced by the HIV-1 Nef protein.* Nat Med, 1996. **2**(3): p. 338-42.
201. Garcia, J.V. and A.D. Miller, *Serine phosphorylation-independent downregulation of cell-surface CD4 by nef.* Nature, 1991. **350**(6318): p. 508-11.
202. Muthumani, K., et al., *HIV-1 Nef-induced FasL induction and bystander killing requires p38 MAPK activation.* Blood, 2005. **106**(6): p. 2059-68.
203. Stewart, S.A., et al., *Human immunodeficiency virus type 1 Vpr induces apoptosis following cell cycle arrest.* J Virol, 1997. **71**(7): p. 5579-92.
204. Watanabe, N., et al., *Induction of M-phase arrest and apoptosis after HIV-1 Vpr expression through uncoupling of nuclear and centrosomal cycle in HeLa cells.* Exp Cell Res, 2000. **258**(2): p. 261-9.
205. Muthumani, K., et al., *Mechanism of HIV-1 viral protein R-induced apoptosis.* Biochem Biophys Res Commun, 2003. **304**(3): p. 583-92.
206. Deniaud, A., C. Brenner, and G. Kroemer, *Mitochondrial membrane permeabilization by HIV-1 Vpr.* Mitochondrion, 2004. **4**(2-3): p. 223-33.
207. Jacotot, E., et al., *The HIV-1 viral protein R induces apoptosis via a direct effect on the mitochondrial permeability transition pore.* J Exp Med, 2000. **191**(1): p. 33-46.
208. Montal, M., *Structure-function correlates of Vpu, a membrane protein of HIV-1.* FEBS Lett, 2003. **552**(1): p. 47-53.
209. Muthumani, K., et al., *HIV-1 Vpr induces apoptosis through caspase 9 in T cells and peripheral blood mononuclear cells.* J Biol Chem, 2002. **277**(40): p. 37820-31.
210. Patel, C.A., M. Mukhtar, and R.J. Pomerantz, *Human immunodeficiency virus type 1 Vpr induces apoptosis in human neuronal cells.* J Virol, 2000. **74**(20): p. 9717-26.
211. Azad, A.A., *Could Nef and Vpr proteins contribute to disease progression by promoting depletion of bystander cells and prolonged survival of HIV-infected cells?* Biochem Biophys Res Commun, 2000. **267**(3): p. 677-85.
212. Nie, Z., et al., *HIV-1 protease processes procaspase 8 to cause mitochondrial release of cytochrome c, caspase cleavage and nuclear fragmentation.* Cell Death Differ, 2002. **9**(11): p. 1172-84.
213. Strack, P.R., et al., *Apoptosis mediated by HIV protease is preceded by cleavage of Bcl-2.* Proc Natl Acad Sci U S A, 1996. **93**(18): p. 9571-6.
214. Akari, H., et al., *The human immunodeficiency virus type 1 accessory protein Vpu induces apoptosis by suppressing the nuclear factor kappaB-dependent expression of antiapoptotic factors.* J Exp Med, 2001. **194**(9): p. 1299-311.
215. Gonzalez, M.E. and L. Carrasco, *Human immunodeficiency virus type 1 VPU protein affects Sindbis virus glycoprotein processing and enhances membrane permeabilization.* Virology, 2001. **279**(1): p. 201-9.
216. Casella, C.R., E.L. Rapaport, and T.H. Finkel, *Vpu increases susceptibility of human immunodeficiency virus type 1-infected cells to fas killing.* J Virol, 1999. **73**(1): p. 92-100.
217. Heinkelein, M., S. Sopper, and C. Jassoy, *Contact of human immunodeficiency virus type 1-infected and uninfected CD4+ T lymphocytes is highly cytolytic for both cells.* J Virol, 1995. **69**(11): p. 6925-31.
218. Laurent-Crawford, A.G., et al., *Membrane expression of HIV envelope glycoproteins triggers apoptosis in CD4 cells.* AIDS Res Hum Retroviruses, 1993. **9**(8): p. 761-73.
219. Perfettini, J.L., et al., *Mechanisms of apoptosis induction by the HIV-1 envelope.* Cell Death Differ, 2005. **12 Suppl 1**: p. 916-23.

220. Roggero, R., et al., *Binding of human immunodeficiency virus type 1 gp120 to CXCR4 induces mitochondrial transmembrane depolarization and cytochrome c-mediated apoptosis independently of Fas signaling.* J Virol, 2001. **75**(16): p. 7637-50.
221. Ji, J., et al., *Apoptosis induced in HIV-1-exposed, resting CD4+ T cells subsequent to signaling through homing receptors is Fas/Fas ligand-mediated.* J Leukoc Biol, 2007. **81**(1): p. 297-305.
222. Biard-Piechaczyk, M., et al., *Caspase-dependent apoptosis of cells expressing the chemokine receptor CXCR4 is induced by cell membrane-associated human immunodeficiency virus type 1 envelope glycoprotein (gp120).* Virology, 2000. **268**(2): p. 329-44.
223. Biard-Piechaczyk, M., et al., *Role of CXCR4 in HIV-1-induced apoptosis of cells with a CD4+, CXCR4+ phenotype.* Immunol Lett, 1999. **70**(1): p. 1-3.
224. Algeciras-Schimnich, A., et al., *CCR5 mediates Fas- and caspase-8 dependent apoptosis of both uninfected and HIV infected primary human CD4 T cells.* Aids, 2002. **16**(11): p. 1467-78.
225. Berger, E.A., *HIV entry and tropism: the chemokine receptor connection.* AIDS, 1997. **11 Suppl A**: p. S3-16.
226. Banda, N.K., et al., *Crosslinking CD4 by human immunodeficiency virus gp120 primes T cells for activation-induced apoptosis.* J Exp Med, 1992. **176**(4): p. 1099-106.
227. Arthos, J., et al., *The role of the CD4 receptor versus HIV coreceptors in envelope-mediated apoptosis in peripheral blood mononuclear cells.* Virology, 2002. **292**(1): p. 98-106.
228. Blanco, J., et al., *Cell-surface-expressed HIV-1 envelope induces the death of CD4 T cells during GP41-mediated hemifusion-like events.* Virology, 2003. **305**(2): p. 318-29.
229. Holm, G.H., et al., *Apoptosis of bystander T cells induced by human immunodeficiency virus type 1 with increased envelope/receptor affinity and coreceptor binding site exposure.* J Virol, 2004. **78**(9): p. 4541-51.
230. Crise, B., L. Buonocore, and J.K. Rose, *CD4 is retained in the endoplasmic reticulum by the human immunodeficiency virus type 1 glycoprotein precursor.* J Virol, 1990. **64**(11): p. 5585-93.
231. Trushin, S.A., et al., *Glycoprotein 120 binding to CXCR4 causes p38-dependent primary T cell death that is facilitated by, but does not require cell-associated CD4.* J Immunol, 2007. **178**(8): p. 4846-53.
232. Liu, Q.H., et al., *HIV-1 gp120 and chemokines activate ion channels in primary macrophages through CCR5 and CXCR4 stimulation.* Proc Natl Acad Sci U S A, 2000. **97**(9): p. 4832-7.
233. Decrion, A.Z., et al., *CXCR4-mediated T cell apoptosis in human immunodeficiency virus infection.* J Gen Virol, 2004. **85**(Pt 6): p. 1471-8.
234. Somma, F., et al., *Engagement of CD4 before TCR triggering regulates both Bax- and Fas (CD95)-mediated apoptosis.* J Immunol, 2000. **164**(10): p. 5078-87.
235. Anand, A.R. and R.K. Ganju, *HIV-1 gp120-mediated apoptosis of T cells is regulated by the membrane tyrosine phosphatase CD45.* J Biol Chem, 2006. **281**(18): p. 12289-99.
236. Luciani, F., et al., *CD95/phosphorylated ezrin association underlies HIV-1 GP120/IL-2-induced susceptibility to CD95(APO-1/Fas)-mediated apoptosis of human resting CD4(+)T lymphocytes.* Cell Death Differ, 2004. **11**(5): p. 574-82.
237. Ullrich, C.K., J.E. Groopman, and R.K. Ganju, *HIV-1 gp120- and gp160-induced apoptosis in cultured endothelial cells is mediated by caspases.* Blood, 2000. **96**(4): p. 1438-42.

238. Vlahakis, S.R., et al., *Chemokine-receptor activation by env determines the mechanism of death in HIV-infected and uninfected T lymphocytes.* J Clin Invest, 2001. **107**(2): p. 207-15.
239. Cicala, C., et al., *HIV-1 envelope induces activation of caspase-3 and cleavage of focal adhesion kinase in primary human CD4(+) T cells.* Proc Natl Acad Sci U S A, 2000. **97**(3): p. 1178-83.
240. Masci, A.M., et al., *HIV-1 gp120 induces anergy in naive T lymphocytes through CD4-independent protein kinase-A-mediated signaling.* J Leukoc Biol, 2003. **74**(6): p. 1117-24.
241. Molina, L., et al., *Proteomic analysis of the cellular responses induced in uninfected immune cells by cell-expressed X4 HIV-1 envelope.* Proteomics, 2007. **7**(17): p. 3116-30.
242. Bachis, A., et al., *M- and T-tropic HIVs promote apoptosis in rat neurons.* J Neuroimmune Pharmacol, 2009. **4**(1): p. 150-60.
243. Peng, F., et al., *Platelet-derived growth factor protects neurons against gp120-mediated toxicity.* J Neurovirol, 2008. **14**(1): p. 62-72.
244. Ohagen, A., et al., *Apoptosis induced by infection of primary brain cultures with diverse human immunodeficiency virus type 1 isolates: evidence for a role of the envelope.* J Virol, 1999. **73**(2): p. 897-906.
245. Wesselingh, S.L. and K.A. Thompson, *Immunopathogenesis of HIV-associated dementia.* Curr Opin Neurol, 2001. **14**(3): p. 375-9.
246. Jones, M.V., J.E. Bell, and A. Nath, *Immunolocalization of HIV envelope gp120 in HIV encephalitis with dementia.* AIDS, 2000. **14**(17): p. 2709-13.
247. Hesselgesser, J., et al., *Neuronal apoptosis induced by HIV-1 gp120 and the chemokine SDF-1 alpha is mediated by the chemokine receptor CXCR4.* Curr Biol, 1998. **8**(10): p. 595-8.
248. Hesselgesser, J., et al., *CD4-independent association between HIV-1 gp120 and CXCR4: functional chemokine receptors are expressed in human neurons.* Curr Biol, 1997. **7**(2): p. 112-21.
249. Alirezaei, M., et al., *Human immunodeficiency virus-1/surface glycoprotein 120 induces apoptosis through RNA-activated protein kinase signaling in neurons.* J Neurosci, 2007. **27**(41): p. 11047-55.
250. Twu, C., et al., *Cardiomyocytes undergo apoptosis in human immunodeficiency virus cardiomyopathy through mitochondrion- and death receptor-controlled pathways.* Proc Natl Acad Sci U S A, 2002. **99**(22): p. 14386-91.
251. Vlahakis, S.R., et al., *Human immunodeficiency virus-induced apoptosis of human hepatocytes via CXCR4.* J Infect Dis, 2003. **188**(10): p. 1455-60.
252. Perfettini, J.L., et al., *Essential role of p53 phosphorylation by p38 MAPK in apoptosis induction by the HIV-1 envelope.* J Exp Med, 2005. **201**(2): p. 279-89.
253. Lelievre, J.D., et al., *A novel mechanism for HIV1-mediated bystander CD4+ T-cell death: neighboring dying cells drive the capacity of HIV1 to kill noncycling primary CD4+ T cells.* Cell Death Differ, 2004. **11**(9): p. 1017-27.
254. Bredell, H., et al., *Identification of HIV type 1 intersubtype recombinants in South Africa using env and gag heteroduplex mobility assays.* AIDS Res Hum Retroviruses, 2000. **16**(5): p. 493-7.
255. Nkosi, S.P., H. Huismans, and M.A. Papathanasopoulos, *Purification and partial characterization of R5, R5X4, and X4 HIV-1 subtype C envelope glycoproteins expressed in insect cells.* J Med Virol, 2005. **76**(4): p. 459-63.
256. Hertzberg, R.P., M.J. Caranfa, and S.M. Hecht, *On the mechanism of topoisomerase I inhibition by camptothecin: evidence for binding to an enzyme-DNA complex.* Biochemistry, 1989. **28**(11): p. 4629-38.

257. Johnson, N., T.T. Ng, and J.M. Parkin, *Camptothecin causes cell cycle perturbations within T-lymphoblastoid cells followed by dose dependent induction of apoptosis.* Leuk Res, 1997. **21**(10): p. 961-72.
258. Fadok, V.A., et al., *Exposure of phosphatidylserine on the surface of apoptotic lymphocytes triggers specific recognition and removal by macrophages.* J Immunol, 1992. **148**(7): p. 2207-16.
259. Martin, S.J., et al., *Early redistribution of plasma membrane phosphatidylserine is a general feature of apoptosis regardless of the initiating stimulus: inhibition by overexpression of Bcl-2 and Abl.* J Exp Med, 1995. **182**(5): p. 1545-56.
260. Schmid, I., et al., *A rapid method for measuring apoptosis and dual-color immunofluorescence by single laser flow cytometry.* J Immunol Methods, 1994. **170**(2): p. 145-57.
261. Lawry, J., *Detection of apoptosis by the TUNEL assay.* Methods Mol Med, 2004. **88**: p. 183-90.
262. Gavrieli, Y., Y. Sherman, and S.A. Ben-Sasson, *Identification of programmed cell death in situ via specific labeling of nuclear DNA fragmentation.* J Cell Biol, 1992. **119**(3): p. 493-501.
263. Davis, C.B., et al., *Signal transduction due to HIV-1 envelope interactions with chemokine receptors CXCR4 or CCR5.* J Exp Med, 1997. **186**(10): p. 1793-8.
264. Hivroz, C., et al., *Human immunodeficiency virus gp120 and derived peptides activate protein tyrosine kinase p56lck in human CD4 T lymphocytes.* Eur J Immunol, 1993. **23**(3): p. 600-7.
265. Doores, K.J., et al., *Envelope glycans of immunodeficiency virions are almost entirely oligomannose antigens.* Proc Natl Acad Sci U S A. **107**(31): p. 13800-5.
266. Yonezawa, A., et al., *Replacement of the V3 region of gp120 with SDF-1 preserves the infectivity of T-cell line-tropic human immunodeficiency virus type 1.* J Virol, 2001. **75**(9): p. 4258-67.
267. Puffer, B.A., et al., *Determinants within gp120 and gp41 contribute to CD4 independence of SIV Envs.* Virology, 2004. **327**(1): p. 16-25.
268. Wells, D.E. and R.W. Compans, *Expression and characterization of a functional human immunodeficiency virus envelope glycoprotein in insect cells.* Virology, 1990. **176**(2): p. 575-86.
269. Chen, B., et al., *Expression, purification, and characterization of gp160e, the soluble, trimeric ectodomain of the simian immunodeficiency virus envelope glycoprotein, gp160.* J Biol Chem, 2000. **275**(45): p. 34946-53.
270. Jones, D.H., et al., *Efficient purification and rigorous characterisation of a recombinant gp120 for HIV vaccine studies.* Vaccine, 1995. **13**(11): p. 991-9.
271. Li, Y., et al., *Glycosylation is necessary for the correct folding of human immunodeficiency virus gp120 in CD4 binding.* J Virol, 1993. **67**(1): p. 584-8.
272. Raska, M., et al., *Glycosylation patterns of HIV-1 gp120 depend on the type of expressing cells and affect antibody recognition.* J Biol Chem. **285**(27): p. 20860-9.
273. Grundner, C., et al., *Factors limiting the immunogenicity of HIV-1 gp120 envelope glycoproteins.* Virology, 2004. **330**(1): p. 233-48.
274. Jarvis, D.L., *Developing baculovirus-insect cell expression systems for humanized recombinant glycoprotein production.* Virology, 2003. **310**(1): p. 1-7.
275. Varadarajan, R., et al., *Characterization of gp120 and its single-chain derivatives, gp120-CD4D12 and gp120-M9: implications for targeting the CD4i epitope in human immunodeficiency virus vaccine design.* J Virol, 2005. **79**(3): p. 1713-23.
276. Bures, R., et al., *Regional clustering of shared neutralization determinants on primary isolates of clade C human immunodeficiency virus type 1 from South Africa.* J Virol, 2002. **76**(5): p. 2233-44.

277. Burton, D.R., et al., *Efficient neutralization of primary isolates of HIV-1 by a recombinant human monoclonal antibody.* Science, 1994. **266**(5187): p. 1024-7.
278. Binley, J.M., et al., *Comprehensive cross-clade neutralization analysis of a panel of anti-human immunodeficiency virus type 1 monoclonal antibodies.* J Virol, 2004. **78**(23): p. 13232-52.
279. Kessler, J.A., 2nd, et al., *Recombinant human monoclonal antibody IgG1b12 neutralizes diverse human immunodeficiency virus type 1 primary isolates.* AIDS Res Hum Retroviruses, 1997. **13**(7): p. 575-82.
280. Roben, P., et al., *Recognition properties of a panel of human recombinant Fab fragments to the CD4 binding site of gp120 that show differing abilities to neutralize human immunodeficiency virus type 1.* J Virol, 1994. **68**(8): p. 4821-8.
281. Saphire, E.O., et al., *Crystal structure of a neutralizing human IGG against HIV-1: a template for vaccine design.* Science, 2001. **293**(5532): p. 1155-9.
282. Rizzuto, C. and J. Sodroski, *Fine definition of a conserved CCR5-binding region on the human immunodeficiency virus type 1 glycoprotein 120.* AIDS Res Hum Retroviruses, 2000. **16**(8): p. 741-9.
283. Moore, J.P., et al., *Exploration of antigenic variation in gp120 from clades A through F of human immunodeficiency virus type 1 by using monoclonal antibodies.* J Virol, 1994. **68**(12): p. 8350-64.
284. Thali, M., et al., *Characterization of conserved human immunodeficiency virus type 1 gp120 neutralization epitopes exposed upon gp120-CD4 binding.* J Virol, 1993. **67**(7): p. 3978-88.
285. Sanders, R.W., et al., *The mannose-dependent epitope for neutralizing antibody 2G12 on human immunodeficiency virus type 1 glycoprotein gp120.* J Virol, 2002. **76**(14): p. 7293-305.
286. Scanlan, C.N., et al., *The broadly neutralizing anti-human immunodeficiency virus type 1 antibody 2G12 recognizes a cluster of alpha1-->2 mannose residues on the outer face of gp120.* J Virol, 2002. **76**(14): p. 7306-21.
287. Gray, E.S., et al., *N-linked glycan modifications in gp120 of human immunodeficiency virus type 1 subtype C render partial sensitivity to 2G12 antibody neutralization.* J Virol, 2007. **81**(19): p. 10769-76.
288. Gray, E.S., et al., *Insensitivity of paediatric HIV-1 subtype C viruses to broadly neutralising monoclonal antibodies raised against subtype B.* PLoS Med, 2006. **3**(7): p. e255.
289. Chen, H., et al., *Reintroduction of the 2G12 epitope in an HIV-1 clade C gp120.* Aids, 2005. **19**(8): p. 833-5.
290. Pantaleo, G., et al., *HIV infection is active and progressive in lymphoid tissue during the clinically latent stage of disease.* Nature, 1993. **362**(6418): p. 355-8.
291. Sunila, I., et al., *gp120 is present on the plasma membrane of apoptotic CD4 cells prepared from lymph nodes of HIV-1-infected individuals: an immunoelectron microscopic study.* Aids, 1997. **11**(1): p. 27-32.
292. Oh, S.K., et al., *Identification of HIV-1 envelope glycoprotein in the serum of AIDS and ARC patients.* J Acquir Immune Defic Syndr, 1992. **5**(3): p. 251-6.
293. Corbeil, J. and D.D. Richman, *Productive infection and subsequent interaction of CD4-gp120 at the cellular membrane is required for HIV-induced apoptosis of CD4+ T cells.* J Gen Virol, 1995. **76 (Pt 3)**: p. 681-90.
294. Marth, J.D., et al., *A lymphocyte-specific protein-tyrosine kinase gene is rearranged and overexpressed in the murine T cell lymphoma LSTRA.* Cell, 1985. **43**(2 Pt 1): p. 393-404.

295. Rudd, C.E., et al., *The CD4 receptor is complexed in detergent lysates to a protein-tyrosine kinase (pp58) from human T lymphocytes.* Proc Natl Acad Sci U S A, 1988. **85**(14): p. 5190-4.
296. Juszczak, R.J., et al., *Effect of human immunodeficiency virus gp120 glycoprotein on the association of the protein tyrosine kinase p56lck with CD4 in human T lymphocytes.* J Biol Chem, 1991. **266**(17): p. 11176-83.
297. Hurley, T.R., K. Luo, and B.M. Sefton, *Activators of protein kinase C induce dissociation of CD4, but not CD8, from p56lck.* Science, 1989. **245**(4916): p. 407-9.
298. Wang, X., et al., *c-FLIPL regulates PKC via AP-2 to inhibit Bax-mediated apoptosis induced by HIV-1 gp120 in Jurkat cells.* Mol Cell Biochem, 2009. **330**(1-2): p. 23-9.
299. Accornero, P., et al., *Differential susceptibility to HIV-GP120-sensitized apoptosis in CD4+ T-cell clones with different T-helper phenotypes: role of CD95/CD95L interactions.* Blood, 1997. **89**(2): p. 558-69.
300. Chang, M.I., et al., *Single-molecule analysis of human immunodeficiency virus type 1 gp120-receptor interactions in living cells.* J Virol, 2005. **79**(23): p. 14748-55.
301. Dobrowsky, T.M., et al., *Monitoring early fusion dynamics of human immunodeficiency virus type 1 at single-molecule resolution.* J Virol, 2008. **82**(14): p. 7022-33.
302. Iyengar, S., J.E. Hildreth, and D.H. Schwartz, *Actin-dependent receptor colocalization required for human immunodeficiency virus entry into host cells.* J Virol, 1998. **72**(6): p. 5251-5.
303. Lynch, G.W., et al., *CD4 is expressed by epidermal Langerhans' cells predominantly as covalent dimers.* Exp Dermatol, 2003. **12**(5): p. 700-11.
304. Lynch, G.W., et al., *Direct evidence for native CD4 oligomers in lymphoid and monocytoid cells.* Eur J Immunol, 1999. **29**(8): p. 2590-602.
305. Steffens, C.M. and T.J. Hope, *Localization of CD4 and CCR5 in living cells.* J Virol, 2003. **77**(8): p. 4985-91.
306. Blanco, J., et al., *R5 HIV gp120-mediated cellular contacts induce the death of single CCR5-expressing CD4 T cells by a gp41-dependent mechanism.* J Leukoc Biol, 2004. **76**(4): p. 804-11.
307. Bleul, C.C., et al., *The HIV coreceptors CXCR4 and CCR5 are differentially expressed and regulated on human T lymphocytes.* Proc Natl Acad Sci U S A, 1997. **94**(5): p. 1925-30.
308. Weissman, D., et al., *Macrophage-tropic HIV and SIV envelope proteins induce a signal through the CCR5 chemokine receptor.* Nature, 1997. **389**(6654): p. 981-5.
309. Kinet, S., et al., *gp120-mediated induction of the MAPK cascade is dependent on the activation state of CD4(+) lymphocytes.* Blood, 2002. **100**(7): p. 2546-53.
310. Popik, W., J.E. Hesselgesser, and P.M. Pitha, *Binding of human immunodeficiency virus type 1 to CD4 and CXCR4 receptors differentially regulates expression of inflammatory genes and activates the MEK/ERK signaling pathway.* J Virol, 1998. **72**(8): p. 6406-13.
311. Baba, M., et al., *A small-molecule, nonpeptide CCR5 antagonist with highly potent and selective anti-HIV-1 activity.* Proc Natl Acad Sci U S A, 1999. **96**(10): p. 5698-703.
312. Samson, M., et al., *Resistance to HIV-1 infection in caucasian individuals bearing mutant alleles of the CCR-5 chemokine receptor gene.* Nature, 1996. **382**(6593): p. 722-5.
313. Cicala, C., et al., *Induction of phosphorylation and intracellular association of CC chemokine receptor 5 and focal adhesion kinase in primary human CD4+ T cells by macrophage-tropic HIV envelope.* J Immunol, 1999. **163**(1): p. 420-6.
314. Berndt, C., et al., *CXCR4 and CD4 mediate a rapid CD95-independent cell death in CD4(+) T cells.* Proc Natl Acad Sci U S A, 1998. **95**(21): p. 12556-61.

315. Machuca, A., et al., *HIV type 2 primary isolates induce a lower degree of apoptosis "in vitro" compared with HIV type 1 primary isolates.* AIDS Res Hum Retroviruses, 2004. **20**(5): p. 507-12.
316. Zhang, C.W., et al., *Expression, purification, and characterization of recombinant HIV gp140. The gp41 ectodomain of HIV or simian immunodeficiency virus is sufficient to maintain the retroviral envelope glycoprotein as a trimer.* J Biol Chem, 2001. **276**(43): p. 39577-85.
317. Bardi, G., et al., *Human immunodeficiency virus gp120-induced apoptosis of human neuroblastoma cells in the absence of CXCR4 internalization.* J Neurovirol, 2006. **12**(3): p. 211-8.
318. Herbein, G., et al., *Apoptosis of CD8+ T cells is mediated by macrophages through interaction of HIV gp120 with chemokine receptor CXCR4.* Nature, 1998. **395**(6698): p. 189-94.
319. Romani, B., R.H. Glashoff, and S. Engelbrecht, *Functional integrity of naturally occurring mutants of HIV-1 subtype C Vpr.* Virus Res. **153**(2): p. 288-98.
320. Grivel, J.C. and L.B. Margolis, *CCR5- and CXCR4-tropic HIV-1 are equally cytopathic for their T-cell targets in human lymphoid tissue.* Nat Med, 1999. **5**(3): p. 344-6.
321. Grivel, J.C., et al., *Human immunodeficiency virus type 1 coreceptor preferences determine target T-cell depletion and cellular tropism in human lymphoid tissue.* J Virol, 2000. **74**(11): p. 5347-51.
322. Meera, S., et al., *Irreversible loss of pDCs by apoptosis during early HIV infection may be a critical determinant of immune dysfunction.* Viral Immunol. **23**(3): p. 241-9.